Singh Sonika (2021) Image analysis of Gray Matter alterations and White Matter lesions in Multiple Sclerosis. PhD thesis, University of Nottingham.

Image analysis of Gray Matter alterations and White Matter lesions in Multiple Sclerosis

Dissertation submitted for degree of Doctor of Philosophy

Submitted by

Miss Sonika Singh, MSc

Department of Neurology,

Nottingham University Hospitals,

Nottingham

Supervisors

Dr. Christopher Tench, PhD

Prof. C Constantinescu, PhD, FRCP

Declaration

I, Sonika Singh, confirm that the work presented in this thesis is my own. Where information has been contributed from other sources and by colleagues, I indicate this in the References and Acknowledgements sections.

Abstract

Multiple Sclerosis (MS) is a frequently disabling neurological disease affecting young adults. The disease has been characterized by recurrent areas of focal inflammation (plaques) in the CNS giving rise to episodic neurological signs and symptoms. Helminth-associated immunoregulation has been investigated by the utilization of controlled hookworm infection in MS. Many studies have reported brain atrophy in patients with MS. This has been demonstrated as a major factor for physical and cognitive impairment in MS. In this thesis, I present our studies using immunomodulation, coordinate-Based Meta-Analysis (CBMA), Meta-Analysis of Networks (CBMAN), and Meta-Regression and voxel based morphometry (VBM) to study disease activity in MS.

1) For a Randomized Double-Blinded Placebo-Controlled Trial, we examined the effect of hookworm treatment on white matter (WM) disease activity.
2) Localised grey matter (GM) Atrophy in Multiple Sclerosis and Clinically Isolated Syndrome (CIS) was investigated by Coordinate-Based Meta-Analysis, Meta-Analysis of Networks, and Meta-Regression of Voxel-Based Morphometry Studies to reveal the significantly consistent regions and networks of GM atrophy in MS or CIS.
3) A further VBM was conducted in the revealed clusters to investigate the difference in GM atrophy between hookworm and placebo arms of the clinical trial, during the course of intervention.

Acknowledgements

This work would not have been possible without the help and support of wide cast of people. I am truly grateful to my supervisors Prof. Cris Constantinescu and Dr Christopher Tench for giving me this opportunity to work on these exciting projects.

I am very thankful for their continuous support. I am very thankful to Dr. Tench for always being there with his advice and innovative ideas. I have learnt a lot from him about analysing critically and thinking out-of-the-box. He has been patient, answering my endless questions. He gave me the skills that shaped me into a better scientist, for which I will always be grateful. I am thankful to Professor Constantinescu, his support, guidance and advice have always been very helpful.

I would also like to acknowledge the guidance provided by Dr. Radu Tanasescu regarding the introduction to the clinical trial and the associated MRI analysis. I would like to thank Dr. Yasser Falah, for nurturing my knowledge of lesion alterations as seen on the MRI. I would also like to thank William Cottam, for nourishing my knowledge regarding the voxel based morphometry project. I would like to thank Nanci Frakich, my friend and colleague, who helped me get values and pictures from the Linux computer at the time of COVID-19 pandemic.

I will forever be grateful to my foster parents, Dr. Ravi Sarin and Mrs. Anurita Sarin, who always believed in my capability despite my health condition and, have always been there for me. I would also like to thank my late grandad who has been a great friend, advisor, and critic. I am extremely thankful to Rishab, my friend and husband. I cannot even imagine my life without him at this stage of my life and, would never have been able to make it this far without his support. I know I always have him to help me through tough times. I am immensely thankful and appreciative for his endless sacrifices to help me pursue my research. The past decade

has not been an easy ride both academically and personally. I am extremely thankful to him for loving and supporting me unconditionally. Words cannot express my gratitude. I would like to thank my parents who supported me in taking the first big leap.

Table of Contents

5	Sample size for each ROI for 20% preservation in GM density.	113

Publications arising from this work

- Radu Tanasescu , Christopher R Tench , Cris S Constantinescu, Gary Telford, Sonika Singh, Nanci Frakich, David Onion, Dorothee P Auer, Bruno Gran, Nikos Evangelou, Yasser Falah, Colin Ranshaw, Cinzia Cantacessi, Timothy P Jenkins, David I Pritchard (2020). Hookworm Treatment for Relapsing Multiple Sclerosis: A Randomized Double-Blinded Placebo-Controlled Trial. JAMA Neurol. 2020 Sep 1;77(9):1089-1098.

- Sonika Singh, Christopher R Tench, Radu Tanasescu, Cris S Constantinescu (2020). Localised Grey Matter Atrophy in Multiple Sclerosis and Clinically Isolated Syndrome-A Coordinate-Based Meta-Analysis, Meta-Analysis of Networks, and Meta-Regression of Voxel-Based Morphometry Studies. Brain Sci. 2020 Oct 30;10(11):798.

Abbreviations

BBB	Blood Brain Barrier
B-cells	B-lymphocytes
CBMA	Coordinate-based Meta-Analysis
CBMAN	Coordinate-based Meta-Analysis of Networks
CDMS	Clinically Definite Multiple Sclerosis
CIS	Clinically Isolated Syndrome
CNS	Central Nervous System
EBV	Epstein-Barr virus
EDSS	Expanded Disability Status Scale
GLM	General Linear Model
GM	Grey Matter
MRI	Magnetic Resonance Imaging
MS	Multiple Sclerosis
NAWM	Normal Appearing White Matter
OCB	Oligoclonal Bands
PPMS	Primary Progressive Multiple Sclerosis
PRMS	Progressive Remitting Multiple Sclerosis
RIS	Radiologically Isolated Syndrome
ROI	Region of Interest
RRMS	Relapsing Remitting Multiple Sclerosis
SPMS	Secondary Progressive Multiple Sclerosis
T-cells	T-lymphocytes
VBM	Voxel Based Morphometry
WM	White Matter
BBB	Blood Brain Barrier
B-cells	B-lymphocytes
CBMA	Coordinate-based Meta-Analysis
CBMAN	Coordinate-based Meta-Analysis of Networks
CDMS	Clinically Definite Multiple Sclerosis
CIS	Clinically Isolated Syndrome
CNS	Central Nervous System
EBV	Epstein-Barr virus
EDSS	Expanded Disability Status Scale
GLM	General Linear Model
GM	Grey Matter
MRI	Magnetic Resonance Imaging
MS	Multiple Sclerosis
NAWM	Normal Appearing White Matter
OCB	Oligoclonal Bands
PPMS	Primary Progressive Multiple Sclerosis
PRMS	Progressive Remitting Multiple Sclerosis
RIS	Radiologically Isolated Syndrome
ROI	Region of Interest
RRMS	Relapsing Remitting Multiple Sclerosis
SPMS	Secondary Progressive Multiple Sclerosis

T-cells	T-lymphocytes
VBM	Voxel Based Morphometry
WM	White Matter

Table of Contents

Chapter 1

Introduction

1.1 Multiple Sclerosis: Natural History

Multiple Sclerosis (MS) is characterized as a chronic inflammatory disease affecting the Central Nervous System (CNS) that often has a relapsing course occurring at random intervals. Such inflammatory episodes, lasting from days to months usually, lead to injured myelin sheaths around nerve axons, damaged oligodendrocytes and, partial damage to neurons and neuronal processes.[1–4] Pathologic evidence of acute as well as chronic inflammation is found in the lesions of the CNS. These lesions are multifocal and centered on draining veins of CNS. The timing of acute MS attacks can be caused by certain factors that have been identified as increasing or decreasing the likelihood of an attack in MS. Pregnancy (last trimester) can be considered as an example when the likelihood of experiencing an attack is decreased as compared to the risk during pre-pregnancy. This risk increases during 3-6 months postpartum.[5] Estrogen level changes could be the probable explanation for these MS attacks. However, nonhormonal physiologic alterations occurring during pregnancy[6] could also be responsible for the observed attack risk. Another factor that can be considered as an influence for risk of attack is infections that are non-specific in nature[7,8]. Some authors have demonstrated that the timing of

some MS attacks could be related to vaccinations although the presented data is not convincing.[9]

The cause of MS is not known. However, the involvement of immune-mediated mechanisms is quite obvious and, most authors favor primary autoimmunity that is probably triggered by environmental events, as the essential pathophysiologic foundation for MS[10]. The pathologic characterization of MS involves demyelinating patches and gliosis causing formation of plaques, occurring in multifocal regions across the CNS white matter (WM).[11] The selective susceptibility of specific CNS pathways to MS lesions is explained in the available literature but, the physiologic foundation of this irregular distribution is not construed properly. Previously, grey matter (GM) and the nerve axons were thought not to be affected however, substantial current research and evidence have highlighted the significance of axonal injury, specifically in case of acute active lesions, and also of demyelination of GM specially in the later stages of MS.[12] Substantial evidence shows that autoreactive CD4+ and CD8+ T-lymphocytes (T-cells), macrophages, B-lymphocytes (B-cells) proliferate and travel across the blood-brain barrier(BBB) and, under the effect of proinflammatory cytokines and various cellular adhesion molecules, enter the CNS.[13,14] These cells, that are activated, lead to injury of CNS tissue found in acute MS lesions. Chronic MS lesions are characterized by gliosis and by a variable degree of loss of axons.

The 10-point expanded disability status scale (EDSS) is a widely used instrument for the quantification of the degree of disability in an MS patient - it was, initially developed in the 1950s and then adapted in several occasions.[15] However, the EDSS is still quite complicated and subjective to score with poor test-retest reliability.[16] Furthermore, it is nonlinear over its range as compared to the actual function level and it emphasizes mobility status more than other neurologic functions.[15] In spite of these limitations, although many other scales have been introduced, MS clinical research and

practice continues to employ EDSS as the standard measure for disability.[17] Another multidimensional clinical outcome measure is the MS Functional Composite (MSFC). The MSFC comprises quantitative functional measures of three key clinical dimensions of MS: leg function/ambulation, arm/hand function, and cognitive function.[16]

The first event of focal demyelination in the CNS is called as clinically isolated syndrome (CIS). About 60% of individuals with CIS suffer from a following relapse and a diagnosis of MS; this gets increased to 80% in case the baseline magnetic resonance image (MRI) demonstrates inflammatory lesions. Approximately, 85% of MS patients demonstrate a biphasic disease course that is marred by alternation in episodes of neurological disability and recovery, which is designated as relapsing remitting MS (RRMS).[1] Following this course, approximately 60-70% of RRMS patients transit into a secondary progressive disease course (SPMS), in 20-25 years, that is characterized by progression in neurological decline. Additionally, some of the MS patients (approximately 10%) exhibit a disease course of steady decline in neurological function that is not accompanied with recovery. They are classified as primary progressive MS (PPMS) patients. Some patients experience frequent relapses in early disease that leads to a rapidly evolving or highly active RRMS.[18] There exists a period of diagnostic uncertainty regarding the transition from RRMS to SPMS. There might be several potential reasons for the delayed diagnosis of SPMS. The earliest indicators of SPMS may be subtle; these involve worsening of symptoms but little change occurs in the neurological examination. The clinician is also likely to be appropriately cautious in labeling a patient as having SPMS, given the lack of available evidence-based treatments for this condition and patients' anxieties regarding its prognosis. In addition, a SPMS label may raise concerns regarding coverage for treatments by a third party.[19]

1.2 Epidemiology

1.2.1 Associations

In accordance with a report by the MS International Federation[20], the median prevalence of MS worldwide increased from 30 per 100,000 in 2008 to 33 per 100,000 in the year 2013. This prevalence varies to a large extent among countries[21] with the highest being in North America (140 per 100,000) and Europe (108 per 100,000) and, it was found to be the lowest in sub-Saharan Africa (2.1 per 100,000) and east Asia (2.2 per 100,00).

Specifically, various environmental risk factors, including infection with Epstein-Barr virus (EBV) [22], latitude[23] and smoking[24] have been put forward. The causative factors of MS are yet to be unraveled and there is no establishment of risk factors that could support prevention of the disease. Numerous systematic reviews and meta-analyses for MS environmental risk factors have been published.[25]

Lazaros and colleagues[26] conducted an umbrella review of systematic reviews and meta analyses of observational studies, from beginning to 2014, for which they searched PubMed and included appropriate studies examining associations between environmental causative agents and MS. There was estimation of 95% prediction interval, further accounting for between-study heterogeneity and evaluating the uncertainty of the effect that can be expected in any new research, regarding that same association.[27,28] With context to meta-analyses having continuous data, the estimate of effect was transformed to an odds ratio (OR) with an established formula.[29]

The 3 systematic reviews included in the umbrella review investigated stress[30], serum prolactin[31] and socioeconomic status[32] as MS risk factors. The umbrella review presented an evaluation of environmental risk factors for MS. The review considered 44 risk factors for an association with MS, that involved surgeries, infections and vaccinations and traumatic events,

comorbid diseases, exposure to toxic environmental agents and biochemical biomarkers. This review confirms 3 risk factors (anti-EBNA IgG seropositivity, smoking, infectious mononucleiosis) for the disease as supported by significant epidemiological credibility. Regarding consistency, smoking and EBV infection demonstrated association with MS without bias. Innumerable mechanisms have been put forward to describe the adverse effects of smoking on MS, having influence on immune system, demyelination, immune-modulatory effects and BBB disruption but, all such effects are still theoretical.[33] Attention has been received by sun exposure and vitamin D as being counted as risk factors for MS. These might explain the latitudinal and geographical trends of MS incidence.[23,25]

Genome wide association studies (GWAS) conducted for MS patients have resulted in the identification of over 100 genetic risk loci.[34]

The aetiology of MS is complex involving genetic as well as environmental influences. The weight of evidence would favor a greater role for the environment over genetics. There is sufficient evidence for profound effect of the environment, with at least four or more directly contributing factors. The reported effect sizes are significantly greater as compared to any identified genetic factor.[35]

The genetic predisposition suggests an explanation for MS cases within families. But this does not entirely explain the geographic variations in the frequency of MS and the risk variability occurring with migration. There is epidemiological support for the “hygiene hypothesis” but with provision for a specific role of EBV towards the development of risk of MS. Although EBV infection is one of many key features of MS epidemiology, the link between the virus and MS cannot clarify, on its own, the declined risk among migrants moving from high to low MS prevalence areas. This decline indicates that either the EBV strains in low risk areas are less liable to cause MS, or that other infectious or non-infectious factors have a modifying effect

on the response of host to EBV or otherwise contribute to determine the risk of MS.[36]

There is a salient latitudinal gradient in the prevalence of MS, with exceptions in Mediterranean Europe and northern Scandinavia. This study has the purpose of evaluating the association between MS prevalence and latitude by meta-regression. The comprehensive review has confirmed a statistically significant positive association between MS prevalence and latitude globally. The exceptions are probably a result of genetic and behavioral-cultural variations.[23]

Handel and colleagues[24] conducted a meta-analysis wherein they performed a Medline search for the identification of researches investigating the risk of MS associated with cigarette smoking. 14 studies were included in the meta-analysis, the studies were analysed in a conservative as well as non-conservative manner. The prior way limited the analysis to studies where smoking was described prior to disease onset. The results of the meta-analysis demonstrate that smoking is associated with MS susceptibility. The research also analysed 4 studies reporting the risk of secondary progressive MS. It was found that the association was not statistically significant and, had considerable heterogeneity.

The results demonstrated that there is an association between smoking and MS susceptibility but this effect on disease progression remained uncertain. Subsequent studies point to an effect of smoking on disease progression as well. For example Manouchehrinia and coworkers[37] showed an association between smoking and disease progression which was confirmed by subsequent studies.

Exposure to infant siblings has an influence on the age of MS onset. A study was conducted by Ponsonby and colleagues[38] on a population of residents of Tasmania, Australia younger than 60 years with at least one grandparent who was born in Tasmania. The cases satisfying these criteria had

abnormalities in the MR images consistent with MS and clinically definite MS as per the neurological review.[39] Interviews were held for the cases and controls between March 1999 and June 2001. The questionnaire intended to examine the environmental factors, particularly sun exposure, contributing towards the development of MS. It included questions regarding the number of siblings and their birthdates, whether their living place was the same, sun exposure in the past, history of cigarette smoking, medical history, whether the subject had been breastfed and sociodemographic features. Type of skin was determined using a spectrophotometer for the assessment of melanin density at the location of the upper inner arm. The type was considered 'fair' if the density of melanin was found to be less than 2%.[40]

The authors found a strong statistically significant inverse association between exposure to infant siblings and MS and, these trends were sustained after adjusting for confounding factors.

The finding that high exposure among controls reduces the risk for developing infectious mononucleosis as well as increased EBV IgG levels is debatable because the risk of infectious mononucleosis and high EBV IgG have been recognized to have a role in the etiology of MS.[36,41]

Higher exposure to infant siblings in the first six years was related to a reduction in the risk of MS. This was probably due to alteration of patterns of childhood infection and associated immune responses. The study found that the increase in contact duration between the index child and a younger sibling aged less than 2 years in the first 6 years of life was associated with reduced MS risk. Among cases, higher contact with infants in early childhood had an association with delayed onset of MS.[38]

According to the proposal put forward by Taylor and colleagues, smoking[42] and the hygiene hypothesis[38] along with ultraviolet radiation exposure[40] add up to be the environmental risk factors that have a significant effect on the

development of MS. Deficiency of vitamin D has a part to play in the causality of MS. It has been well established as a risk factor for MS with an association between low vitamin D and the significantly elevated risk of MS development.[43]

MS has been found to be frequent in the developed areas of the world as compared to the ones that are developing.[44] Considering these epidemiological observations, a variety of risk factors have been proposed that include Epstein-Barr virus, low vitamin D, smoking and sanitation.[44,45] However, the most enthralling is the inverse correlation between helminth infections and incidence of autoimmune disease.[46]

Authenticating this hypothesis, studies that are longitudinal and involve translocating subjects for the evaluation of MS prevalence in the FrenchWest Indies over a duration of 20 years confirm that incidence of MS is increased in regions with significantly reduced parasite infections.[47]

Being more specific, MS prevalence decreased significantly when a critical threshold (10%) of helminth (Trichuris trichura) infection was exceeded in any given population.[48] The administration of anti-helminth drugs lead to elevated MS activity.[49] This propounds the direct involvement of helminths in the suppression of autoimmune diseases and might be the protective environmental factor against MS development.

1.3 Pathophysiology

1.3.1 Inflammation and Demyelination

MS is primarily an immune-mediated disease that involves the auto-aggressive T-cells crossing the BBB imposing demyelination and axonal loss subsequently leading to disability. The formation of gadolinium-enhancing lesions, due to an overt breach of BBB, is a crucial event in MS.[50] Recent developments in MS drug therapies highlight leukocyte passage across BBB in the disease pathophysiology. It has been reported by

histopathological studies that inactive MS lesions as well as normal appearing WM (NAWM) show abnormalities[51]. In addition, it has been demonstrated by MRI studies that structural alterations[52,53] and BBB dysfunction[54] might be heralding myelin damage and leukocyte infiltration.

1.3.2 Neurodegeneration in MS

This is an early part of the disease that undergoes self-perpetuation over time. The use of immunotherapy has been able to disclose considerable insights into the disease pathogenesis: for instance, while the reduction of relapses can postpone progression and disability[55], it does not stop the disease evolution. This suggests that progressive worsening might require directly targeting the neurodegeneration and the processes causing it which arise without any association with immune attacks in the later disease stages. Therefore, while SPMS may not stand as a distinct phase arising as a direct consequence of RRMS, it could be the product of other pathophysiological mechanisms.[56]

In recent years, the requirement of novel therapeutic strategies to specifically target neurodegeneration has been apparent, shifting the balance from neuroaxonal damage towards neuroprotection and/or regeneration. It would be inaccurate to consider neurodegeneration as a secondary phase of MS; it is an early allied process that is already proceeding since the time of diagnosis.[57]

Damage of the axons is detectable even in MS lesions where axons are still myelinated[58], and loss of axons can possibly provide the best correlate of neurological disability. Disturbances in axonal transport also promote progressive degeneration.[59]Disconnection of relapses with progression of disability is, however, challenging due to immunological involvement being implicated in the progression course. Epidemiological studies have demonstrated how to achieve delay in MS progression if the clinical EDSS score of 3.0 has not been reached yet; however, if that clinical threshold has been crossed, the disability is not as much responsive to any

management.[60] This information supports the necessity to counteract inflammation as early as possible to be able to delay the self-perpetuating neurodegenerative processes.[61]

1.3.3 Neuroprotection

Glial as well as endothelial cells can play a role in the promotion of recovery from stress and injury via the secretion of neurotrophic factors like brain-derived neurotrophic factor (BDNF), nerve growth factor (NGF) and neurotrophin-3.[62]

Furthermore, the importance of the maintenance of regulatory T-cell (T_{reg}) populations has been highlighted by many studies for the prevention of autoimmune neuro-inflammatory damage in the EAE animal model of MS.[63]

1.4 Course and Classification

1.4.1 Classification

The course of MS is quite diverse. Jean-Martin Charcot was the first person to describe a neurological triad consisting of intention tremor, nystagmus, scanning and staccato speech representative of MS, with the recognition of latent symptoms.

In 1952, Douglas McAlpine and Nigel Compston[64] produced simple line diagrams of the classic MS disease courses as shown in **Figure 1** and, provided description to attacks, remission and chronic progression as a result of MS onset or following several attacks.

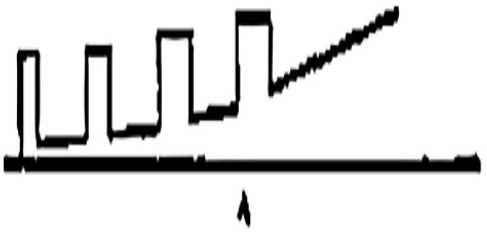

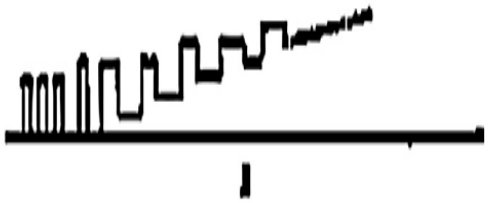

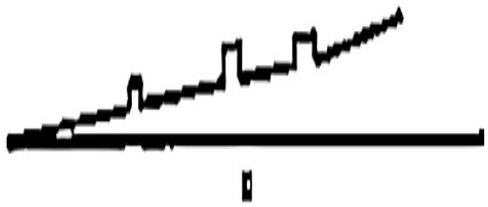

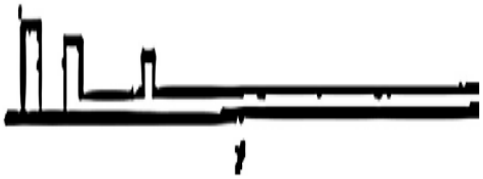

Figure 1: Adapted from [64]; Line diagrams of the different courses of MS.

The requirement for single common classifications became persuasive during the 1990s (the era of clinical trials), due to the unavailability of biological or imaging biomarkers. As a result of a survey issued in 1952 by the US Advisory Committee on Clinical Trials of New Agents in MS of the National Multiple Sclerosis Society (NMSS), Lublin and Reingold[65] classified four disease subtypes. These included relapsing–remitting (RR), secondary–progressive (SP), primary–progressive (PP) and progressive–remitting (PR).

However, different views have arisen recently with the arrival of imaging techniques. These include opinions like—confirmation of suspected RRMS by asymptomatic lesions observed on MR images following a single inflammatory event. Furthermore, new MRI lesions, with or without attacks, have the capability to predict future disability in progressive forms[66] along with drug efficacy[67,68], thereby indicating the importance of the need for identifying inflammatory activity in such patients.

Attacks and new/enlarging T2-weighted lesions and/or new contrast-enhancing lesions on MRI are now considered to be the markers of this disease activity. In 2014, the NMSS Advisory Committee, after revisions of previous definitions, published a novel classification along with new definitions. (**Table** 1)

FORMS	**EVENTS**
Attack, relapse, bout, exacerbation	• Acute or subacute episodes of new or increasing neurologic dysfunction followed by full or

	partial recovery, in the absence of fever or infection''[69] • ''Although a new attack should be documented by contemporaneous neurological examination, in the appropriate context, some historical events with symptoms and evolution characteristic for MS, but for which no objective neurological findings are documented, can provide reasonable evidence of a prior demyelinating event''[70] • ''30 days should separate the onset of the first event from the onset of a second event''[71]
Activity	• Clinical: attacks • AND/OR imaging (MRI): occurrence of contrast-enhancing T1 hyperintense or new or unequivocally enlarging T2 hyperintense lesions.[71]
Progression	• Worsening for those solely in a progressive phase of the illness • Progressive disease: - Clinical: steadily increasing objectively documented

	neurologic dysfunction/disability without unequivocal recovery (fluctuations and phases of stability may occur) - Imaging (MRI): imaging measures of progression are not established or standardized and not (yet) useful as phenotype descriptors for individual patients.[71]
Worsening	• ‘‘Documented increase in neurologic dysfunction/disability as a result of relapses or progressive disease’’ • ‘‘Confirmed accumulation of disability would be defined by a worsening of EDSS that persists over x months’’[71]
Clinically isolated syndrome	• ‘‘The first clinical presentation of a disease that shows characteristics of inflammatory demyelination that could be MS, but has yet to fulfill criteria of dissemination in time’’[65] • ‘‘A CIS is, by definition, always isolated in time (i.e. monophasic). Clinically, it is usually also isolated in space

	(i.e. monofocal) with signs indicating a lesion in the optic nerve (a common presentation in many reported CIS studies), spinal cord, brainstem or cerebellum, or (rarely) a cerebral hemisphere. However, some patients with a CIS have clinical evidence for dissemination in space (i.e. multifocal)''[72]
Benign and malignant MS	''These terms, especially the term benign, which should always be a retrospective determination, are often misunderstood and misused. In a long-term disease like MS, the severity and activity of the disease can change significantly and unpredictably. We recommend that these terms be used with caution''[69]

Table 1: Adapted from[73]; Definitions of events or forms in MS.

This classification defined CIS as a single attack. Radiologically Isolated syndrome (RIS) was defined in cases where incidental imaging findings, signifying inflammatory demyelination, were visualized in the lack of clinical signs or a history of attack and/or progression.[65] Nonetheless, three classic disease forms were retained—RRMS, PPMS, SPMS—while asserting the inability of defining the 'transition point' where RRMS converts to SPMS. Among all the points, ''the MS Phenotype Group believes that disease

activity detected by clinical relapses or imaging as well as progression of disability can be meaningful additional descriptors in either relapsing or progressive disease''. This further led to two categorization levels: clinical phenotype (CIS, RRMS, PPMS, SPMS) and disease process (active or not; progressive or not).

1.4.2 Course

Most of the MS patients (85%) experience sequential acute clinical relapses (RRMS) at the start of the disease, ultimately experiencing progression (SPMS). The major predictive factor for recovery after an MS relapse is the length of time period of persistence of the episode, longer duration corresponding to worse stance.[74] According to the literature, the proportion of patients who demonstrate incomplete recovery after their first episode range from 16% to 30%.[3] Some data suggests that the recovery rates from relapses may be as low as 50%; therefore, it is essential to prevent relapses in order to prevent the risk of accumulating permanent disability.

The development of a second clinical episode i.e. in a different location of the CNS leads to the diagnosis of clinically definite (CD) MS.[39,71,75] The probability of the same is very high in the immediate repercussion of the initial episode and, diminishes thereafter.[3,76,77]This has been reported, for the placebo arms, in several randomized controlled trials recruiting CIS patients. The median time to experiencing the second attack in these studies was calculated to be ~2years.

In recent years, radiologic evidence guides the diagnosis of CDMS demonstrating dissemination in space and time.[70] According to the 2017 revisions to the McDonald diagnostic criteria for MS, with a typical CIS, fulfillment of clinical or MRI criteria for DIS, and no better explanation for the clinical presentation, demonstration of CSF oligoclonal bands (OCBs) in the absence of atypical CSF findings permits a diagnosis of MS to be

made, even if the MRI findings on the baseline scan do not meet the criteria for DIT and in advance of either a second attack or MRI evidence of a new or active lesion on serial imaging.[78] This recommendation allows the presence of CSF OCBs as a substitute for the requirement of fulfilment of DIT in this situation.[79]

One large study, that enrolled 532 patients, reported a much longer median time for conversion to CDMS (7.1 years). This could partially be due to the utilization of 'CDMS' rather than 'second attack' that are not necessarily equivalent outcomes.[39] The reason could also be the overrepresentation of optic neuritis patients (52%) and, the inclusion of large proportion (30%) of patients without the presentation of abnormalities on baseline brain MRI. None of the clinical parameters (eg. Onset age, gender, mono- or multifocality of initial symptoms or recovery degree since initial episode) have shown consistent influence on the likelihood of a patient experiencing a second clinical attack.[76,80]

MRI abnormalities observed at clinical disease onset do impact this occurrence. Hence, the occurrence of and/or the number of MRI lesions have been steadily reported as a strong factor increasing the probability of a second neurologic episode within 1-3 years.

There is an association of T2 lesion volume on brain MRI and the likelihood of a second attack, with higher volumes leading to greater risk.[81] Furthermore, researchers have demonstrated T1 gadolinium-enhancing lesions as a stronger predictor of development of a second episode.[82,83]

The presence of new T2 lesions or gadolinium-enhancing lesions observed on a brain MRI performed 3 months following the baseline MRI[84] or 12 months following the initial episode forecast the occurrence of a second episode. The repeated MRIs in both studies improved the prediction specificity.

1.4.3 Clinical Features

A person is suspected to have MS when there is presentation of a CIS. It can be mono- or polysymptomatic depending on the lesion (s) location. The most common presentations involve optic neuritis, spinal cord and brainstem syndromes. The less common presentations include cortical presentations like dominant parietal lobe syndromes.

MS relapses are known to develop over hours to days followed by reaching a plateau and then recovering. Gross clinical recovery from relapses is often complete in early disease, however, they leave behind some damage. For instance, acute optic neuritis may result in contrast sensitivity, colour vision and depth perception abnormalities even after the recovery of visual acuity. There is loss of neuronal reserve and therefore, recovery from relapses becomes incomplete leading to accumulation of neurological deficits followed by sustained disability.

For each clinical attack, roughly 10 ‘asymptomatic’ lesions are observed on MRI. A combination of location and lesion volume give rise to symptoms – a small lesion in an eloquent region is likely to cause symptoms. Many more lesions are visible at the microscopic level along with lesions in the deep and cortical GM, along with macroscopic lesions or those visible on MRI.

The development of SPMS takes place 10-15 years after the onset of RRMS with a steady evolution from distinguished relapses to slowly progressive disease. Instead of a discrete transition between the disease categories, there is occurrence of relapses on a background of progression before progression taking over. The progressive brain atrophy and impaired cognition in early stages of the disease signify that clinical onset marks the initiation of neurodegeneration.

5%-15% of cases present with PPMS, demonstrating gradual progressive disability accrual involving one dominant neuronal system. Patients commonly present with a progressive spastic paraparesis, but sensory ataxia, cerebellar ataxia; progressive visual and cognitive failure are well-described PPMS variants.

Pediatric MS is rarer as compared to adult onset disease, with a highest reported incidence of 2.9/100,000.[85] It is diagnosed on the basis of repeated demyelination episodes separated by time and space. It has been found to be challenging to distinguish paediatric MS from acute disseminated encephalomyelitis, due to pediatric MS being multifocal at onset. Physical recovery in this form of disease is seen to be more complete despite relapse rates being higher.

Thus, MS can be considered as a disease existing within a spectrum ranging from relapsing ('inflammatory dominant') to progressive ('neurodegeneration dominant'), in keeping with the 2013 revisions to the clinical course of MS.[69]

1.4.3.1 Relapses

These are referred to as acute attacks, flare-ups or exacerbations, involving acute or sudden onset of focal neurological disturbances. Examples of typical MS relapses include blurred vision in one eye (optic neuritis), weakness of a body part (motor system relapse), persistent tingling or numbness of a body part (sensory system relapse), or loss of coordination (cerebellar system relapse).

Relapses are a characteristic feature of the RRMS subtype. Most patients demonstrate a recovery within six weeks, although improvements can take months for some. Recovery can comprise of a complete return to baseline, partial return or no improvement; with some degree of improvement being typical early in the disease. It is essential for deficits to persist for a minimum of 24 hours for it to be considered a relapse.

New abnormalities lasting for a few seconds to minutes, like paroxysmal attacks (stereotypic neurologic deficits lasting less than a minute, occurring multiple times a day) or (Lhermitte's sign (tingling sensation radiating down the neck, arms or back on neck flexion) are also considered as relapses in case they occur repeatedly over several weeks.[86]

Sequential relapses are considered discrete only in case they occur 30 days apart with a month of clinical stability in between. Clinical relapses are known to always change a patient's condition but don't always demonstrate changes on neurological examination. Greatest deficit in a relapse typically develops over a period of several days but can develop much faster over hours or minutes or gradually over weeks.

Factors such as pH, temperature or electrolyte balance can cause temporary disruption of nerve conduction resulting in neurologic abnormality. Hence, it is important to differentiate between relapse and pseudo-exacerbation, latter being a neurologic deterioration associated with a physiologic change like fever or infection. Deficits due to pseudo-exacerbation disappear after correction of the precipitating factor.

About 85% of MS patients begin with relapsing-remitting disease.[1] Relapses in MS can either involve a single neural system, as in optic neuritis, or several anatomically different systems, as in combined motor and sensory problems. The former is more likely and common in the first MS relapse.

Relapses involving sensory, visual or brainstem systems demonstrate a better prognosis as compared to those with the involvement of motor, cerebellar or sphincter systems. A low rate of relapse, in the first 2 years, accompanied with excellent recovery indicates a better prognosis as compared to a high relapse rate accompanied with poor recovery. With a disease duration of more than equal to five years, an increased rate of relapses, poly-regional relapses involving multiple systems and incomplete recovery from relapses signify a worse prognosis.[87]

1.4.3.2 Progression

Contradictory to the relapsing MS form, progressive MS is characterized by slow deterioration and increase in neurologic deficits. Once relapsing patients enter a progressive disease phase, they either discontinue with experiencing relapses or continue to experience exacerbations

superimposed on gradual worsening. Documenting a progressive course necessitates at least six months of observation. Slow deterioration is the principal defining feature of progressive MS, occurring independently of acute relapses without reflecting residual deficits from relapses.[86] Progressive MS is a more severe disease form as compared to benign or relapsing-remitting MS and, possesses a worse prognosis.[86]

1.5 MRI in MS

There has been growing involvement of MRI techniques in the evaluation of MS. The roles include initial evaluation of patients suspected of having the disease to secure or reject the diagnosis of MS[88,89]. It has also been used as a prognostic tool at first presentation of symptoms with extreme probability of acute inflammatory CNS demyelination, in provision of primary outcome measures for phase I/II clinical trials and as a source of critical supportive outcome measures in phase III trials of MS therapeutics.

The value of MRI in MS stems largely from its extreme sensitivity to alterations in regional proton relaxation times occurring with processes that bring about change in tissue water content and constraints on hydrogen molecule motion, specifically those linked to tissue-bound and free water molecules. However, the current MRI techniques and methodology continue to be insensitive towards the detection of underlying disease processes that lead to these alterations. As a result, there is a limit on the specificity of MRI signals and plentiful overinterpretations of imaging results to imply specific changes in histopathologic tissue alterations.

Many lesion patterns and distributions observed on conventional and even advanced MRI neither reflect a histopathology nor are disease specific. Therefore, a broad differential diagnosis persists in case MRI is considered isolated from the clinical history, laboratory investigations and physical and neurologic findings.

However, understanding the sequence of events associated with the formation of MRI-visible lesions, and the characteristic topography of lesions in the brainstem, cerebrum and spinal cord assist in the determination of the likelihood of MS in a patient and, provide reasonable markers that can be utilized for the inference of therapeutic effects on the developing underlying disease process.

Since the introduction of McDonald diagnostic criteria for MS in 2001 up till the 2017 revisions, they are based on the size, number and location of brain and spinal cord lesions believed to be typical of the disease.[90]

An update to the standardized approach of imaging MS patients that has been developed by the Consortium of MS Centers provides the minimum required sequence to support in the diagnosis and monitoring of MS that can be performed on variable clinical scanners. It involves 3D T1-weighted, 3D T2-weighted, 3D T2 FLAIR and post-single-dose gadolinium-enhanced T1-weighted imaging, all with a non-gapped section thickness of <=3mm, and a DWI sequence of <=5mm section thickness.

The breakdown of BBB can be detected by gadolinium contrast. It occurs with the development of new lesions and reactivation of old lesions. The enhancement has an average duration of 3 weeks for individual brain lesions,[91] with most enhancing for 2-6 weeks.

MS brain lesions rarely enhance persistently for more than 3 months with single-dose gadolinium. Mostly, all newly enhancing lesions will lead to residual T2 hyperintense lesion, following the resolution of the enhancement.[92] The detection of new or enlarging T2 lesions in comparison to a previous scan can indicate new inflammatory activity even in the absence of contrast enhancement.

Current conventional MRI techniques consist of several series of image acquisitions based on pulse sequences employed to provide optimal tissue

contrast for the purpose of routine clinical diagnostic work. These have continued to be the foundation for addressing disease activity in patients recruited in clinical trials.[88]

1.5.1 MS lesions

An MS lesion is defined as a focal hyperintense region on T2-weighted (T2, FLAIR or similar) or a proton-density (PD) sequence. The shape of characteristic MS lesions is round to ovoid ranging from a diameter of a few millimetres to more than one or two centimetres. In addition, the lesions should be a minimum of 3mm in their long axis to fulfill the diagnostic criteria; however, the topography should also be considered.

Lesions should be visible on at least two consecutive slices in order to exclude small hyperintensities or artefacts. However, in higher slice thickness acquisitions, smaller lesions may be detectable on a single slice.

MS lesions are typical of development in both hemispheres with mildly asymmetric distribution in initial stages. They might have an occurrence in any region of CNS, comparative to disorders causing WM lesions but have a tendency to occur in specific areas of WM, like the corpus callosum, periventricular and juxtacortical WM, infratentorial regions (specifically the pons and the cerebellum) and spinal cord (preferably the cervical segment).[90]

1.5.2 MRI techniques

Since the dawn of the MRI era, it was quite evident that due to its sensitivity in revealing focal WM abnormalities, it has the capability to become a valuable tool for the assessment of MS. This has been the case in the diagnostic workup of MS, while also playing a major role in the elucidation of mechanisms underlying disease progression as well as in the monitoring of accumulation of abnormal features underlying disability. For the

development of imaging strategies that can provide an accurate estimate of the extent of disease-related damage, considerable effort has been dedicated.

Guidelines have been established for the integration of magnetic resonance findings into diagnosis of patients presenting with CIS suggestive of MS,[70] and specific acquisition protocols have been put forward for the longitudinal monitoring of change in patients with clinically definite MS.[93]

Furthermore, regarding MS research, conventional MRI has been substantially enhanced by quantitative MR techniques that demonstrate greater sensitivity and specificity for the assessment of heterogeneous pathological substrates of the disease. This is not only in context of focal T2-visible lesions but also in normal appearing WM (NAWM) as well as GM.

More recently, novel imaging techniques that are capable of gauging pathological processes in relation with the disease which had been neglected previously (eg iron deposition and perfusion abnormalities) and the advent of high and ultra-high field magnets have facilitated the provision of further understanding of the pathobiological features of MS.[94]

1.5.2.1 MRI as a diagnostic tool in MS

Various MRI platforms with different magnetic field strengths are utilized at present for diagnosing MS, and the most frequently applied magnet strengths are 1.5 Tesla (1.5T) or 3T. 3T magnetic strength has been shown to have increased sensitivity for detecting MS lesions due to improved signal-to-noise ratio and resolution;[95] however, utilization of 3T MRI as compared to 1.5T MRI has not been demonstrated to facilitate early MS diagnosis.[96] Still, 3T MRI is considered preferable in the current MAGNIMS criteria, with inclusion of both field strengths in the recommendations.[97,98]

Inspite of the significant improvements in the most recent changes made to the McDonald criteria, a few aspects have elicited criticism. Relevantly, simplification of the criteria has led to it being less restrictive, that might further lead to an overdiagnosis of MS.[98,99] Additionally, collection and interpretation of CSF is not required in accordance with the most recent guidelines. Therefore, prudence is needed when McDonald criteria are employed for differentiation of MS from other potential CNS pathologies; however, in case of uncertain presentations, CSF samples might increase diagnostic specificity.

Susceptibility-weighted imaging (SWI) has been suggested to be a sequence for better diagnostic values. SWI at 7T has demonstrated remarkable detection of central veins.[100,101] According to the literature, periventricular inflammatory lesions can be depicted with diagnostic accuracy, by using FLAIR in combination with T2* at 3T. After validation, this presents to be a highly useful tool in clinic for differentiation between MS and other WM pathology.[102] Such novel measures have the capability to facilitate the differential diagnosis of MS and support the representation of demyelinating lesions associated with MS.

Generally, the use of MRI has become a well-established tool for diagnostic purposes and facilitates the early diagnosis of MS. This offers the opportunity to initiate immune-modulatory treatment as soon as possible. Yet different pathologies need to be assessed with prudence and excluded before a patient is committed to long-term treatment. In summary, the McDonald criteria have a high sensitivity but are not as specific for the MS diagnosis and vigilance is still required when confirming MS.[103]

1.5.2.2 MRI as a prognostic tool in MS

An important role is played by MR imaging for the prognosis of disease development and monitoring of disease progression. Multiple studies have focused specifically on the predictive value of T2-hyperintense lesions, T1-hypointense lesions, referred to as black holes (BH), along with implication of overall atrophy observed on MRI with the progression of disease. These individual modalities have been employed for predicting the development of MS from CIS, RIS and for the general prediction of long-term disability.[103]

1.5.2.3 Lesion Evolution

On conventional MRI, new lesions arising in earlier NAWM are almost always distinguished by a nodular area of Gd-enhancement on T1-weighted images.[104] This is nearly customarily associated with a hyperintense lesion in the same location on T2-weighted images.[105] Approximately 65% of the larger enhancements correspond to hypointense lesions observed on non-contrast T1 MRI[106]. Most enhancements fade away over a period of 4-6 weeks, and 50% of the hypointensities experience spontaneous resolution within 4 weeks. Return to the T1-isointense state or mild T1 hypointensity might be an indication of extensive or partial remyelination.[107]

Hypothetically more aggressive lesions have a ring-like propagation of enhancement over a few weeks or longer before the enhancement begins to fade, have a central spherical hypointensity on T1-weighted images, have more complicated appearances on T2-weighted images and are persistent over time. An incomplete enhancement ring (“open ring sign”), open where the lesion abuts GM, characterizes MS.[108] There can be an observation of a complete ring specifically in case lesions are confined to WM. Vigilant inspection of regions around some of the larger T1-hypointense lesions

contracting over time signifies this apparent repair to be at the expense of surrounding tissue loss. Along with the center of such lesions likely undergoing gliosis and contraction, there is occurrence of regional ventricular enlargement and loss of cortical volume directed toward the lesion.

Even though T1-hypointense lesion evolution has profound link with enhancements, the relationship might be more complex. Frequency of enhancement is age-dependent, being lesser among older MS patients of all disease subtypes.[109] Still, hypointense lesions are more commonly observed in case of longer disease duration and among progressive disease subtypes. The conflicting behaviour of these apparently inter-related MRI metrics might suggest that whereas some hypointense lesions result directly from new inflammatory events that are readily monitored by enhancements on MRI, other hypointense lesions may evolve in a different way.

With regards to advanced imaging, monitoring of lesion evolution is more complex. Newly-enhanced lesions that occur within previously conventional MRI-defined NAWM provide informative regions for retrospective scrutiny for change that occurs before lesion evolution on conventional MRI. Retrospective analyses suggest that regional abnormalities in magnetization transfer imaging (MTR) develop in NAWM months before the enhancement is visible on conventional MRI.[110] However, these changes unfortunately have not shown enough robustness for prospective use.

MRI findings, as an outcome measure, are used by most clinical trials for the investigation of treatment efficacy. Number and size of T2-hyperintense lesions and contrast-enhanced T1-weighted lesions are focused on. The effect of treatment on lesion burden was evaluated in treatment studies by a recently conducted meta-analysis of various trials. It demonstrated that treatment effects on MRI lesions over short time periods (6-9 months) also

have the ability to predict relapses over longer periods of follow-up.[111] The overall analysis of these 31 studies showed that there is association between new or enlarging T2-hyperintense lesions and contrast-enhanced T1-hypointense lesions and, number of relapses. Thus, the use of MRI was proposed as a primary endpoint for treatment trials.

MRI has been employed in many observational studies for identification of patients at high risk for treatment failure as determined by clinical disease progression.

Three or more new T2 lesions or new enhanced lesions within the first 2 years foretold worse disease progression, and follow-up after 15 years provided confirmation of these findings.[112] In the presence of more effective therapeutic options, achievement of multi-metric disease stability or 'no evidence of disease activity' (NEDA) has been emphasized. The definition of NEDA has basis in the absence of new disease activity on MRI and, in the absence of relapses and disability. It has been used for the assessment of positive treatment response for RRMS patients after 2 years.[113] The original criteria are now referred to as NEDA3, given the latest proposed expansion to NEDA4, involving brain atrophy and suggested to be an improved metric for disease stability.[114] It needs to be considered that NEDA is a developing measure and, there are contradictory studies concerning the prognostic potential of NEDA for the purpose of long-term disease stability.[115] Nevertheless, the availability of new treatment modalities offers a more aggressive 'treatment to target' approach and might provide a prospect to achieve NEDA. The existence of new activity on MRI is a crucial marker for the clinical setting, which can be inferred as a suboptimal treatment response and a change of treatment needs to be considered on a case-by-case basis. There is unavailability of guidelines regarding the timing of obtaining MR images for best objective assessment.

In RRMS patients on DMT with long disease durations, who are clinically and radiographically stable or patients with longstanding progressive MS, further imaging should be customized according to individual circumstances. In addition, younger patients with progressive disease should undergo MR imaging frequently. There might be occurrence of new lesions in patients with progressive MS and adjusting therapy can be considered. Patients with untreated CIS should be scanned every 1–3 months for the initial 6 months and, in case stable repeating MRIs every 6–12 months is recommended, if possible, unless there is occurrence of new clinical symptoms. Largely, these imaging recommendations permit close monitoring in order to assess disease activity and treatment response for the achievement of NEDA.[103]

1.6 Gray Matter Pathology in MS

1.6.1 Gray Matter Pathology and Diagnosis of MS

There has been clear demonstration of cortical lesions occurring in all MS phenotypes through neuroimaging studies[116], not only in the late disease stages but also early on. Indeed, cortical lesions have been visualized prior to the development of WM lesions[117], as well as in radiologically isolated syndrome (RIS)[118] and CIS[116]. As with cortical demyelination, GM atrophy can be detected very early in the disease and accelerates over time[119].

Similar to cortical lesions, GM atrophy measures are apparently predictive; Calabrese and colleagues[120] showed that in comparison to CIS patients meeting the DIS criteria, CIS patients and atrophy of either the superior frontal gyrus, cerebellum or thalamus had double the risk of conversion to clinically definite MS. However, it should be kept in mind that the predictive power of GM atrophy may be less than GM lesions in CIS.

1.6.2 Gray Matter Atrophy in MS

In addition to the well-known local inflammatory and demyelinating lesions that are routinely observed in the WM, MS is also associated with degeneration and consequent GM volume loss that is often referred to as GM atrophy.

Brain GM atrophy is typically measured in vivo using standard 3D T1-weighted images acquired by MRI, and automated analysis methods. Previous studies have demonstrated decreased volume of subcortical GM structures as well as reduced volume or thickness of cortical regions[121].

1.6.3 Evolution of GM atrophy

It is not very clear which particular brain regions are most likely to develop GM atrophy in the early phase of the disease, whether the atrophic process is primary or secondary, or to what extent its evolution is distinct between disease types[122–124].

Partially, this can arise from methodological issues, like unknown sensitivities of different measurement methods to atrophy in different GM regions. The simultaneous evolution of focal lesions and other pathological changes, along with the varying and partly unknown effects of different treatments on GM atrophy, further obfuscate the understanding of natural evolution of GM in MS.

In relapse-onset MS, GM atrophy has been observed already in the earliest phases of the disease[122,125]. Moreover, there might be a difference in GM atrophy between the disease types[123,126], as well as between patients with and without evidence of disease activity[127]. Scientific literature has some evidence of early and articulate GM atrophy in specific regions: for example, the involvement of the cingulate cortex was found to occur throughout the

disease course, in PPMS[128]. Also, significant GM volume loss occurred in the right precuneus in RRMS patients with progressive disability[129]. Moreover, atrophy of specific DGM structures, specifically the thalamus, also occurs in MS patients[151–153]. Atrophy of the thalamus apparently occurs early and prominently, worse in men, and has an association with cognitive decline[132]. However, it remains unclear as to what extent these observations could be biased by the size and partially limited contrast with the neighboring WM of the thalamus. In general, more research is required for the validation of the dynamic alterations and anatomical patterns observed in previous studies.[133]

1.7.4 Brain atrophy and the risk of disease progression

Brain atrophy is detected in early disease stages, even in stages without clinical symptoms.[134,135] The rate of brain atrophy is greater in CIS patients that progresses to MS when compared with patients who show no worsening over the disease course. This has an impact on the early prognosis of the disease[136].

A sub-analysis from the ETOMS study (which dealt with the assessment of the efficacy of subcutaneous interferon beta 1-a in CIS patients) demonstrated a significant difference in mean annual percentage brain volume change (PBVC) between patients who had disease progression versus those who did not [137].

An observational study performed by Pérez-Miralles et al.[138] reported similar findings showing a greater decrease of PBVC in 176 CIS patients who progressed to MS when compared to those who did not progress.

These findings established a prognostic role for brain atrophy and conversion to MS in patients who had first demyelinating event.

The study by Di Filippo et al.[139] demonstrated the prognostic role of brain atrophy and the risk of progression to MS following a first clinical event. In the concerned studies, the CIS patients that progressed to MS during a follow-up of 6 years had an atrophy rate of 0.5% vs -0.2% of those who did not; thereby producing this as an important prognostic factor for conversion to MS.

Steenwijk and colleagues[140] performed a study looking particularly at cortical atrophy in patients with long-standing MS, that suggested largely non-random patterns. A commonly held view of MS, previously, involved a multifocal and multi-phasic immune-mediated WM inflammatory demyelinating disorder. Indeed, the suppression of such a process has reinforced the progress in DMT till date. It is now quite clear that demyelinating lesions are possibly as extensive in GM as they are in WM, and there is substantial neuro-axonal loss in NAWM, WM lesions, cortical GM and deep GM. It is also unambiguous that GM pathology is present in early RRMS that increases with time.

Brain tissue loss does not have a uniform occurrence; in progressive MS, it is most apparent in the GM, having an effect on some cortical and DGM regions more than others[122–124]. In vivo, significant associations of GM atrophy with physical disability, cognitive impairment and progressive MS have been identified by MRI-clinical correlation studies. There are compelling reasons to make an attempt in order to better understand the GM atrophy mechanisms and the further reflected neurodegenerative process.

Steenwijk and coworkers[140] reported on their work observing patterns of cortical GM atrophy in MS. The authors employed source-based morphometry (SBM), an evolved voxel-based morphometry (VBM) approach. Both SBM as well as VBM support the identification of regional

disease effects on MRI scans without the need for a priori-defined regions of interest.

Furthermore, VBM looks for regions consistently different between groups and, SBM looks for regions where MRI features tend to differ together, further determining how they are weighed in different groups. Practically, this further means that SBM might have greater sensitivity towards distributed but connected regional disease effects, as occurs in case of a damaged brain network.

In consistency with previous VBM studies, the SBM analysis confirms that GM atrophy does not have an even occurrence throughout the cortex. However, it also shows that underlying this are overlapping regional 'patterns' of non-random cortical atrophy. Steenwijk et al. hypothesize that these patterns of atrophy are initiated by the tract-mediated effects of WM lesions on cortical 'hubs' (i.e. cortical regions that are located centrally in structural networks), with subsequent network-mediated (trans-synaptic) degeneration further extending from these hubs.

The literature supports such a network-based interpretation[141], but does not necessarily exclude alternative explanations.

Steenwijk and colleagues[140] have discovered an essential new feature of cortical GM atrophy in MS; that it not only occurs in some cortical regions more than others but also that regions of predilection can be linked in a non-random way. These findings could have several explanations, and their elucidation would be worthwhile provided the clinical importance of GM atrophy in MS, and the potential to discover novel mechanisms for rationally based therapies aiming to prevent this striking neurodegenerative aspect of MS.

1.7.5 Review of measurement techniques

There has been development of various methods for the measurement of anatomical changes in the brain. Some of the measurement techniques produce single-subject measurements while others, such as VBM, provide statistical tests that are group-based.

In this section, the predominant interest is the application of brain GM atrophy measures between two different groups of MS patients from the WIRMS clinical trial[142] (HW and Placebo). This VBM analysis involves the measurement of GM density in a priori ROI derived from the coordinate-based meta-analysis[143] results.

1.7.6 Group-level analysis methods

VBM is an extension of voxel-wise segmentation-based techniques such as SIENAX or SPM, that comprise of the transformation of GM segmentation maps into a common space. One can then continue with the investigation of differences between groups and correlations with other variables for each voxel or vertex in the common space separately (followed by appropriate corrections for multiple testing).

The key strength of such methods is that they allow the study of anatomical patterns undergoing atrophy without any a priori selection of ROIs. Prominent regions and anatomical patterns can, therefore, be detected from the data.

The statistical method employed in brain morphometric analyses is the general linear model (GLM). This is utilized due to its ability to incorporate a multitude of effects.[144]

1.7.6.1 General Linear Model

The General Linear Model (GLM) arises from regression and correlational methods and can be construed as a general multiple regression model.
The GLM has been successfully used in the analysis of brain structures because of its flexibility to handle both categorical (e.g. groups of subjects), and continuous variables (e.g. test scores). It can be used to examine regions of interest (ROI) from which various morphometric markers can be extracted, but it has been most successful in whole brain analysis using a voxel based approach for GM.
The GLM is employed for modelling and statistical hypothesis testing in almost all areas of neuroimaging. This is due to its great flexibility - it can be used to analyze within-subject as well as between-subject data.

1.7.6.1.1 Linear Modelling

Regarding its foundation, the GLM is a way to model an observed signal in terms of one or more explanatory variables, also known as regressors. Signal here could direct towards the series of measurements associated with individuals in a group, e.g., the cortical thickness in different patients at a given anatomical location. The GLM makes an attempt for the explanation of this series of measurements in terms of one or more regressors (also called explanatory variables), which consist of series of values that represent patterns that are expected to be found in the measured signal.

The GLM is fundamentally a linear model, which means that it has the ability to scale the regressors and add them together in order to best explain the data. Many GLMs involve more complex relationships with time or subject ID. The linearity depends on how the regressors can be combined together to explain the data.

The simplest GLM is the one modelled with a single regressor; here the model only contains one parameter that is fit, which is the scaling value for this regressor; this scaling is β. This has a close relation to Pearson's correlation, as correlation provides one way for measuring the similarity of two signals (the regressor and the data in this case) whereas the GLM models how well one signal (the regressor) can fit another (the data).

To determine the best value of the scaling parameter, the GLM examines the difference between the data and the scaled regressor (the fitted model). This difference is known as the residual error, or more concisely just as the residuals.

In equation form, the GLM can be expressed as:

$Y = X \beta + \varepsilon$, where Y represents the data, X represents the regressor, β represents the scaling parameter and ε represents the residual errors.

In the case of working with neuroimaging data, there would be a separate GLM for each location in an image - that is, for a particular voxel location there is extraction of one value from each subject and, analysis of these values is performed in one GLM. This is then repeated for every voxel location, running a separate GLM, but (typically) using the same regressors for all these GLMs as it is the dependent variable that changes.

Altering the scaling parameter will change the model fit and hence the residuals, and the best fit is the one that corresponds to the smallest residual9s (quantified by the sum of squared values). This is known as minimising the residuals (or finding the least squared error) and can be performed using the GLM. The fitted or estimated parameter value is often denoted as $\hat{B}$ and represents a value that is estimated or calculated from the noisy data. This is in contrast to β (without the hat), which usually represents an ideal or theoretical value.

When using the GLM it is not only the β value that we are often interested in, but also the uncertainty surrounding its estimation: we need to know both in order to perform any statistical testing. The uncertainty in the value of any given $\hat{B}$ is affected by the noise (i.e., the size of the residuals) but also, in

the case of multiple regressors, by whether there is a correlation between individual regressors.[145]

1.8 Focus of interest

In this study, we examine the new disease activity by means of alterations in WM lesions for patients recruited in the WIRMS clinical trial, as can be seen in chapter 3. Further, as can be seen in chapter 4, we conducted coordinate-based meta-analysis, meta-analysis of networks, and meta-regression to summarize the evidence from VBM of regional GM changes in patients with MS and CIS, and whether these measured changes are relatable to clinical features. The eight significant clusters, that were the result of the meta-analysis, were used as ROI for VBM to analyze GM atrophy in placebo versus hookworm-treated patients, in the change from the initial visit to final visit (chapter 5). This is followed by the general discussion and conclusions (chapter 6) and future directions (chapter 7).

Chapter 2

Methods

This chapter mentions the methods used in the included research.

2.1 WIRMS

2.1.1 Cohort

The cohort in the WIRMS study involved adults with relapsing MS.

2.1.2 MRI acquisition

Acquired images were: 3D axial T1 weighted fast spoiled gradient echo (1×1×1mm isotropic, 256×256×156 matrix), post gadolinium (Gadovist, standard dose; Gd) acquisition of axial T2 weighted fast spin echo, and axial T2 weighted fluid attenuated inversion recovery images (0.98×0.98×3mm, matrix 256×256×60) which achieved about 13 minutes' delay between Gd injection and post Gd axial T1 weighted spin echo.

2.1.3. Reproducibility Analysis

Bland-Altman plot is constructed to describe agreement between two quantitative measurements by constructing limits of agreement. These statistical limits are calculated by using the mean and the standard deviation (*s*) of the differences between two measurements. The graph is a scatter plot XY, where the Y-axis shows the difference between the two paired measurements (A-B) and the X-axis represents the average of these measures ((A+B)/2).

For the purpose of assessing the reproducibility of the MRI outcomes two people independently measured: (i) newly enhancing T1 lesions and (ii)

sum of new and enlarging T2-weighted lesions. Bland Altman analysis was then performed. The Bland and Altman analysis is a way to evaluate a bias between the mean differences, and to estimate an agreement interval, within which 95% of the differences of the second method, compared to the first one, fall.[146]

2.1.4 T2 lesion load at baseline

The total number of T2/FLAIR lesions were counted on the initial MRI (**Figure 2A**) for all patients. This was done to analyze, after the unblinding, whether the 2 arms were matched for T2-weighted lesions at baseline and to check that the patients were not atypical.

2.1.5 Contrast-enhancing lesions

The number of contrast (gadolinium) enhancing lesions were observed on T1 contrast-enhancing MRI for each patient at all visits (**Figure 2B**). This was done to analyze whether the 2 arms were matched for contrast-enhancing lesions at baseline.

2.1.6 Newly enhancing T1 lesions

Newly enhancing old lesion has been characterized as a lesion that is contrast-enhancing on a visit and was visible on the previous visit but was not contrast-enhancing (**Figure 2 C, D, E**). The number of newly enhancing lesions on T1-weighted MRI have been counted on all visits.

T1-weighted contrast-enhancing images were acquired post-Gadolinium and for image analysis they were registered to the equivalent image from the previous visit. The images were investigated for each MR slice and the two MR images automatically swapped periodically to highlight (newly enhancing lesions appear to ‘flash’ as images are swapped) newly enhancing lesions on the following visit, which were observed and counted.

The number of newly enhancing lesions on T1-weighted MRI were counted on all visits.

The non-enhancing T1 lesions always have corresponding hyperintense lesions on FLAIR/T2. Newly enhancing lesions are characterized as those already visible on FLAIR in the previous visit MRI and are newly enhancing on T1 Gd+ MRI. Therefore, if we consider a patient, an 'old newly enhancing lesion' must: not have been enhancing on T1 but should have been visible on the Flair/T2 at the previous visit.

2.1.7 New T2 lesions

The number of new lesions on FLAIR has been counted comparing initial with final MRI, following rigid registration, for all patients. T2 spin echo images were registered using rigid registration and visualized slice by slice with automated switching between the 2 images. This efficiently highlighted new and enlarging lesions for observation.

A new lesion has been characterized as the one visible on the final MRI and not on first MRI. Lesions that were simultaneously new/enlarged and enhancing were only counted/considered once. T2 spin-echo or FLAIR images were registered using rigid registration and visualized slice by slice accompanied with automated switching between the 2 images. This enabled efficient emphasis of new and enlarging lesions. (**Figure 3A, B**).

2.1.8 Enlarging T2 lesions

The enlarging lesions on FLAIR were counted comparing the initial MRI with final MRI. The lesions on first MRI were marked as Regions of Interest (ROIs) and an enlarging lesion was characterized as the one that had expanded out of the ROI outline (**Figure 4A, B**).

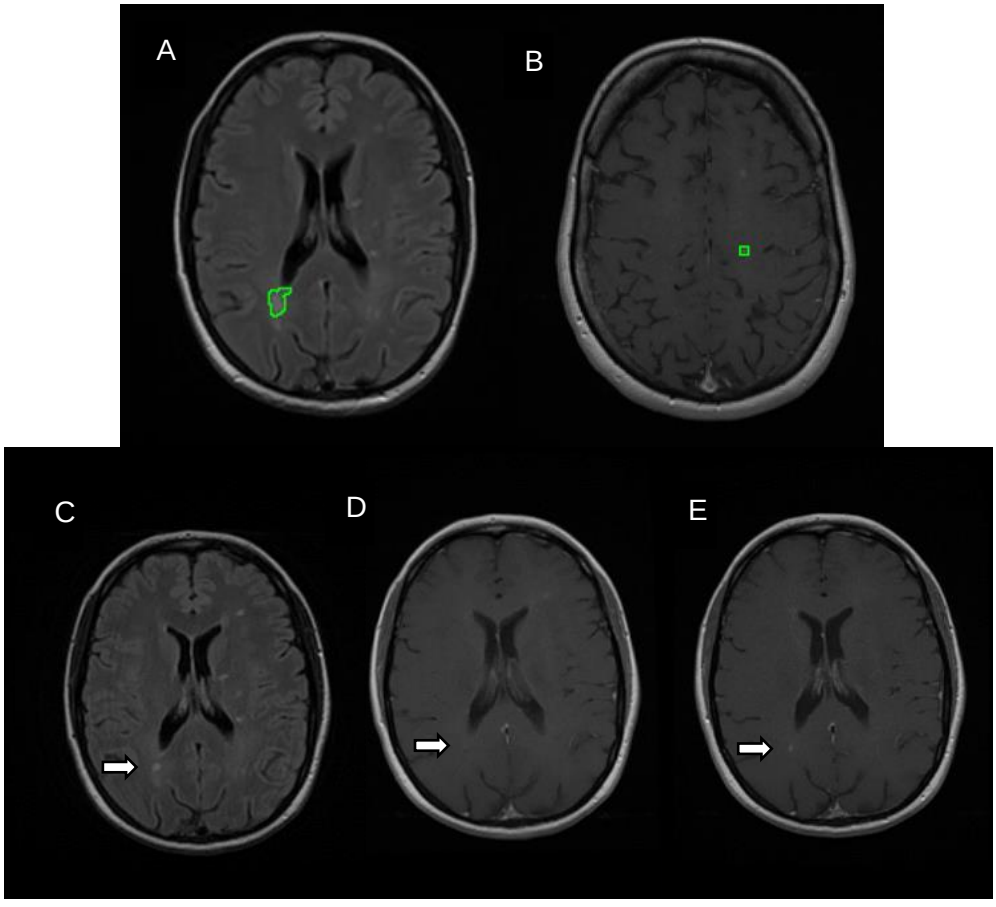
A
B
C
D
E

Figure 2: (A) Demonstration of lesion (marked with ROI) on FLAIR; (B) Demonstration of contrast-enhancing lesion (marked with ROI) on T1-weighted Gd+ MRI (C) patient xx V9 FLAIR MRI (marked with arrow) (D) patient xx V9 T1 (marked with arrow). (E) patient xx V10 T1 (marked with arrow).

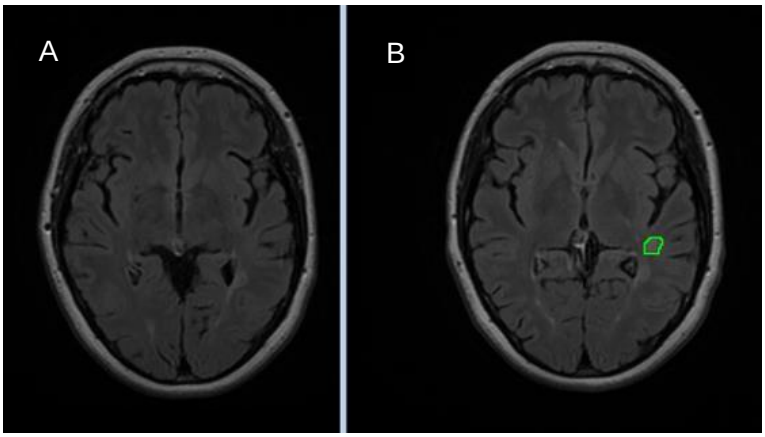

Figure 3: (A) initial FLAIR MR image (B) Demonstration of new T2 lesion (ROI) on final FLAIR MR image; time interval of 6 months between the two scans.

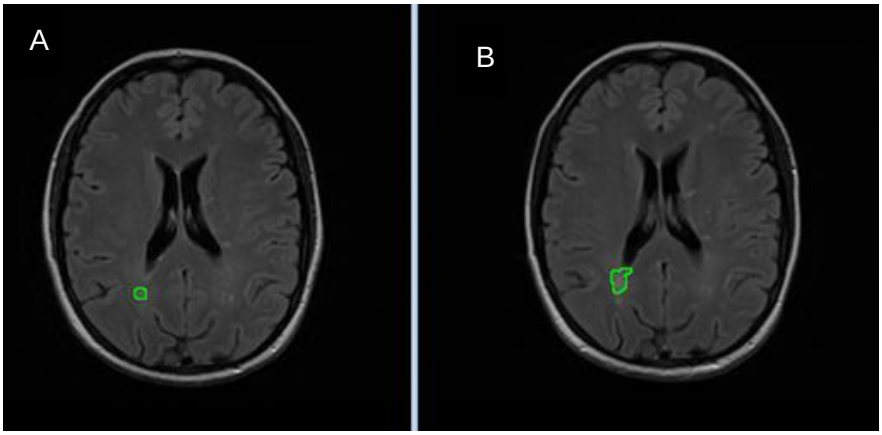

Figure 4: (A) Demonstration of enlarging T2 lesion (ROI) on initial FLAIR image (B) Demonstration of enlarging T2 lesion (ROI) on final FLAIR image

2.1.7 Total lesion volume (TLV)

Total lesion volumes were calculated using software NeuROI (https://www.nottingham.ac.uk/research/groups/clinicalneurology/neuroi.aspx).

2.2 Coordinate based random effect size meta-analysis

All CBRES and CBMAN analyses are performed using NeuRoi (https://www.nottingham.ac.uk/research/groups/clinicalneurology/neuroi.aspx), which is available to use freely. Details about the algorithms incorporated into CBRES and CBMAN are presented in [147,148]. In both algorithms a clustering algorithm[149] is used to determine where the coordinates reported by multiple independent studies are spatially concordant (clustered). Once clusters are formed, the reported Z scores are converted to standardised effect sizes by dividing by the square root of the number of subjects. In CBRES, a random effect meta-analysis of these

effect sizes is performed in each cluster. In CBMAN, the test statistic is the correlation of standardised effect sizes performed pairwise between clusters. Where a study does not report a coordinate within a cluster, or where no effect sizes are reported by a study, the contribution to the cluster is estimated using the study censoring threshold. The significant results of the CBRES meta-analysis are clusters of reported coordinates where the estimated effect size is statistically different to zero after controlling the false cluster discovery rate (FCDR), a type 1 error control method based on the false discovery rate (FDR)[150]. The expected proportion of clusters incorrectly declared significant is controlled at 5% by default. Clusters indicate both spatial and effect size concordance across studies, which is an unlikely chance event suggesting that atrophy at the location of the clusters is a general feature of MS.

Significant results reported by CBMAN are clusters where standardised reported statistical effects are correlated between clusters. This indicates a significant pattern of reported effect that is represented as a network of nodes (clusters) and edges (correlations). The FDR is used to control type 1 error rate of the effect size correlations. The clusters analysed by CBMAN and CBRES are identical, since the same clustering algorithm is employed, but the results may differ due to the different hypotheses tested.

A feature of both CBRES and CBMAN is that the results declared significant are reported as a functionof the FDR. Any that just miss the threshold for significance can therefore be explored. Analysis can also be performed on subgroups of studies. This estimates a subgroup-specific effect size in each of the clusters found significant during the full analysis (using all studies); this is useful since clusters may not be significant if the subgroup is small, yet the effect size might be of interest. Furthermore, the use of standardised effect sizes makes meta-regression possible by looking for significant correlation between a specified covariate and the standardised effect size in each cluster.

2.3 Voxel Based Morphometry

FSL's standard VBM processing pipeline was adopted, and the processing steps have been briefly described below. The basic VBM protocol, defined in[151] consists of five steps: 1. Template creation 2. Spatial normalisation 3. Segmentation 4. Smoothing 5. Statistical Analysis.

Using the FSL 5.01 tools[152] on Centos 7 operating system, brain extraction was performed on all individual 3D T1-weighted images using BET[153]. Following this, tissue-type segmentation was carried out using FASTv4.1[154]. FAST does not use prior information for determining the different tissue classes, instead it applies a hidden Markov random field model with the Expectation Maximization algorithm to associate each intensity value from the anatomical image with a specific mixture of GM, WM and CSF probabilities. The resulting GM probability images were normalized to ICBM152 standard space by using the standard FSL template and the affine registration tool FLIRT[155,156], followed by nonlinear registration executed by FNIRT[157]. The resulting images were flipped and averaged to create a symmetric, study-specific template. In a second iteration, the native GM probability maps were non-linearly re-registered to the customized template.

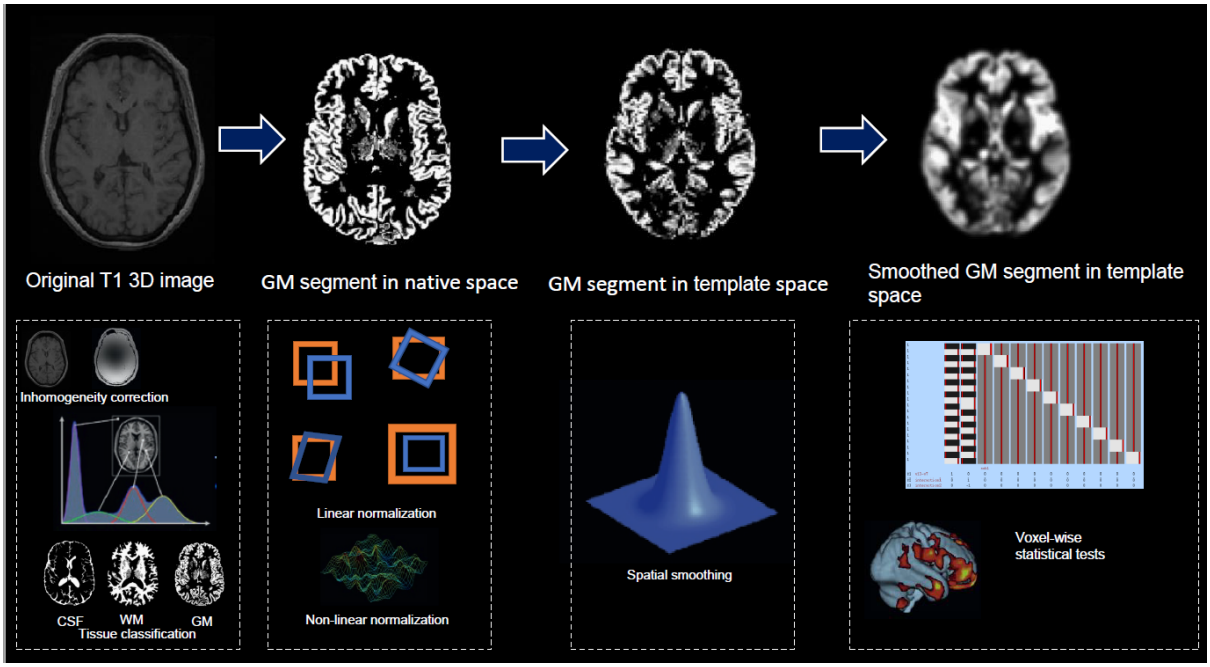

Figure 1: Workflow of a VBM analysis. The analysis is based on 3D structural brain images. First, the T1-weighted 3D images undergo correction for inhomogeneities followed by classification into different tissue types. The gray matter segment (i.e., the tissue of interest) is spatially normalized to match a study-specific template. Subsequently, the normalized gray matter segment is smoothed with an isotropic Gaussian kernel. Finally, the smoothed normalized gray matter segments are entered into a statistical model for conduction of voxel-wise statistical tests and mapping of statistically significant effects.

Chapter 3

Imaging analysis for hookworm treatment in RRMS

Abstract

IMPORTANCE Studies suggest gut worms induce immune responses that can protect against multiple sclerosis (MS). To our knowledge, there are no controlled treatment trials with helminth in MS.

PURPOSE To determine whether hookworm treatment has effects on MRI activity and T regulatory cells in relapsing MS.

DESIGN, SETTING, AND PARTICIPANTS This 9-month double-blind, randomized, placebo-controlled trial was conducted on relapsing MS patients without disease-modifying treatment.

INTERVENTIONS Patients were randomized (1:1) to receive either 25 *Necator americanus* larvae transcutaneously or placebo. The MRI scans were performed monthly during months 3 to 9.

MAIN OUTCOMES AND MEASURES The primary end point was the cumulative number of new/enlarging T2/new enhancing T1 lesions at month 9.

RESULTS The median cumulative numbers of new/enlarging/enhancing lesions were not significantly different between the groups by preplanned

Mann-Whitney *U* tests, which lose power with tied data (high number of zero activity MRIs in the hookworm group.

3.1 Worms as therapeutics

MS has been considered as a Th1-Th17-mediated inflammatory auto-immune response that is an organ-specific inflammatory autoimmune disorder[158,159].

Helminth parasites potently manipulate the regulatory T cells in the host. A numerical expansion in both natural and induced regulatory T-cells (T regs) is accompanied by qualitative changes to activation markers and increased suppressive function. These T regs suppress excessive inflammation caused by autoimmunity.

Different groups have made an attempt to identify and utilize the protective effect of helminth-derived single components for the modulation of immune response in autoimmune diseases, in recent animal studies[160].

3.2 Helminths in MS clinical trials

Recommendations for clinical trials of helminth therapy in autoimmunity have been published recently.[161] Trichuris suis and Necator (N.) americanus are the helminth species employed in clinical trials of helminth therapy in MS. They are selected due to their safety profiles with regards to controlled infection.

N. americanus is a gastrointestinal pathogen infecting over 500 million people. It is encountered only in humans making it a ‘family heritage’ and an evolutionary ‘old friend’ that has accompanied humans during historical migration[162]. N. americanus infection is generally benign following the establishment of adult worms in the gut.[162–164]. There is a possibility of

gastrointestinal symptoms due to acute infection but dose-ranging studies have demonstrated that light infection is asymptomatic[165,166].

A successful parasite-host relationship thrives on commensalism, where the parasite causes little-to-no overt damage to its host, and approaches mutualism, that consists of derivation of some benefits for the host, from the parasite[164,167,168]. This helminth satisfies this profile due to its possible benefits in treating MS or other chronic inflammatory diseases[168].

There has been evaluation of the safety and therapeutic validity for various inflammatory diseases where low dose of *N. americanus* infection has been demonstrated to be safe as well as tolerable[163,167,169,170].

Clinical trials of helminth therapy in MS have recently been reviewed[171].

HINT (Helminth-induced immunomodulation therapy) study- This study was conducted by Fleming and colleagues at the University of Wisconsin, USA. In the first part of this trial (HINT 1), Trichuris suis ova (TSO) was administered orally every 2 weeks for 3 months to treat five RRMS subjects. MRI of brain was performed at baseline, monthly for 3 months and at 2 months after the end of treatment with TSO.

Results: The mean number of new active brain lesions was 6.6 at baseline, 5.8 at 2 months post-treatment and 2.0 after 3 months of treatment.

It was noted by the authors that the encouraging MRI results require prudent interpretation due to the small number of subjects and the short observation period[172].

The study reported no adverse clinical effects in the subjects.

HINT (Helminth-induced immunomodulation therapy) 2 study- *This was a follow-up exploratory clinical trial.* It had a baseline versus treatment design and, involved 15 RRMS patients naïve to treatment[172]. The recruited patients underwent 5 months of pre-treatment observation followed by 10

months of treatment with Trichuris suis ova (administered orally every 2 weeks).

The primary outcome measures involved safety and tolerability of Trichuris suis ova and changes in the number of contrast-enhancing lesions as observed during monthly brain MRI scans with gadolinium contrast[44]. No significant safety and tolerability issues were observed. The study reported no serious side effects or adverse events associated with the treatment. The cohort showed 35% reduction in active lesions when observation MRIs were compared to treatment MRIs. There was an association observed between TSO and elevation in Treg cells as well as modification in Th2 immune response, according to the immunological tests. The modest reduction observed in contrast-enhancing lesions during the treatment course suggested the requirement of further investigation of TSO for the assessment of its effectiveness in RRMS[173].

Pilot study for SPMS- A study of helminth therapy in SPMS was conducted by Benzel and colleagues at the Charite University, Berlin, Germany[174]. The study recruited four SPMS subjects and, consisted of 6 months of treatment with 2,500 TSO that were administered orally every 2 weeks. The patients were observed to be clinically stable during the study, and treatment was well tolerated[174].

Rosche and colleagues[175] have started work on a phase II study with an aim to recruit 50 RRMS patients who will be administered either TSO or placebo for a period of 12 months (Trichuris suis ova in relapsing-remitting multiple sclerosis (TRIOMS) and clinically isolated syndrome).

Comparing HINT2 and TRIOMS, the latter included fifty RRMS or CIS patients with clinical activity as well as not undergoing any standard therapies. The patients were randomized to obtain Trichuris suis ova every 2 weeks or placebo. The authors aimed to assess the safety, tolerability and influence on disease activity, along with the in vivo mechanisms of action of

the helminth ova by means of laboratory, neurological, immunological exams and MRI over a period of 12 months followed by a follow-up of 6 months. However, the results for this study have not been posted yet.

TRIMS A was an open label, MRI assessor-blinded study, involving 10 RRMS patients. The patients were treated with TSO orally for a period of 3 months. Six out of ten patients were concomitantly administered β-interferon. MRI was done every 3 weeks. It was concluded by the investigators that TSO was well tolerated and safe but none of the clinical, immunological or MRI signals observed indicated a benefit[176].

The trial was designed to test safety instead of drug effectiveness. In addition, the association of disease-modifying therapies in more than half of the recruited patients, the brief follow-up and the small patient sample do not allow any conclusions to be drawn from this study with regards to effectiveness of helminth therapy.

WIRMS[142] was the first phase II randomised double-blinded placebo-controlled of treatment with hookworms in relapsing MS that had been held at the University of Nottingham (Worms for Immune Regulation of MS (WIRMS))[177]. The trial recruited 72 RRMS patients for treatment with dermally administered hookworm (Necator americanus) larvae or placebo.

The primary endpoint consisted of cumulative number of new or enlarging contrast-enhancing lesions at 9 months following intervention. In addition, several immunological parameters reflecting expression and activity of Tregs as well as Th2 shift were secondary and exploratory outcome measures. MRI scans were conducted monthly. Safety analysis in between the administration and deworming as per January 2015 advocated good tolerability and safety of this treatment.

Pilot MS studies with helminths have demonstrated a very decent safety profile, along with encouraging effects on clinical, radiological and

immunological outcomes. Phase II study results are essential for confirming the favorable indications hinted by epidemiological, preclinical and observational along with pilot therapeutic studies concerning effectiveness of helminth therapies in MS[171].

WIRMS clinical trial: MRI analysis

3.3 Study introduction

The purpose of this study was to determine whether infection, that is controlled with a clinically safe number of hookworm larvae, demonstrated protection towards reducing MRI activity in relapsing MS and lead to the induction of immunoregulatory mechanisms that suppress the overactive immune system.

The worms for immune regulation in MS (WIRMS) study[142] proposed to be the first controlled parasite exposure study in 36 patients with relapsing remitting MS (RRMS) with 25 hookworm larvae versus 36 patients with placebo (water). Sample size calculation for this study was based on Tubridy et al.[178] for frequent gadolinium MRI (primary end point); that itself reported MRI disease activity in 80% of the study population. Assuming new lesion distribution similar to that study, using the Mann-Whitney U test to compare placebo and HW groups, 36 patients per arm (1:1 randomization) are needed to show 70% reduction (relative risk 0.3) between month 3 and month 9 with approximately 95% power (2-tailed significance of 5%).[178]

Patients were observed clinically for relapses and disability scores, immunologically and radiologically for monthly MRI scans over a period of 1 year. The primary outcome of this study considered the cumulative number of new and active T2 lesions. The induction of Tregs were considered as the immunological secondary outcome measure. Relapse rate was the secondary clinical outcome measure.

The study has potentially examined therapeutic immunomodulation employing controlled parasitic infection in MS.

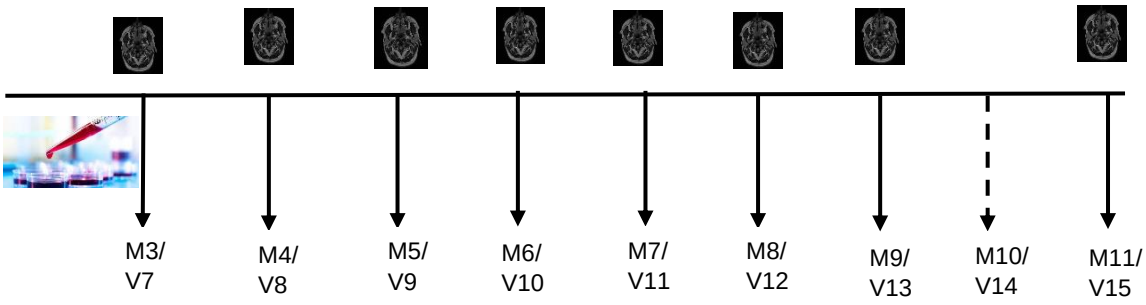

Figure 6: MRI timeline for the clinical trial; long arrows represent visits at which MRI was conducted; worms were administered at month 3/visit 7; M stands for month; V stands for visit.

3.3.1 Primary outcome of the clinical trial: Newly active lesions

The primary outcome of the WIRMS trial was MRI detectible disease activity between visits 7 and 13. This is a sum of new lesions, enlarging lesions, and newly enhancing lesions. These are defined as

- **New lesions**: Comparing visit 13 to visit 7, a new lesion should be on 13 but not 7.
- **Enlarging lesions**: Comparing visit 13 to visit 7, an enlarging lesion should be bigger at V13 than it was at V7.
- **Newly enhancing old lesion**: looking at all visits 8, 9, 10, 11, 12, and 13 a newly enhancing lesion is one that is enhancing and was visible in the previous visit but not enhancing. Lesions can newly enhance more than once. The newly active lesions are a sum of these three components.

  All outcome measures were assessed by raters blinded to the treatment arm.

3.4 Results

The study found no quantitative differences in the T2 lesion load on MRI at the baseline (V7) scan between participants assigned to receive HW (hookworm) or placebo. According to the data, the number of newly enhancing T1 lesions was numerically higher in the HW arm as compared to placebo at V8.

At visit 13, the cumulative number of new T2 lesions, newly enhancing lesions or enlarging lesions was calculated to be 141 in the HW group and 117 in the placebo group. Sixteen of the HW-treated patients (53%) versus eight of the placebo-treated patients (26%) had no detectable MRI activity.

3.4.1 Reproducibility analysis

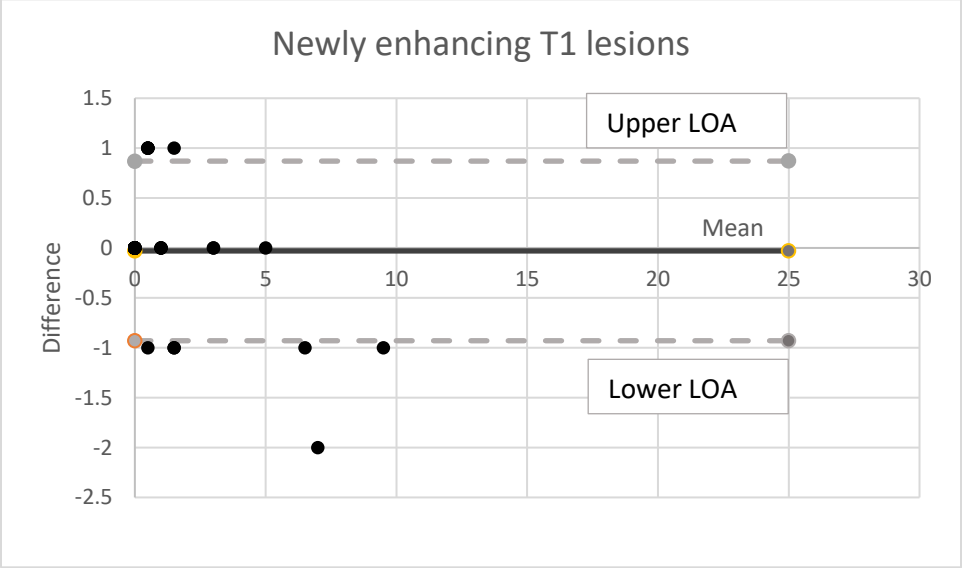

Figure 7: Bland Altman plot showing agreement of newly enhancing T1 lesion counts between two observers. Dashed lines = upper and lower limits of agreement; Bold line = Bias

Figure 8: Bland Altman plot showing agreement of new and enlarging T2 lesion counts between two observers. Dashed lines = upper and lower limits of agreement; Bold line = Bias.

The plot for newly enhancing T1 lesions (**Figure 7**), the bias of -0.03 units means less than 1 lesion difference between the two observers on average. The narrow limits show unbiased limits of agreement.

Regarding the difference plot for new and enlarging T2 lesions (**Figure 8**), the bias lies at 0. This suggests that observer 2 measures 0 lesions more

or less than observer 1. The narrow limits show unbiased limits of agreement. Many outliers are very close or on the line of limit of agreement.

3.4.2 T2 lesion load and Total Lesion Volume at baseline

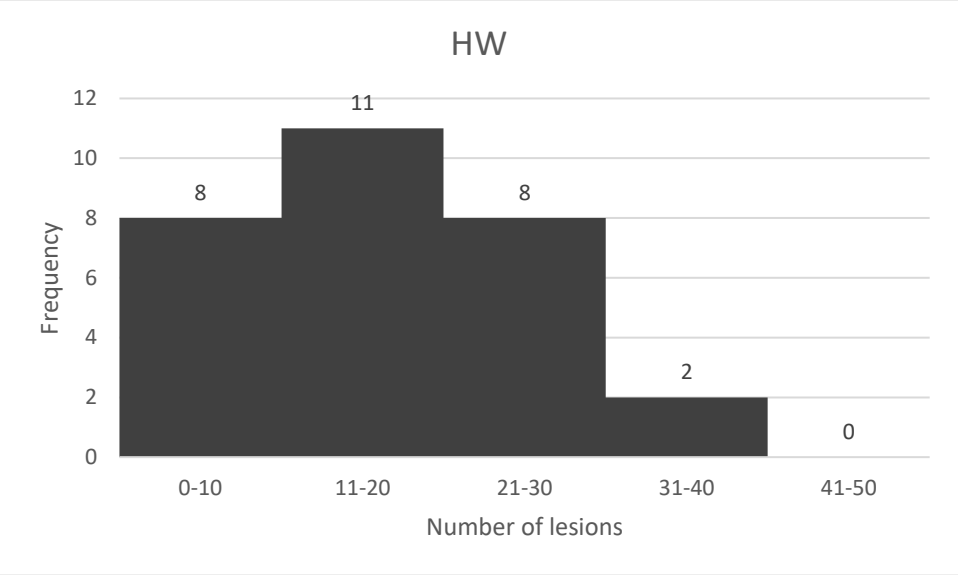

Figure 9: Histogram demonstrating the number of T2-weighted lesions at V7 for all HW-treated patients.

As demonstrated in **Figure 9**, 8 patients show 0-10 T2-weighted lesions at the first visit. None of the patients' scans demonstrate more than 50 T2-weighted lesions, at V7, with 1 patient having the highest lesion load (41-50) in the cohort.

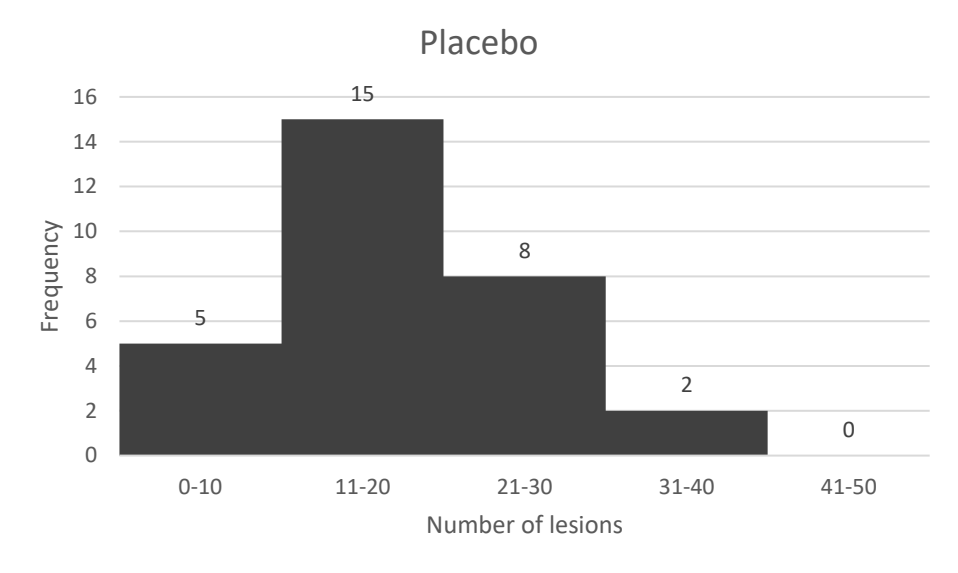

Figure 10: Histogram demonstrating the number of T2-weighted lesions at V7 for all placebo-treated patients.

As demonstrated in **Figure 10**, 10 patients show 0-10 T2-weighted lesions at the first visit. None of the patients' scans demonstrate more than 50 T2-weighted lesions, at V7, with 1 patient having the highest lesion load (41-50) in the cohort.

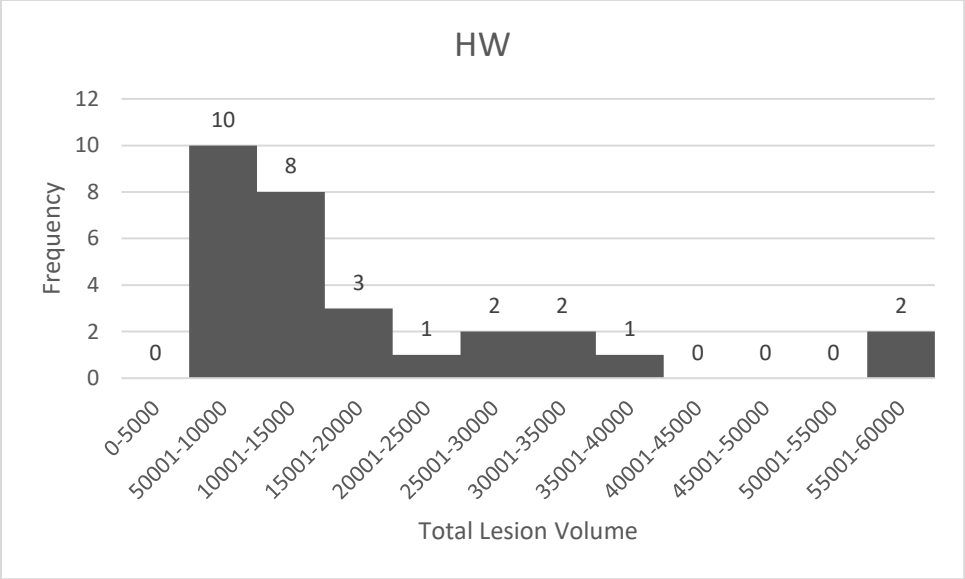

Figure 11: Histogram showing TLV at V7 in the HW arm.

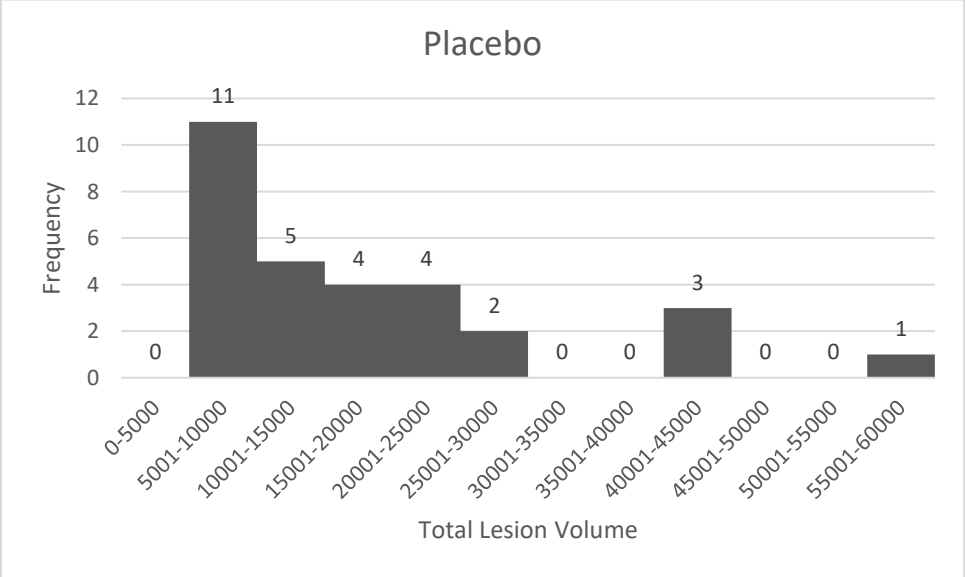

Figure 12: Histogram showing Total Lesion Volume (TLV) at V7 in the Placebo arm.

Regarding **Figure 11**, most patients (10) have TLV) ranging from 5001-10000 mm^3 in the HW arm. None of the patients' scans demonstrate TLV more than 60000mm^3 with two patients' scans having highest TLV.

As shown by the histogram (**Figure 12**), most patients (11) have a total lesion volume (TLV) ranging from 5001-10000 mm^3 at V7. None of the patients' scans demonstrate TLV of more than 60000 mm^3 with one patient's scan showing highest TLV.

3.4.3 Contrast-enhancing lesions at baseline

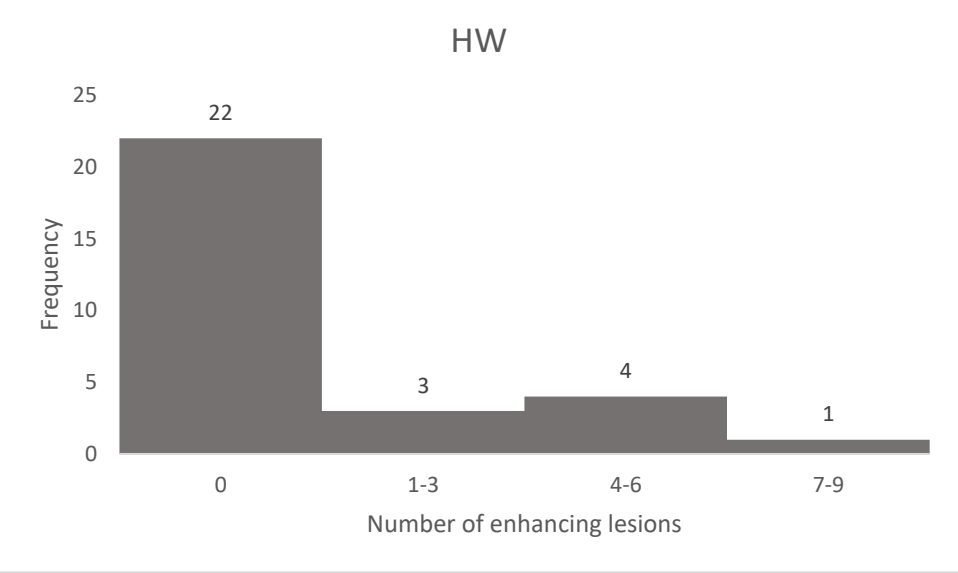

Figure 13: Histogram demonstrating the number of contrast-enhancing lesions at V7 for HW-treated patients.

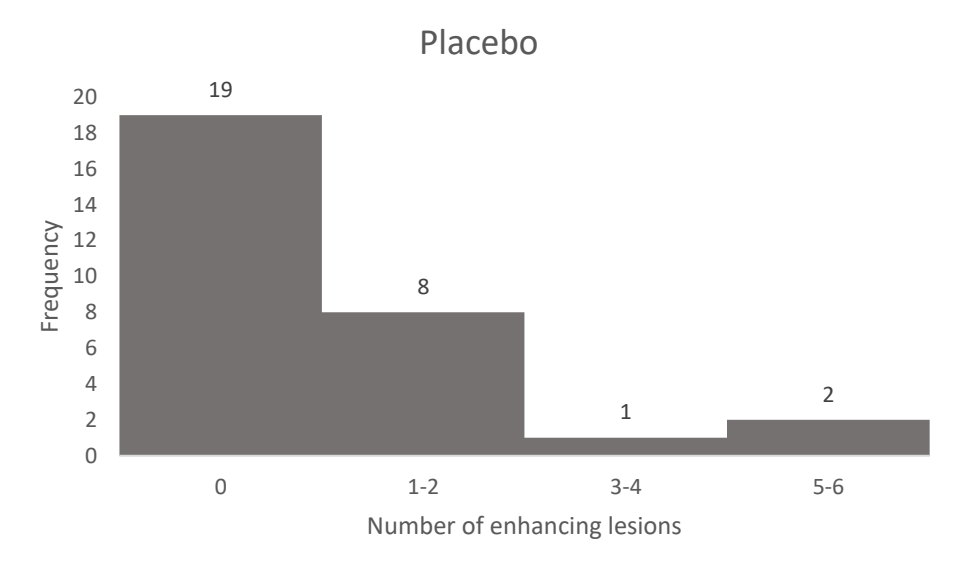

Figure 14: Histogram demonstrating the number of contrast-enhancing lesions at V7 for placebo-treated patients.

As demonstrated in **Figure 13,** 22 patients in the HW group show 0 contrast-enhancing lesions. 1 patient shows 7-9 enhancing lesions at the first visit. None of the patients' scans demonstrate more than 9 enhancing lesions with 1 patient having the highest lesion load in the cohort.

As demonstrated in **Figure 14**, 19 patients in the placebo group show 0 contrast-enhancing lesions. 2 patients show 5-6 enhancing lesions at the first visit. None of the patients' scans demonstrate more than 6 enhancing lesions with 2 patients having the highest lesion load in the cohort.

3.4.4 Newly enhancing T1 lesions

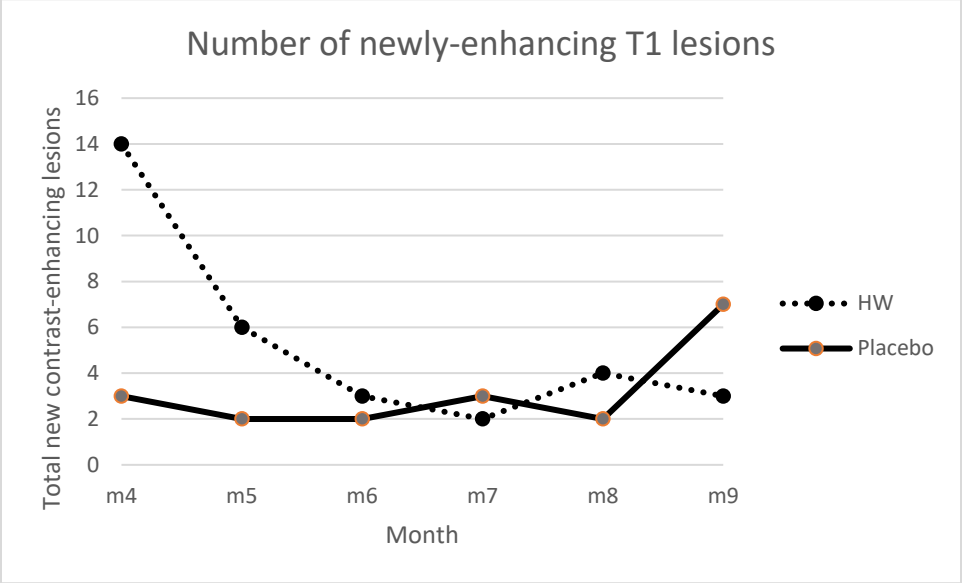

Figure 15: The chart shows the number of newly enhancing T1 lesions in the two arms.

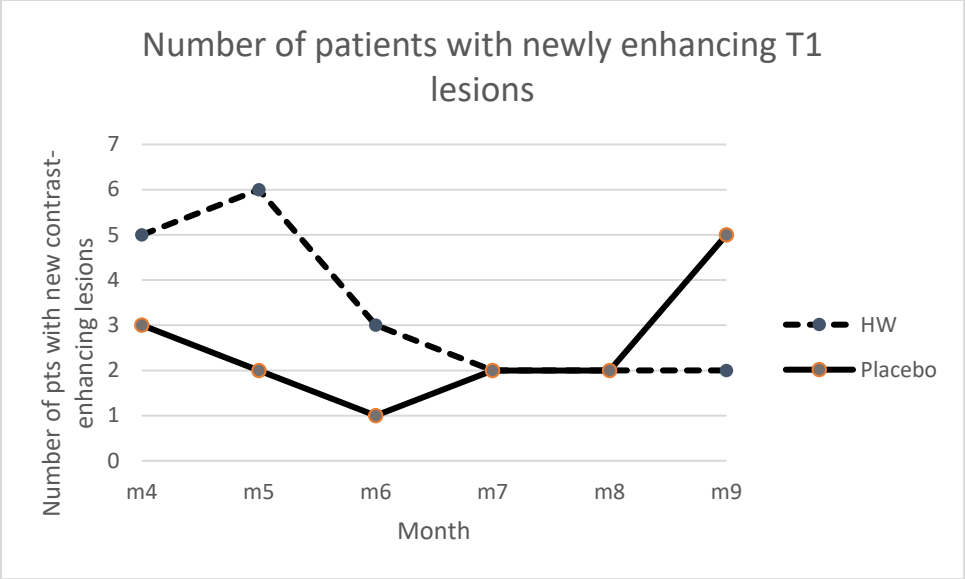

Figure 16: The chart shows the number of patients with newly enhancing T1 lesions at each visit.

The number of newly enhancing T1 lesions was found to be higher in the HW arm at V8. (**Figure 15)**

The graph shows the number of patients with newly enhancing T1 lesions that is found to be higher in the Placebo arm at V13. (**Figure 16**)

The number of newly enhancing lesions and patients with newly enhancing lesions was found to be numerically higher in the HW arm vs placebo at month 4 (V8) but was observed to shift downward between months 4 and 9 while there appears to be an upwards trend in the placebo arm

3.4.5 Primary Outcome: New disease activity

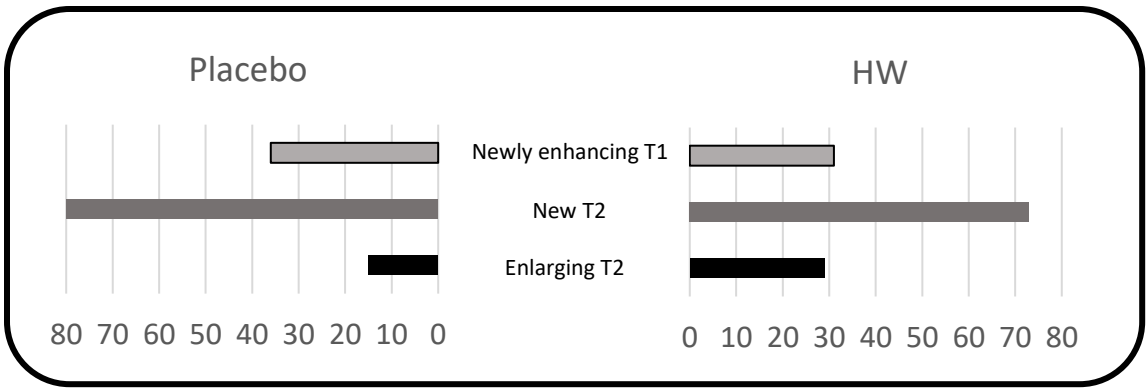

Figure 17: Bar chart showing the summary of the components of the primary outcome measure (total number of newly enhancing T1, new T2 and enlarging T2 lesions) in the two arms.

As can be seen in the bar chart (**Figure 17)**, the total number of newly enhancing T1 lesions was 36 in the placebo arm and 31 in the HW arm. The total lesion count of new T2 lesions was lesser in the HW arm (73) as compared to placebo (90). Lesion count for enlarging T2 lesions was observed to be numerically higher in the HW arm (29) as compared to the placebo arm (15).

Regarding the clinical trial, in the 71 randomized participants, the estimated difference in median range (placebo–HW) was 0 to 2 (*P* = .19; Mann-Whitney *U* test results adjusted for ties) when means were imputed and 0 to 3 (*P* = .26; Mann-Whitney *U* test results adjusted for ties) when maximum values were imputed.

3.5 Discussion

MRI has been widely accepted as a more sensitive disease activity marker as compared to clinical assessment. This has been commonly observed in clinical practice where MS patients often have new MRI lesions without new clinical symptoms.

The analysis of lesion activity on serial MRI has been accepted widely as a measure of treatment effects. Contrast-enhancing lesions indicate foci of active inflammation, while T2-weighted lesions persist and accumulate; hence, the presence of enhancing lesions gives indication of currently active disease, while the overall T2 lesion burden provides a marker for cumulative disease progression.

Early in the disease, T2 disease burden and the accumulation predict future disease severity.[179,180] Therefore, MRI scanning in patients with MS is utilized for the purpose of diagnosis, counseling patients regarding disease severity and prognosis, and deciding the requirement for disease-modifying drug therapy and as a tool to screen and test new therapies. The variability in lesion quantification as a clinical trial metric has been well studied and its importance emphasized in the literature [181].

3.5.1 Reproducibility Analysis

The observations for new and enlarging T2 lesions could not be made for 5 patients due to the missing scans, the reason being either unavailability of V7 scans or dropouts. The observations for newly enhancing T1 lesions could not be included for 13 patients in the final analysis due to 3 dropouts and 10 patients with missing scans.

Both the Bland-Altman plots demonstrate good agreement between the 2 observers suggesting the reproducibility of results.

3.5.2 T2 lesion load at baseline

Regarding the WIRMS study, number of T2 lesions were matched at baseline for the two arms.

3.5.3 Alterations in T1 lesions

Regarding the WIRMS trial, 51% of HW-treated patients demonstrated no new, enlarging or enhancing lesions during the study. This raises the possibility that the HW had an anti-inflammatory effect.[182] The number of newly enhancing T1 lesions was found to be higher in the HW arm at V8.

Regarding the chart showing the number of patients with newly enhancing T1 lesions, this was found to be higher in the Placebo arm. The reason for this is that it was the same HW-treated patients that had enhancements however, there were many enhancements. The placebo group, on the other hand, had fewer enhancements, but always different patients so, there were more patients with enhancements overall.

Re-enhancing T1 lesions represent larger areas of inflammation according to the study conducted by Campbell and colleagues[183].

3.5.4 New disease activity

The 2 arms in the WIRMS trial were matched for MRI activity at baseline. There was no new disease activity observed, during the trial, in 51% of patients treated with HW.[182]

The number of newly-enhancing lesions and patients with newly-enhancing lesions was higher in the HW arm versus placebo at month 4 but showed a dip between visits 8 and 13 whereas it shifted upwards in the placebo arm. Accepting the small number of lesions, a trend towards reducing MRI activity with treatment in the HW arm can be hypothesized.

3.5.5 Total Lesion Volume

In a study conducted by Lewanska and colleagues[184], the mean total T2 lesion volume at baseline for the placebo group was calculated to be

between 10,000 and 15,000 mm^3 for RRMS patients administered with either two different doses of intravenous immunoglobulin or placebo. This signifies that the population recruited for this study is representative of RRMS.

3.5.6 WIRMS clinical trial

In this 36-week phase 2 trial of HW in relapsing MS, no difference was observed between the cumulative number of active MRI lesions in the 2 groups (primary outcome). However, the higher proportion of scans with no new disease activity in HW group i.e. 51% of patients treated with HW showing no new, enlarging or enhancing lesions, indicates a beneficial effect. The 2 arms in the WIRMS trial were matched for clinical and MRI activity at baseline.[178]

Sample size calculation for the clinical trial was based on Tubridy et al.[178] for frequent gadolinium MRI (primary end point). Assuming the new lesion distribution to be similar to that study, utilizing the Mann-Whitney U test for the comparison between placebo and HW groups, there was a requirement of 36 patients per arm (1:1 randomization) for demonstrating 70% reduction between month 3 and month 9 with approximately 95% power.[178]

The primary outcome for the WIRMS clinical trial was the number of new, enlarging or newly enhancing lesions by month 9. The results showed that eighteen of the patients treated with HW (51%) and 10 of the patients treated with placebo (28%) had no detectable MRI activity. The per-protocol analysis involving 54 patients with complete data sets, demonstrated 16 patients in the HW group vs 8 patients in the placebo group with no MRI changes.

There was a higher number of tied zero-activity counts than expected in the HW arm, meaning a higher number of MRI scans with no disease activity, considering the sample used to power the study, in which 6 out of 31 patients demonstrated no new activity over the trial period.[178] This resulted in the planned Mann-Whitney U test being inappropriate because it loses power in the presence of ties.[185] The high rate of no detectable MRI activity in HW arm, although resulted in reduced study power, suggested a treatment effect.

Chapter 4

Localised Grey Matter Atrophy in Multiple Sclerosis and Clinically Isolated Syndrome—A Coordinate-Based Meta-Analysis, Meta Analysis of Networks, and Meta-Regression of Voxel-Based Morphometry Studies

Abstract

Background: Atrophy of grey matter (GM) is observed in the earliest stages of multiple sclerosis (MS) and is associated with cognitive decline and physical disability. Localised GM atrophy in MS can be explored and better understood using magnetic resonance imaging and voxel-based morphometry (VBM). However, results are difficult to interpret due to methodological differences between studies. Methods: Coordinate based analysis is a way to find the reliably observable results across multiple independent VBM studies. This work uses coordinate based meta-analysis, meta-analysis of networks, and meta-regression to summarise the evidence from voxel based morphometry of regional grey matter (GM) changes in patients with multiple sclerosis (MS) and clinically isolated syndrome (CIS), and if these measured changes are relatable to clinical features. Results: Thirty-four published articles reporting forty-four independent experiments using VBM for the assessment of GM atrophy between MS or CIS patients and healthy controls were identified. Analysis identified eight clusters of consistent cross-study reporting of localised GM atrophy involving both cortical and subcortical regions. Meta-network analysis identified a network-like pattern indicating that GM loss occurs with some symmetry between hemispheres. Meta-regression analysis indicates a relationship between disease duration or age and the magnitude of reported statistical effect in some deep GM structures.

Conclusions: These results suggest consistency in MRI detectible regional GM loss across multiple MS studies, and the estimated effect sizes and symmetries can help design prospective studies to test specific hypotheses.

4.1 Introduction

Areas of inflammation, axonal loss, demyelination and gliosis, occurring throughout the brain and spinal cord, are the distinctive features of Multiple Sclerosis (MS)[186]. Although MS has been considered a condition affecting the white matter (WM) and the hyperintense lesions on T2 weighted images are for MS diagnostics, there is a limited association between lesion accrual and disability. Atrophy measures appear to be a more specific marker of MS pathology than lesion volumes [187], as demonstrated by the association of atrophy in the brain and spinal cord with increasing disability [188]. In addition, progressive ventricular enlargement, another indicator of atrophy, has been shown to predate clinically definite MS in patients with clinically isolated syndrome (CIS) [189].

Atrophy of GM is already observed in the initial disease stages [122] and an association has been observed with cognitive decline and physical disability [190]. The underlying mechanism for GM atrophy is unknown, but several hypotheses have been postulated including primary GM damage involving neuronal loss, demyelination, reduced synapses, decreased oligodendrocytes and axonal transection [191]. An association has been demonstrated between GM loss and WM lesion load even in patients with short disease duration [136,192–194].

The importance of GM loss in MS necessitates careful analysis using advanced imaging methods such as voxel-based morphometry (VBM). Multiple VBM analyses of MS or CIS patients compared to healthy control groups have been published and significant changes interpreted as

atrophy. VBM has been shown to be robust against various processing steps with false positives randomly distributed about the brain [195] However, studies often involve small sample sizes, and with lack of power comes increased chance that any observed effect is a false positive [196]. Moreover, uncorrected p-values are commonly employed, inflating the false positive rates [197]. A further complexity of VBM was highlighted by a study [198] comparing detectable GM changes by different software packages- FSL [199], FreeSurfer [200,201], SPM (Statistical Parametric Mapping Functional Imaging Laboratory, University College London, London, UK). The study examined agreement between these packages by using an MS cohort with a common disease type with matched controls and highlighted pronounced differences.

Given the problems with single studies, there is potential for meta-analyses to reveal which of the observed effects are most likely to indicate MS specific GM changes. Results can add to the understanding of GM pathology in MS, and provide specific hypotheses for testing. In the absence of the original images, a coordinate based meta-analysis (CBMA) is possible using only the summary reports tabulated in the large majority of VBM publications. Results indicate effects most reliably detectable by VBM.

The primary aim of this meta-analysis was to determine the locations of consistent regional GM changes in MS and CIS patients by means of a coordinate based random effect size (CBRES) [147] meta-analysis and coordinate based meta-analysis of networks (CBMAN) [148]. Each of these algorithms cluster the reported coordinates where there is spatial concordance. CBRES performs conventional random effect meta-analysis, of the reported Z scores standardised by study sample size, in each cluster. CBMAN looks for network-like patterns of GM loss by considering significant correlations of standardised statistical effects between pairwise clusters. Secondary analyses involving subgroup analysis and meta-

regression are also performed using CBRES. The coordinate data used in this analysis is made available on the Nottingham Research Data Management Repository [dataset](DOI: 10.17639/nott.7049) for validation purposes [202].

4.2 Materials and Methods

4.2.1 Search strategies

A literature search was conducted using PubMed - with the following search term combinations- ("multiple sclerosis"[All Fields] OR "ms"[All Fields] OR CIS[All Fields] OR "clinically isolated syndrome"[All Fields]) AND ("voxel based morphometry"[All Fields] OR VBM[All Fields]) AND ("atrophy"[MeSH Terms] OR "atrophy"[All Fields]) AND ("grey matter"[All Fields] OR "gray matter"[All Fields] OR GM[All Fields]), Web of science, using the following search terms-TS=("multiple sclerosis" OR MS OR CIS OR "clinically isolated syndrome") AND TS=("voxel based morphometry" OR VBM) AND TS=(atrophy) AND TS=("grey matter" OR "gray matter" OR GM) and Science direct, using the following search terms- TITLE-ABSTR-KEY("multiple sclerosis" OR MS OR "clinically isolated syndrome" OR CIS) and TITLE-ABSTR-KEY("voxel based morphometry" OR VBM) and TITLE-ABSTR-KEY("grey matter" OR "gray matter" OR GM) and TITLE-ABSTR-KEY(atrophy).

Study selection

Inclusion criteria are (a) involved participants with MS or CIS (b) compared patients to healthy controls (c) performed whole brain VBM for assessing GM atrophy (d) reported coordinates for GM volume changes in either Talairach [203] or Montreal Neurological Institute (MNI) reference space. Exclusions were made due to unreported coordinates or unavailable full text. Two independent researchers assessed these criteria of the individual studies and the MNI or Talairach coordinates.

Study properties

Information extracted for analysis: the censoring threshold i.e. the smallest Z value the study considered as significant, the reported

coordinates, and either the Z score, estimated degrees of freedom and t statistic, or uncorrected p-value; t-statistics and uncorrected p-values are converted automatically to Z scores.

Coordinate based Meta-analysis

All CBRES and CBMAN analyses are performed using NeuRoi (https://www.nottingham.ac.uk/research/groups/clinicalneurology/neuroi.aspx), which is available to use freely.

Details about the algorithms incorporated into CBRES and CBMAN are presented in [147,148] . In both algorithms a clustering algorithm [204] is used to determine where the coordinates reported by multiple independent studies are spatially concordant (clustered). Once clusters are formed the reported Z scores are converted to standardised effect sizes by dividing by the square root of the number of subjects. In CBRES, a random effect meta-analysis of these effect sizes is performed in each cluster. In CBMAN, the test statistic is the correlation of standardised effect sizes performed pairwise between clusters. Where a study does not report a coordinate within a cluster, or where no effect sizes are reported by a study, the contribution to the cluster is estimated using the study censoring threshold.

The significant results of the CBRES meta-analysis are clusters of reported coordinates where the estimated effect size is statistically different to zero after controlling the false cluster discovery rate (FCDR); a type 1 error control method based on false discovery rate FDR [150]. The expected proportion of clusters incorrectly declared significant is controlled at 5% by default. Clusters indicate both spatial and effect size concordance across studies, which is an unlikely chance event suggesting that atrophy at the location of the clusters is a general feature of MS.

Significant results reported by CBMAN are clusters where standardised reported statistical effects are correlated between clusters. This indicates a significant pattern of reported effect that is represented as a network of nodes (clusters) and edges (correlations). FDR is used to control type 1 error rate of the effect size correlations. The clusters analysed by CBMAN

and CBRES are identical, since the same clustering algorithm is employed, but the results may differ due to the different hypotheses tested. A feature of both CBRES and CBMAN is that the results declared significant are reported as a function of the FDR. Any that just miss the threshold for significance can therefore be explored.

Analysis can also be performed on subgroups of studies. This estimates a subgroup specific effect size in each of the clusters found significant during the full analysis (using all studies); this is useful since clusters may not be significant if the subgroup is small, yet the effect size might be of interest. Furthermore, the use of standardised effect sizes makes meta-regression possible by looking for significant correlation between a specified covariate and the standardised effect size in each cluster.

Experimental Procedure

Multiple experiments reported on the same subjects were pooled into single independent experiments to prevent correlated results inducing apparent concordance that is not due to a generalizable MS process [205].

All planned analyses were performed controlling the FDR at 0.05. For each the next most significant clusters were explored, and reported, to make sure that none had just been missed at this threshold.

Main analysis

The main meta-analysis was performed using both CBRES and CBMAN and involved all studies meeting the inclusion criteria.

Subanalyses

Subanalyses for CIS, benign MS (BMS), Relapsing Remitting MS (RRMS), Primary Progressive MS (PPMS) and Secondary Progressive MS (SPMS) studies were performed; subtypes as defined in the reporting studies. This analysis estimates effects of the respective subgroup within significant clusters discovered using all studies.

Meta-regression

Regression analyses were performed for covariates that might influence the grey matter volume: mean age (years), MS disease duration

(years; excluding CIS studies with no MS disease duration), MSFC, and EDSS (all studies and including RRMS studies only).

4.3 Results

4.3.1 Included studies and sample characteristics

The literature search yielded 237 potential studies of which 34 met the inclusion criteria (Figure 1). The 34 included research papers reported 45 whole brain VBM experiments comparing MS subtypes and controls (See supplementary materials for study details).

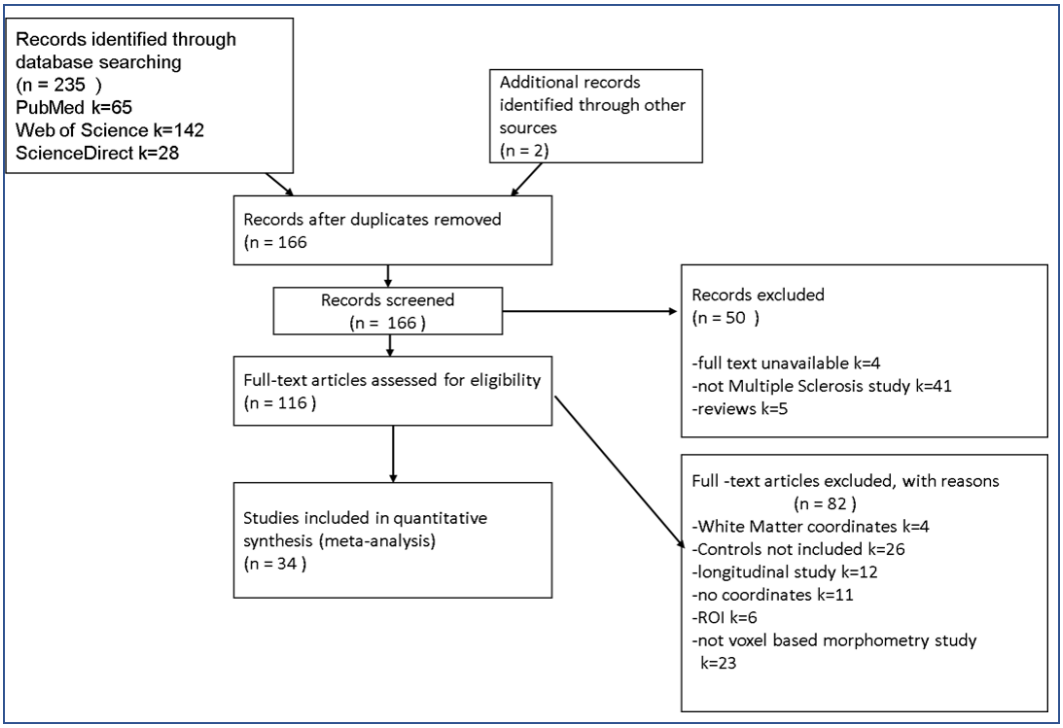

Figure 1. This is a figure with the PRISMA flowchart [206] showing the inclusion and reasons for exclusion of studies in the meta-analysis.

Studies included in the analysis were conducted between 2006 and 2018 and involved a total of 1561 patients and 1182 controls. The studies by MS subtype were 4 CIS, 24 RRMS, 7 PPMS, 3 BMS, and 2 SPMS; 4 studies were not specific to any single MS subtype. Mean patients age was 40.49 years (SD =.64). The number of controls varied in size from 9

to 90 and patients varied from 9 to 249. The mean (standard deviation (SD)) EDSS was 2.7 (1.5). The mean disease duration was 9.26 (6.51) years. Across the studies the duration of disease, excluding the CIS studies, was 1.66 to 30.50 years.

4.3.2 Primary Meta Analysis

The analysis found 8 significant clusters involving basal ganglia and cortical regions; effect sizes are given in Table 1 and the complete list of Talairach regions, automatically detected (26), covered by each cluster given in online materials [dataset](DOI: 10.17639/nott.7049) (21). Significant clusters and a depiction of the covariance of standardised effect sizes between clusters are shown in Figure 2. Forest plots for the most significant clusters according to CBRES are shown in Figure 3. In figure 4 a scatter plot of standardised effect sizes reported in the left and right thalamic clusters shows clear correlation detected by CBMAN. The first non-significant cluster according to CBRES was at a FCDR of 0.18. The first non-significant edges discovered by CBMAN were at FDR 0.057, where a further 9 significant edges and two extra clusters (right Caudate peaking at Talairach coordinates {12,4,20}mm and another covering mostly the left/right cingulate gyrus peaking at {-4, -18, 44}mm) are found.

Table 1: shows significant clusters detected by CBRES and CBMAN algorithms for the main meta-analysis and estimated effects from the subanalyses. The column ‘main analysis’ shows effect size, standard deviation and false cluster discovery rate for each significant cluster estimated using CBRES. The subsequent columns show the estimated effect size for the subanalyses; - signifies no contribution of the subgroup to the cluster. *Cluster 7 is discovered by the CBMAN algorithm only.

Cluster Number	Talairach labels	Talairach coordinate of density peak (x,y,z)mm	Main analysis Mean (SD); FCDR	CIS subanalysis Mean	BMS subanalysis Mean	RRMS subanalysis Mean	PPMS subanalysis Mean	SPMS subanalysis Mean
1	Right Thalamus	(12.0 -28.0 8.0)	-1.27 (0.25);**0.00025**	-1.01	-1.76	-1.23	-0.94	-1.80
2	Left Thalamus	(-14.0 -28.0 8.0)	-1.25 (0.26);**0.00025**	-1.04	-1.74	-1.11	-1.25	-1.70
3	Left Putamen	(-28.0 2.0 6.0)	-0.96 (0.24);**0.00033**	-0.96	-1.28	-0.81	-0.96	-1.52
4	Left Superior Temporal Gyrus/insula	(-48.0 -18.0 2.0)	-0.85 (0.19); **0.007**	-0.66	-	-0.85	-0.77	-1.09
5	Right Superior Temporal Gyrus/Insula	(38.0 -18.0 12.0)	-0.84 (0.2);**0.009**	-	-	-0.83	-0.55	-1.22
6	Right Postcentral Gyrus	(36.0 -26.0 48.0)	-0.87 (0); **0.0014**	-0.67	-1.18	-0.90	-0.78	-1.20
7	Left Pre- & Postcentral Gyrus*	(-46.0 -18.0 38.0)	-0.69 (0.3); 0.18	-0.69	-1.03	-0.82	-0.79	-1.57
8	Right putamen	(26.0 4.0 8.0)	-0.8 (0.31); **0.03**	-	-1.25	-0.69	-0.48	-1.27

1

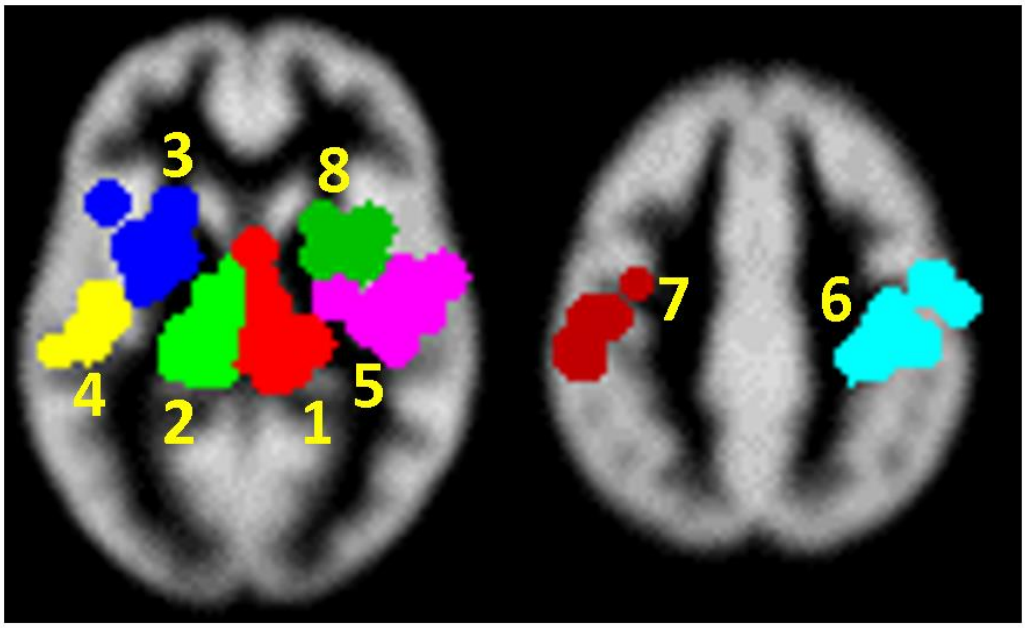
3
8
7
6
4
2
1
5

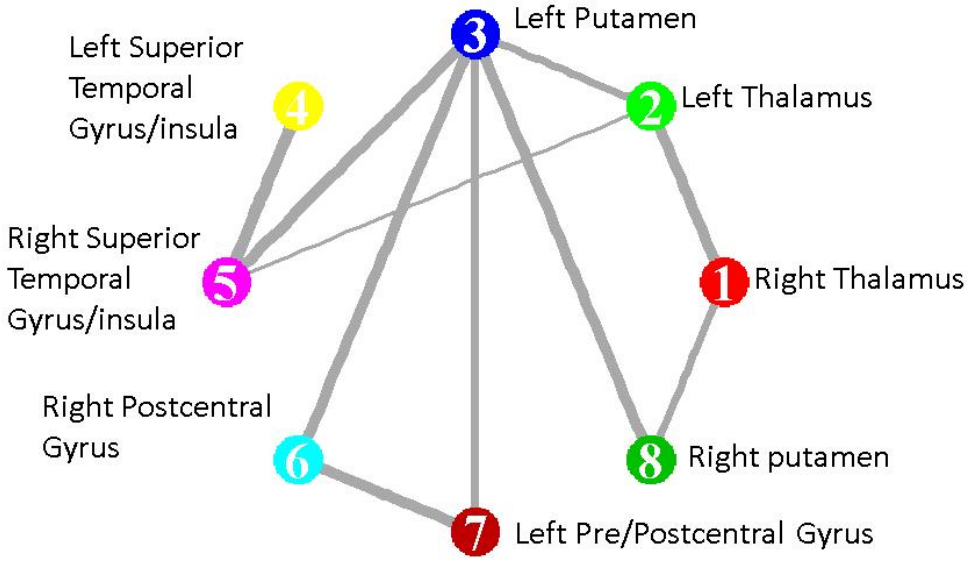
Left Putamen
Left Superior Temporal Gyrus/insula
Left Thalamus
Right Superior Temporal Gyrus/insula
Right Thalamus
Right Postcentral Gyrus
Right putamen
Left Pre/Postcentral Gyrus

Figure 2: Top: Significant clusters of GM atrophy detected using CBRES and CBMAN algorithm. Cluster (7) is detected only by CBMAN. Bottom: The network edges found to connect the clusters significantly by CBMAN; line thickness indicates correlation strength of the standardised effect sizes between connected clusters.

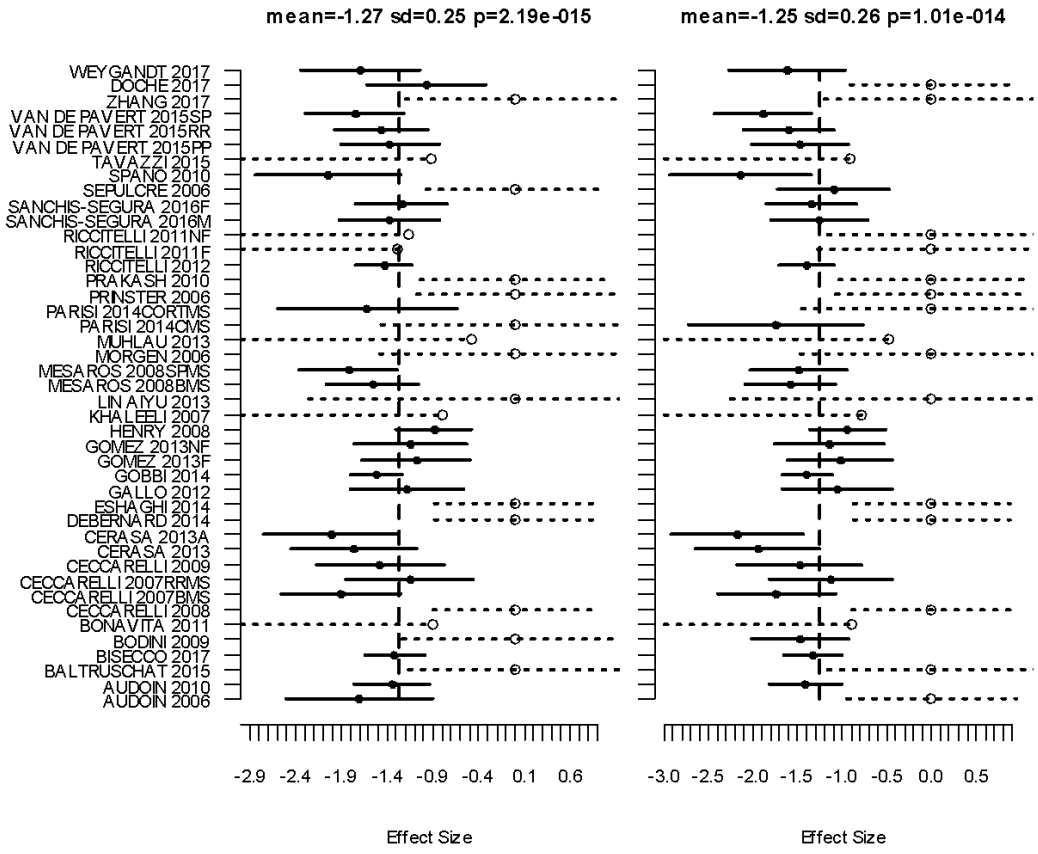

Figure 3: Forest Plots for the two most significant clusters (left and right Thalamus) of GM atrophy reported by the 45 VBM experiments. Markers with solid circle indicate the effect size reported by the study in the respective cluster. The solid horizontal lines span ± 1.96 times the within

study standard deviation of the effect size. Censored values are depicted by open circle markers and the intervals by dashed lines (···o···).

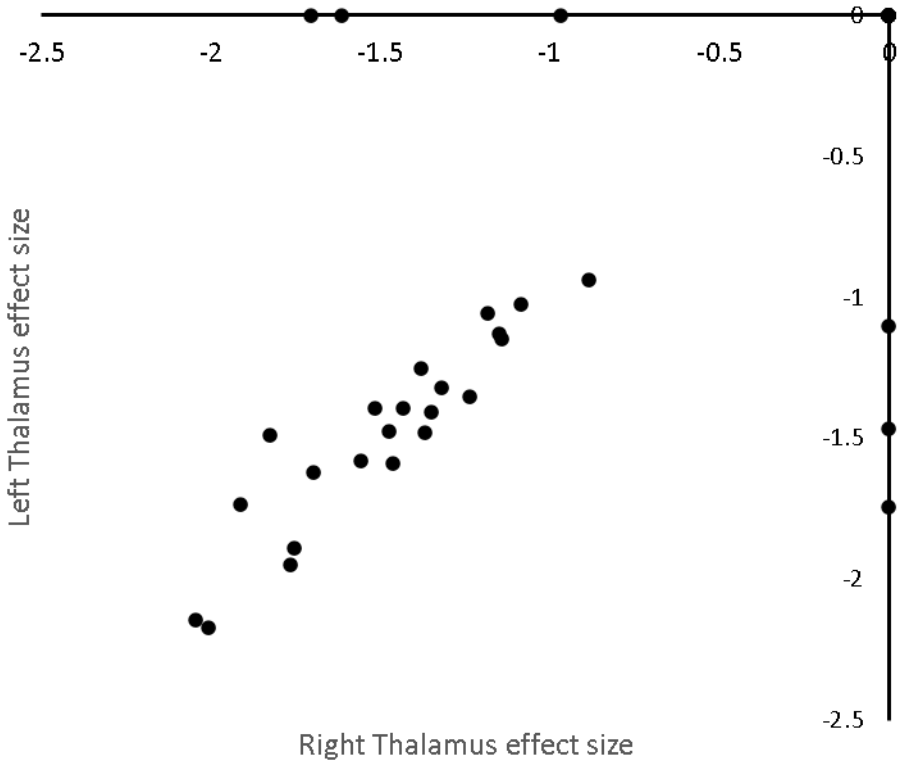

Figure 4. Relationship between standardised effect sizes reported in the left and right thalamic clusters. Markers that fall on the axes are censored.

4.3.3 Subanalyses

Results from the subanalysis are given in table 1, which shows estimated effects sizes considering only the respective subgroup within each of the clusters from the primary meta-analysis. It is apparent that the estimated effects are lowest in magnitude in CIS and PPMS groups and highest in the SPMS and BMS groups, while RRMS generally falls in the middle.

4.3.4 Metaregresion

4.3.4.1 Age

A single cluster was found with age as a significant covariate; table 2. The first non-significant cluster was at FCDR 0.18.

Table 2: The table shows significant clusters for the Age and Disease Duration meta-regression. The location indicates the most commonly reported Talairach labels covered by the cluster.

Location	**Talairach coordinates (x,y,z)mm**	**Change in standardised effect per year (% of mean effect)**
Age		
Left Thalamus	(-14.3 -28.3 10.4)	-0.025 (2%)
Disease Duration		
Right Thalamus	(10.0 -30.0 7.0)	-0.049 (3.7%)
Left Thalamus	(-14.3 -25.2 6.1)	-0.046 (3.8%)
Left Claustrum, Putamen, and Insula	(-31.0 0.3 8.8)	-0.032 (3.4%)

4.3.4.2 MS Disease Duration

This analysis included 39 of the independent experiments reported MS disease duration due to exclusion of CIS studies where MS disease duration is zero. Three clusters were found with disease duration as a significant covariate; table 2. The first non-significant cluster was found to be at FCDR 0.1.

4.3.4.3 MSFC

Regression analysis was not performed because only 9 out of 44 studies reported MSFC.

4.3.4.4 EDSS

No significant clusters with EDSS a covariate. The first non-significant cluster was found at FCDR 0.1.

4.4 Discussion

The results of 34 voxel-based morphometry studies of MS and CIS are summarised using CBMA, showing that GM atrophy in MS not only occurs in some regions more than in others and that regions of predilection are not independent. Eight regions were identified using two algorithms testing different null hypotheses. Results indicate a consistent pattern, rather than independent clusters, of reported effects both spatially and in terms of effect size.

The pattern of localised GM atrophy involves both cortical and subcortical regions. Considering the correlation of reported statistical effect size suggests that these regions do not develop independently, but rather together and with some hemispheric symmetry as shown in figure 2. Meta-regression analysis suggests that the standardised effect magnitude increases with disease duration by several % per year of disease on average. This is also reflected in the mean statistical effect size estimates

within the disease type subgroups, where the estimates for the CIS group tend to be lower than the RRMS group, which are in turn lower than the SPMS group. The PPMS subgroup reported intriguingly low statistical effect sizes while the BMS group almost as large as the SPMS group in some clusters, which might reflect that BMS is indistinct from MS with long enough follow up. These estimates should be considered with caution because of the small subgroup sizes, however they could be prospectively tested.

GM tissue damage is an important pathological process in MS that underlies neurological disability [123]. It has been suggested that distribution of cortical GM atrophy is related to the effects of WM lesions on cortical regions that are network hubs, with trans-synaptic degeneration then extending from these hubs [140], or that the preferential accumulation of WM lesions in some regions would induce tract-mediated effects through secondary retro- or anterograde degeneration. The relationship between GM atrophy and WM abnormalities is weaker in people with PPMS or SPMS [207]. The loss of volume is the result of many dynamic processes, with a balance between destructive and reparative mechanisms with interaction among neurons, oligodendrocytes, axons, microglia, astrocytes, inflammatory cells, endothelial cells and water distribution [208].

In the thalamic clusters the standardised effect sizes were found to correlate negatively with disease duration. Both imaging and pathology studies have demonstrated the involvement of thalamus in early RRMS [209], CIS [210] and pediatric MS [211]. Cifelli and colleagues [212] conducted a study of normalised thalamic volume measurements in SPMS patients. Volumes of manually outlined thalami were normalised by intracranial volumes and showed a mean decrease of 17%. Thalamic volume loss may be due in part to disconnection created by WM lesions [213,214].

Atrophy of the left and right putamen MS has also been detected. The putamen is a part of the dorsal striatum and the basal ganglia and, plays a

role in the regulation of movement, coordination, motor function and cognition [215–217]. It is also involved in modulation of sensory and motor aspects of pain. [218] Thus, a pathology like, neurodegeneration, might be expected to cause a broad spectrum of clinical manifestation from motor dysfunction to psychiatric disorder. [219,220]. Previous studies have demonstrated progressive atrophy of the putamen in both RRMS and SPMS [125]. Kramer and colleagues [221] recently reported a significant relationship between putamen volume and disease duration in MS, which was also indicated by the present study.

Pre- and postcentral gyrus (bilateral) is consistently reported. The clusters have density peaks reported in the right precentral and the left postcentral gyrus, but the coordinates forming the clusters cover both pre- and postcentral gyrus on each side. Li et al [222] used diffusion tensor imaging (DTI) and demonstrated neuroconnectivity changes in the left postcentral gyrus, and reduced communicability correlating with the 25-foot walk test results.

Clusters covering the left/right superior temporal gyrus and insula ware also detected. The superior temporal gyrus is associated with auditory and speech comprehension [223,224] and perception of emotions in facial stimuli [225,226]. In addition, it is an essential structure in the pathway containing prefrontal cortex and amygdala that are responsible for social cognition processes [225,227]. The study conducted by Achiron and colleagues [228] suggested correlation between reduced cortical thickness in superior temporal gyrus and global cognitive score, attention, information processing speed and motor skills. The insula is primarily a visceral-somatic region [229]. Studies have shown relation between functional connections of the basal ganglia and insula and fatigue severity in case of MS patients [230–232].

A similar coordinate based meta-analysis in MS was performed by Chiang et al at the same time as the present study [233]. That study used the popular ALE algorithm and produced similar results. The study also used functional meta-analytic connectivity modelling (fMACM) [234] to explore functional coactivation of clusters as a network, estimated using non MS studies. By contrast the present study investigates the network like properties of GM atrophy and uses the included MS specific studies.

There are limitations to CBMA are that bias and methodological issues in the primary studies might be reflected in the results. Therefore, CBMA results should be considered hypothesis generating and used to inform robust prospective studies. To this end the presented results provide a-priori regions of interest for testing as well as statistical effect size estimation for sample size calculations.

4.5 Conclusions

This CBMA of VBM studies of MS and CIS has identified a pattern of related cortical and subcortical GM atrophy. Relationships are indicated by the covariance of reported statistical effects. Disease duration was found to be a significant covariate of the standardized reported effect sizes in the thalamic clusters and a cluster covering the left claustrum/putamen/insula. The estimated statistical effect sizes may be important for powering prospective studies of GM atrophy in MS to test specific hypotheses.

Appendix A

Table A1: The table shows demographics for the included studies.

A1: The table shows demographics for the included studies.

STUDY	CONTROLS				PATIENTS				
	n	MEAN AGE	SD/RANGE	FEMALES	SUBTYPE	N	MEAN AGE	SD/RANGE	FEMALES
AUDOIN 2006	10	37	31-52	4	EARLY RRMS	21	36	27-55	16
AUDOIN 2010	37	28	8	-	CIS	62	29	20-46	-
BALTRUSCHAT 2015	15	30.47	5.91	7	RRMS	17	32.82	6.41	11
BISECCO 2017	52	37.3	13.1	33	RRMS	125	36.8	10.7	82
BODINI 2009	23	35.1	7.9	12	EARLY PPMS	36	44.8	11.13	15
BONAVITA 2011	18	39	10	10	RRMS	36	CI- 40.9	8.7	11
	-	-	-	-			CP- 40.5	6.9	10
CECCARELLI 2008	21	40.9	24-62	14	CIS	28	30.7	21-43	15
CECCARELLI 2007BMS	20	36.8	6.8	13	BMS	19	41.5	5.6	15
CECCARELLI 2007RRMS	-	-	-	-	RRMS	15	33.3	7.8	12
CECCARELLI 2009	17	51.3	26-68	11		18	49.6	38-73	10
CERASA 2013	20	36.9	5.8	14	RRMSnc	14	38.6	8.5	11
CERASA 2013A	-	-	-	-	RRMSc	12	38.9	8.7	10
DEBERNARD 2014	25	35.2	10.3	17	EARLY RRMS	25	37.2	8.6	22
ESHAGHI 2014	19	37.6	34.4, 41.9	9	PPMS	36	42.8	39.4, 46.6	12
GALLO 2012	15	36.3	20-53	10	RRMS	30	35.9	19-51	20
GOBBI 2014	90	39.7	13.7	51	MIXED_MS	123	41.7	10.3	71
GOMEZ 2013F	18	31.06	5.67	8	RRMS_fatigue	32	37.72	5.9	21
GOMEZ 2013NF	18	-	-	-	RRMS_nonfatigue	28	34.96	5.87	18
HENRY 2008	49	38	11	34	CIS	41	37	10	29

KHALEELI 2007	23	35.1	23-56	12	EARLY PPMS	46	43.5	19-65	19
LIN AIYU 2013	11	39.5	13.2	7	RRMS	11	38.5	12.2	7
MESAROS 2008BMS	21	45.7	25-66	11	BMS	60	46.2	35-63	37
MESAROS 2008SPMS	21	45.7	25-66	-	SPMS	35	46.5	30-63	25
MORGEN 2006	19	31.7	7.5	-	RRMS	19	33.05	8.26	-
MUHLAU 2013	49	36.4	13	33	CIS or RRMS	249	36.8	10.7	62
MORGE low PASAT	19	31.7	7.5	-	RRMS	10	36.7	8.05	-
PARISI 2014CMS	9	54.4	12.1	6	CMS	9	50.2	11	7
PARISI 2014CORTMS	9		-	-	CORT-MS	9	48.9	9.9	7
PRINSTER 2006	34	43.2	13.2	15	RRMS	51	38.6	7.5	36
PRAKASH 2010	15	45.8	1.8	15	RRMS	21	44.2	1.9	21
RICCITELLI 2012	88	39.7	18-65	51	RRMS	78	40.2	20-63	55
RICCITELLI 2011F	14	38.7	8.4	8	RRMS Fatigue	10	38	7.7	6
RICCITELLI 2011NF	14	-	-	-	RRMS nonfatigue	14	38.6	8.5	8
SANCHIS-SEGURA 2016M	35	25.54	5.35	-	RRMS male	22	38.68	8.72	-
SANCHIS-SEGURA 2016F	28	27.96	7.85	-	RRMS female	34	40.85	10.18	-
SEPULCRE 2006	15	43.2	10.9	6	PPMS	31	43.7	9.87	13
SPANO 2010	20	40.5	11.07	12	BMS	10	44.5	6.5	8
TAVAZZI 2015	31	47.9	14.5	20	PPMS	18	46.9	8.1	6

TAVAZZI 2015	31	47.9	14.5	20	PPMS	18	46.9	8.1	6
VAN DE PAVERT 2015PP	30	37.8	11.8	18	PPMS	25	52.5	9.8	14
VAN DE PAVERT 2015RR	30	-	-	-	RRMS	30	42.5	9.6	20
VAN DE PAVERT 2015SP	30	-	-	-	SPMS	25	52.8	7.6	14
ZHANG 2017	29	37.79	10.29	17	RRMS	39	38.26	9.05	23
DOCHE 2017	16	37.1	10.2	12	RRMS	23	34.2	9.3	19
WEYGANDT 2017	21	49.1	11.7	13	HI-LB MS	18	49.8	7.7	10

1

Table A2: The table shows clinical characteristics of patients in the included studies.

	DISEASE DURATION (y)	SD/RANGE	MSFC	EDSS	SD/RANGE	PASAT 3'	SD/RANGE	education	SD/RANGE	BPF (mm3)	SD/RANGE
AUDOIN 2006	2.15	1.2-3.8	-0.348	1	0-3	-	-	-	-	-	-
AUDOIN 2010	0.33	0-0.5		1	0-3.5	40	10	13	3	0.831	0.043
BALTRUSCHAT 2015	4.53	3.5	-	2.24	1.09	48.12	6.94	12	2.72	0.84	0.023
BISECCO 2017	9.6	8.7	-	2	0-6	-	-	12.9	3.7	-	-
BODINI 2009	3.3	0.9	-	4.5	1.5-7	47.65	11.24	-	-	-	-
BONAVITA 2011	11.86	7.08	-	2.8	1.1	-	-	12.5	3.9	0.82	0.03
	10.91	4.67	-	2.6	1.7	-	-	12.3	3.6	0.83	0.03
CECCARELLI 2008	0	0	-	0	0-1	-	-	-	-	-	-
CECCARELLI 2007BMS	20	15-30	-	2	1.0-3.0	-	-	-	-	-	-

CECCARELLI 2007RRMS	6	2.0-10.0	-	1.5	1.0-3.5	-	-	-	-	-	-
CECCARELLI 2009	10.7	4.0-21.0	-	5.5	3.0-7.0	-	-	-	-	-	-
CERASA 2013	8.8	4.4	-	2	1.5-4.5	-	-	13	5.0-17.0	-	-
CERASA 2013A	12.1	8.7	-	2.5	1.0-4.0	-	-	13	5.0-17.0	-	-
DEBERNARD 2014	2.4	1.5	0.4 (0.6)	1.5	0-4.5	0.16	0.99	13.5	2.7	-	-
ESHAGHI 2014	3.3	2.9,3.6	-1.2 (-0.7,-1.6)	4	1.5,7	-	-	-	-	-	-
GALLO 2012	9.2	3.0-22	-	2.1	1.0-5.5	-	-	-	-	-	-
GOBBI 2014	12.6	1.0-44	-	2	0-7.0	36.6	1.0-59	-	-	-	-
GOMEZ 2013F	7.44	5.15	-	3.2	1.68	-	-	-	-	-	-
GOMEZ 2013NF	5.14	3.69	-	1.96	1.2	-	-	-	-	-	-
HENRY 2008	0.3	0.25	1.9(1.7)	1.1	0.8	-2.1	2.3	-	-	n GMV = 940(52)	-
KHALEELI 2007	3.3	2.0-5.0	-	4.5	1.5-7	-	-	-	-	-	-
LIN AIYU 2013	30.5	11.1	-	3.4	2.3	-	-	12.3	4.7	-	-
	DISEASE DURATION (y)	SD/RANGE	MSFC	EDSS	SD/RANGE	PASAT 3'	SD/RANGE	education	SD/RANGE	BPF (mm3)	SD/RANGE
MESAROS 2008BMS	22.7	15-40	-	1.5	0-3.0	-	-	-	-	-	-
MESAROS 2008SPMS	16.2	7.0-27	-	6	4.0-7.0	-	-	-	-	-	-
MORGEN 2006	1.66	1.43	-	1	0-3.5	31	22-56	15 (college level)	-		-
MUHLAU 2013	-	-									

MORGE low PASAT	2.02	1.78	-	2	0-3.5	27	22-31	15 (college level)	-			-
PARISI 2014CMS	14	4-20	-	3	1.5-6	-	-	10.6	2.9	765 ml	31 ml	
PARISI 2014CORTMS	8	2-31	-	4	1.0-6.0	-	-	8.4	3.2	655 ml	110 ml	
PRINSTER 2006	13.1	6.4	-	2.6	1.5-4.5	-	-	-	-	-	-	
PRAKASH 2010	7.3	0.1	-	2.2	0-6	43	2.3	15.6	0.4	-	-	
RICCITELLI 2012	10	1-28	-	1.5	1-4.5	-	-	-	-	-	-	
RICCITELLI 2011F	8.2	6.2		1.5	1.5-2.0	-	-	-	-	-	-	
RICCITELLI 2011NF	10.6	6.6	-	1.5	0-1.5	-	-	-	-	-	-	
SANCHIS-SEGURA 2016M	6.45	5.53		2.5	0-6.5	35.23	20.01	5	1-6	0.83	0.33	
SANCHIS-SEGURA 2016F	8.82	7.47		2.38	0-6.5	33.35	23.04	4	1-6	0.83	0.27	
SEPULCRE 2006	3	2-5	-0.26(-6,16-0.79)	4.5	3.5-7	-0.002	-3.73-1.24	-	-	-	-	
SPANO 2010	17.1	4.5	not for all pts	1.75	1-3	-	-	-	-	-	-	
TAVAZZI 2015	12.4	7.73	-	6	3.0-8.0	-	-	-	-	-	-	
VAN DE PAVERT 2015PP	12	7.4	-0.62 (0.81)	6	0-6.5	-0.7	1.38	-	-	-	-	
VAN DE PAVERT 2015RR	11.5	10.5	-0.41 (0.76)	1.75	1.0-6.5	-0.69	1.32	-	-	-	-	
VAN DE PAVERT 2015SP	24	8.2	-0.77 (0.66)	6.5	4.5-8.5	-0.94	1.12	-	-	-	-	
ZHANG 2017	7.69	5.96	-	2.24	1.58	CI n CP separate values		11.9	3.68	-	-	

DOCHE 2017	4.5	4.6	-0.70 (1.04)	1.5	1.2	-	-	-	-	-	-
WEYGANDT 2017	11.7	7.2	-	4	2.5-6.0	-	-	11	-	GM fraction=0.41	0.04

Appendix B

Figure B1: This figure shows forest plots for significant clusters 3-8.

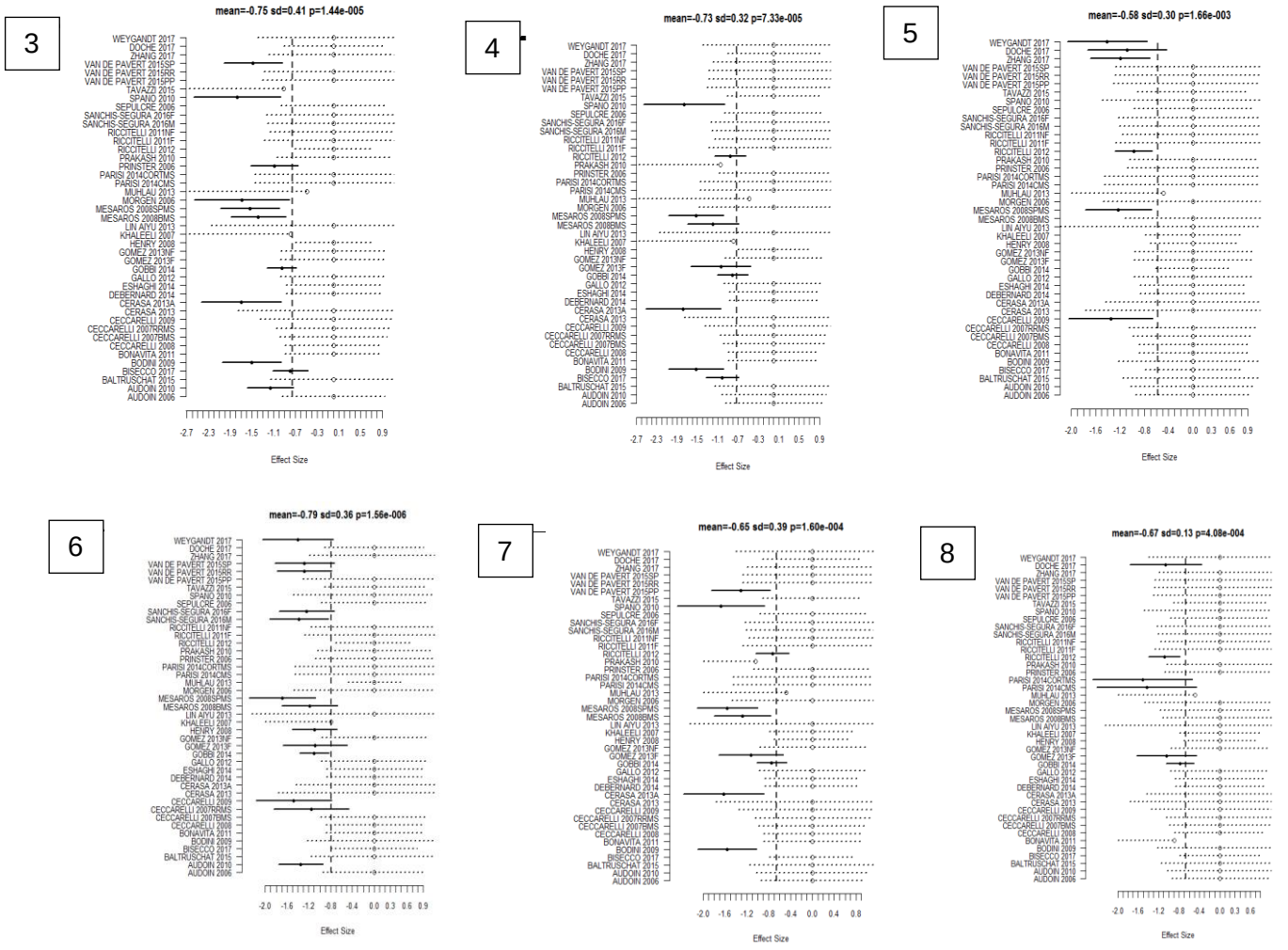

Chapter 5

Voxel-based morphometry reveals brain GM volume alterations in hookworm-treated MS patients

Abstract

Previous literature and the coordinate-based meta-analysis[143] conducted has demonstrated a preferential loss of grey matter (GM) in the dorsal striatum, primary somatosensory cortex, insular cortex, auditory cortex and the relay station of the brain as identified cortically and subcortically in multiple sclerosis (MS) and clinically isolated syndrome (CIS) patients. The objective of this study was to assess GM atrophy in the whole brain and regions of interest (ROI) by the utilization of standard voxel-based morphometry (VBM) pipeline.

5.1 Introduction

MS has been described as a chronic demyelinating disease of the CNS, affecting WM. However, it has been demonstrated by pathological[12,235] and MR imaging[236–240] studies that it also involves cortical regions and deep GM. A reduction in brain and specifically GM volumes has been detected in MS,[241] even in the early disease stages,[242] but it is unknown whether some GM areas are more susceptible to volume loss as compared to others. Understanding of the potential differential susceptibility to GM loss may help illuminate the clinical presentation and improve our understanding of the clinico-radiological dissociation present in some MS patients.[243] The measurement and evaluation of regional atrophy could also be useful in

monitoring disease progression, by identifying areas more sensitive to volume loss, and in the planning of clinical trials.

It is legitimate to argue that an inflammatory misbalance is at the origin of MS. Research on pro-inflammatory mechanisms in MS has been largely performed; and, the potential mechanisms that actively participate in resolving inflammation involve T-regs.[244] Regarding the WIRMS clinical trial[142] that was a 9-month double-blind, randomized, placebo-controlled trial conducted to determine whether hookworm treatment effects

MRI activity and T regulatory cells in relapsing MS (chapter 3); the proportion of CD4+foxp3+CD127neg cells, that may be more specific for true Treg cells, was found to be significantly increased by HW.

Measurement of brain atrophy is also considerably influenced by the amount of tissue fluids[245], which is increased by active inflammation and vasogenic edema in WM plaques, and decreased during treatment with agents with strong anti-inflammatory properties (pseudoatrophy effect)[245,246]. As per the results of the WIRMS study[142], more than half of the HW-treated patients demonstrated no new disease activity during the trial compared to about 28% in the placebo arm, suggesting that the HW probably had an anti-inflammatory effect. Voxel based Morphometry (VBM) analysis is an accurate method for the assessment of tissue-specific brain atrophy, that allows the comparison of local GM between groups of subjects involving the segmentation of brain volumes into GM, WM and CSF, normalization to a standard space, and GM atrophy quantification on a voxel-by-voxel basis.[151,247] The output comprises of a statistical parametric map (SPM) highlighting regions where there is a statistically significant difference in WM or GM among the groups.

The purpose of this study was to evaluate the difference in GM density in the MS patients recruited in the WIRMS trial. Although, the duration of the clinical trial is not long enough to observe an effect, we hypothesize higher GM atrophy in placebo-treated patients in the whole brain and specifically

in regions of GM atrophy (ROIs) unveiled by the coordinate-based meta-analysis[143].

5.2 Aim

The purpose of this VBM study was to investigate:

(i) Statistically significant differences in GM density of whole brain and a-priori defined ROIs, between groups (Placebo and HW) in the change from V7 (Figure 1; chapter 3) to V13(Figure 1; chapter 3), using general linear model (GLM).

(ii) GM density changes in ROIs between HW and Placebo groups, by extraction of GM density values.

5.3 Methods

5.3.1 Subjects

56 RRMS patients (28 HW, 28 Placebo) recruited in the WIRMS clinical trial, with complete data.

5.3.2 Structural MRI

3D axial T1-weighted fast spoiled gradient echo (1x1x1 mm isotropic, 256 x 256 x 156 matrix).

5.3.3 Data Analysis

All the structural MRI post-processing (**Figure 1**) was performed by a single observer. Whole brain and regional volumetry measurements were performed on the 3D T1-weighted images, using a standard VBM approach. The 3D MR datasets of all placebo and HW-treated patients were

processed using the following main steps: (i) normalization of all images to the MNI template. This was done by first estimating the optimum 12-variable affine transformation to match images and then optimizing the normalization using 16 nonlinear iterations. (ii) the spatially normalized images were segmented into GM, WM and CSF in accordance with the tissue probability maps. A nonlinear deformation field is estimated that best overlays the tissue probability maps on the individual subjects' image. The accuracy of the segmentation was assessed by examining axial slices of each subject's GM, WM and CSF image in the individual's space. The accuracy of warping was assessed by displaying axial slices from each subject with edges from the atlas image. (iii) The normalized GM images were modulated by the Jacobian determinants based on the voxel to compensate for the effect of spatial normalization, as it may result in volume changes due to affine transformation (global scaling) and non-linear warping (local volume change). (iv) The normalized and modulated GM images were smoothed using a 12 mm full-width half-maximum (FWHM) Gaussian kernel as done before[248].

Following the above steps, I used Randomise that is FSL's tool for nonparametric permutation inference on neuroimaging data. Randomization was performed in the whole brain as well as in ROIs using the following command:

randomise -i GM_mod_merg_s2 -o GM_mod_merg_s2 -d design.mat -t design.con -m GM_mask -n 5000 -T -V

where,

design.mat and design.con are text files containing the design matrix and list of contrasts respectively.

-n 5000 option facilitates **the command** to generate 'n' permutations of the data when building up the null distribution to test against.

-T option ensures that the test statistic is TFCE (threshold-free cluster enhancement).

This command runs randomise with the generation of tstat maps demonstrating the comparison between groups.

Further, ROIs were extracted for cortical/subcortical regions from NeuRoi. The randomization was performed in the whole brain as well as in ROIs. The corrected p value image was thresholded at 0.05 by setting the min to 0.95 and max to 1 in fslview. Further, the statistically significant clusters for the contrasts were highlighted in the whole brain and ROIs.

(1) The GM segmentation was binarized in the whole brain and in ROIs at 0.5, using fslmaths.
(2) The GM density values were extracted for each ROI, using fslmeants.

5.3.4 Defining ROIs

The defining of ROI was performed in NeuRoi by filtering the image of all clusters found, as a result of coordinate-based meta-analysis, to extract individual ROIs. This was done by setting the upper and lower threshold to the required cluster number.

5.3.5 Statistical analysis

An analysis of variance (ANOVA): 2-groups, 2-levels per subject (2-way Mixed Effect ANOVA) was used to compare GM volumetry measurements between the placebo and HW groups. The following a-priori contrasts were assessed: (1) Placebo vs HW, in the change from V7 to V13, (2) V7-V13. A family-wise error (FWE) correction at $p < 0.05$ for multiple comparisons at voxel level across the whole brain was used.

5.4 Results

The patients did not demonstrate any area of significant GM loss in the whole brain as well as in the ROIs when comparing HW and Placebo-treated patients, in the change from V7 to V13 (FWE correction for multiple comparisons, $p < 0.05$). **Figure 23** shows the scatter plots for GM density values in the two arms for the eight ROIs. **Figure 22** shows the ROIs constructed for the analysis. No statistically significant difference in GM density (**Table 4**) was observed between the two groups at V13.

Figure 22: Demonstration of ROIs constructed for the analyses; A. Right Thalamus B. Right Insula C. Right Precentral Gyrus D. Right Putamen E. Left Thalamus F. Left superior temporal gyrus G. Left Postcentral gyrus H. Left Putamen

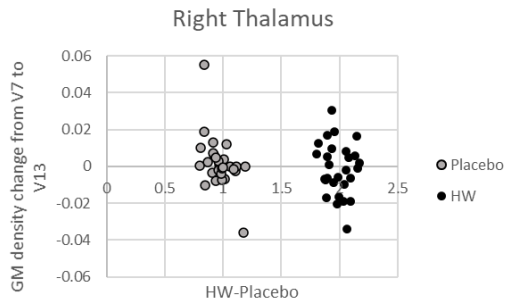
Right Thalamus
GM density change from V7 to V13
HW-Placebo
Placebo
HW

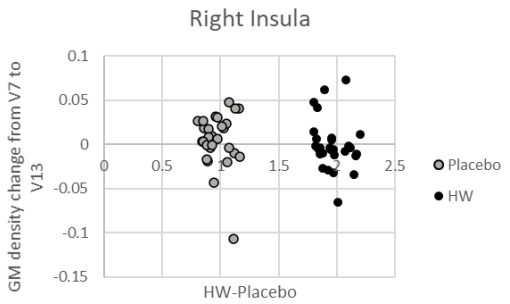
Right Insula
GM density change from V7 to V13
HW-Placebo
Placebo
HW

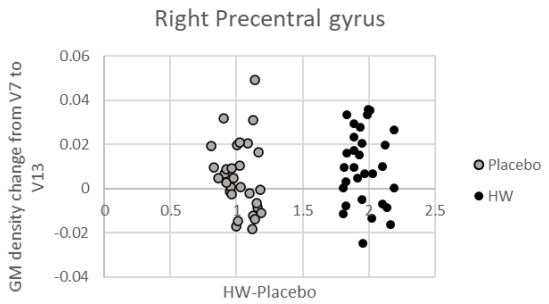
Right Precentral gyrus
GM density change from V7 to V13
HW-Placebo
Placebo
HW

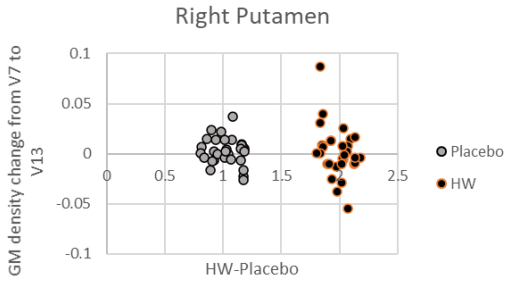
Right Putamen
GM density change from V7 to V13
HW-Placebo
Placebo
HW

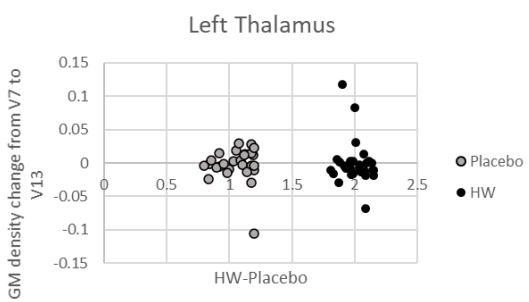
Left Thalamus
GM density change from V7 to V13
HW-Placebo
Placebo
HW

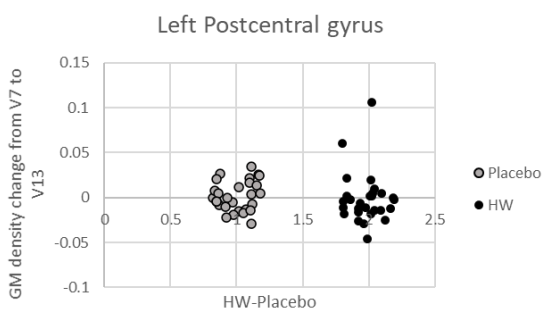
Left Postcentral gyrus
GM density change from V7 to V13
HW-Placebo
Placebo
HW

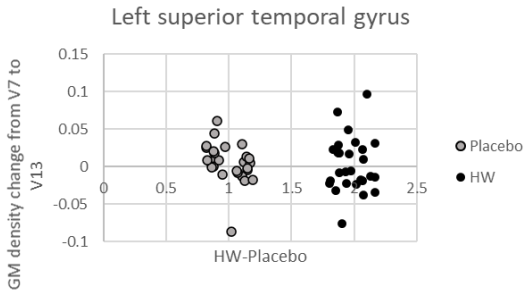
Left superior temporal gyrus
GM density change from V7 to V13
HW-Placebo
Placebo
HW

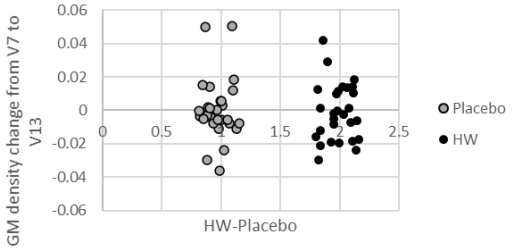
Left Putamen
GM density change from V7 to V13
HW-Placebo
Placebo
HW

Figure 23: Scatter plots demonstrating GM density values for the change from V7 to V13 in Placebo and HW groups for respective ROIs.

ROI	Mean (Placebo)	Mean (HW)	Difference of means	95% CI
Left Putamen	0.353	0.334	0.019	(0.003, 0.034)
Right Putamen	0.517	0.486	0.031	(0.01, 0.045)
Left Superior Temporal gyrus	0.417	0.403	0.015	(-0.003, 0.033)
Left Postcentral gyrus	0.270	0.258	0.012	(0.001, 0.023)
Left Thalamus	0.236	0.231	0.005	(-0.006, 0.017)
Right Thalamus	0.415	0.413	0.002	(-0.021,0.021)
Right Insula	0.403	0.363	0.040	(0.014, 0.066)
Left Precentral gyrus	0.272	0.257	0.015	(-0.0005, 0.030)

Table 4: Difference in GM density values between the two groups in each ROI with 95% confidence intervals.

5.5 Discussion

The key objective of this study was to define the change in GM density in the MS patients recruited as part of the WIRMS clinical trial, by means of VBM. In previous studies, it was hypothesized that regional GM atrophy occurs in MS and, they have demonstrated reduction of GM volume in several cortical and subcortical regions in MS patients[249–254]. In MS patients recruited in the trial, no statistically significant regions of difference in GM atrophy were observed in Placebo or HW-treated groups. The same result was observed in each of the ROIs. This result was expected because MS patients were treated with hookworms only for a period of 9 months and, this intervention period would not be enough to observe any difference in GM atrophy between the two groups. All disease-modifying treatments reduce the rate of brain volume loss and/or GM atrophy in RRMS.[255]
However, according to the hypothesis that HW have an anti-inflammatory effect, we would expect lesser GM atrophy in the HW arm and, some degree

of detectable atrophy would be expected in a non-treated/placebo-treated patient during this time-period.

The included subjects had hypointensities on T1-weighted MRI and, this factor might confound the GM segmentations. because of some of the T1 lesions having the same intensity as GM. For the reduction of potential technical biases when performing VBM analysis, masking of T1 lesions from the GM maps could be done in order to avoid misclassification of MS lesion as GM. Registration of the included scans looked reasonable as observed in movie mode for GM_mod_merg. The reason that a smoothing of 2mm was chosen is that, based on visual assessment of the imaging data, it provided a reasonable middle ground between removing noise and maintaining the underlying anatomy. In addition, a threshold of 50% was applied to the masks in order to ensure the inclusion of GM pixels exclusively.

Further, for calculating the sample sizes for the situation where a treatment preserves 20% of the GM density, the calculated sample size (80% power; 1-sided test) for each ROI is shown in Table 5.

ROI	Standardized effect sizes/5	Sample size (80% power; 1-sided test)
Right Thalamus	0.254	192
Left Thalamus	0.252	195
Let Putamen	0.192	336
Left Superior temporal gyrus/Insula	0.17	428
Right Superior temporal gyrus/Insula	0.168	439
Right Postcentral gyrus	0.174	409
Left Pre- and Postcentral Gyrus	0.138	650

Right Putamen	0.16	484

Table 5: Sample size for each ROI for 20% preservation in GM density.

Chapter 6

General Discussion and Conclusions

The predominant, although sometimes confronted, view specifies MS to be an autoimmune disease in which immunopathology in the CNS undertakes a central role[256]. Regarding a specific autoimmunity mechanism in MS, many authors have favoured a primary abnormality of immunoregulation. In MS, there is a numerical or functional deficit of Treg cells, and DMT increases Treg cell number as well as activity.[257] Elevated inflammatory responses may reflect defective immunoregulation[258].

If microbial deprivation according to hygiene hypothesis, causes abnormal immunoregulation and if helminths have the ability to promote normal immunoregulation, the question that naturally would arise is whether controlled helminth infection might be therapeutic in MS and related conditions.44

The WIRMS research project involved the analysis of new disease activity in the recruited RRMS patients. This was done by the observation of newly enhancing T1, new T2 and enlarging T2 lesions on MR images and was the primary outcome of the clinical trial. In addition, I looked at the contrast-enhancing T1 lesions, T2 lesion load and total lesion volume at baseline in the two arms. As controlled helminth infection has the potential to lead to immune regulation, the disease activity was analysed in recruited relapsing MS patients with the utilization of MRI (primary outcome of the clinical trial). The clinical study did not detect a difference between the cumulative number of active MRI lesions in the placebo and hookworm (HW) groups. However, the higher proportion of scans with no new disease activity in the HW group suggests a beneficial effect.

A subsequent clinical trial of HW infection should be conducted, as this phase 2 clinical trial showed a satisfactory safety profile. However, it would require higher power and will need to examine larger cohorts of patients.

In the next chapter, a Coordinate-Based Meta-Analysis, Meta-Analysis of Networks, and Meta-Regression of Voxel-Based Morphometry studies[143] has been conducted to examine the influence that MS/CIS has on GM atrophy. This meta-analysis found eight significant clusters of GM atrophy in MS and CIS. These regions involved basal ganglia and the cortex. ClusterZ found 3 clusters with significant correlation for MS disease duration in the bilateral Thalamus and Left claustrum/putamen/insula and 1 cluster with significant correlation for age in the Left Thalamus.

GM tissue damage is an important pathological process in MS that underlies neurological disability.[123] Previous literature shows differences in GM atrophy between MS subtypes involving a selective myriad of brain regions along with an increased extent of atrophy in common regions, such as the thalamus, in the progressive phase of the disease.[259]

The CBMA results comprise of clusters of coordinates located where significant effect has been reported in similar anatomical locations, consistently by studies. This represents the concordance of brain structures reported along with indication of their relevance. Consistent reported coordinates are determined statistically relative to a null hypothesis that the coordinates in different studies are independent. The results provided by this study provide a quantitative summary of published evidence for a common pattern of regional GM atrophy in MS and CIS.

When we compare the effect sizes for the primary metaanalysis and subanalyses in this study, the effect sizes get reduced in the subanalyses and the p values get larger. The effect sizes get decreased in the case when the number of studies, which contribute to a cluster, is small. So, as the number of subanalysis studies contributing to the defined clusters (by

all studies) become less, the effect sizes also get small. However, the p values are bigger for the subanalyses. This is because of the small number of subanalysis studies contributing to a cluster and, therefore, lower significance.

The metaregression performed here with ClusterZ is a novel technique. The post hoc regression conducted performs a mean analysis to reveal the clusters with a significant mean. Further, it performs regression analysis only in the revealed clusters. For Metaregression of disease duration, I have removed the CIS studies (4) due to a disease duration of zero or few months.

I tried to perform meta-regression tests on global GM volumes, brain parenchymal fraction, Multiple Sclerosis Functional Composite (MSFC), PASAT scores, years of education (Supplementary Table 1) and disease-modifying therapy administered (Supplementary Table 2) but could not do that due to unavailability of the respective values in all included studies.

Further, as an application of the regions of interest (ROI) found for GM atrophy, voxel-based morphometry (VBM) was conducted on 3D T1-weighted MR scans acquired from relapsing MS patients recruited in the WIRMS clinical trial. This involved the analysis of GM density change in the two arms, during the period of intervention.

Therefore, the outcome of the subsequent clinical study should involve GM volume change, along with WM disease activity. Although MS is classically considered a WM disease, the involvement of GM in the pathogenic process has been confirmed by pathology studies and MRI studies.[190] The phase III trial of HW in relapsing MS will examine the effect of immunoregulation on WM lesions as well as regional GM atrophy, over a longer period of intervention.

Conclusion

The WIRMS clinical trial proved that treatment with hookworm was safe and well tolerated. The primary outcome did not reach significance, likely because of a low level of disease activity. An increase in T regs was observed with HW infection, suggesting an immunobiological effect of HW.

The CBMA of VBM studies of MS and CIS has identified a pattern of related cortical and
subcortical GM atrophy. Relationships are indicated by the covariance of reported statistical effects. Disease duration was found to be a significant covariate of the standardised reported effect sizes in the thalamic clusters and a cluster covering the left claustrum/putamen/insula.

The VBM experiment did not find any statistically significant difference in GM density, between the placebo and hookworm arms, in the whole brain as well as in ROIs.

Chapter 7

Future Directions

7.1 WIRMS clinical study

A phase III clinical trial with higher power can be designed with a focus on WM as well as GM involvement in MS or CIS can be conducted.

A subsequent clinical trial of hookworm (HW) infection should be conducted as this phase 2 clinical trial showed a satisfactory safety profile. However, it would require higher power and will need to examine larger cohorts of patients. With probability in group 1 (HW) = 0.43 and in group 2 (Placebo) = 0.69; calculated by the number of patients with active MRI divided by the total number of patients in the group; the total sample size required is 105 i.e., 52 per group. Also, it would be a good option to power the study by the number of patients with no new disease activity, instead of calculating new lesions.

Additionally, the study can be conducted by utilizing the data from the current study for the detection of biological differences between: (1) HW-treated patients with negative or positive disease activity (binary outcome); (2) HW-treated patients with reduction or stabilization of total lesion volume.

7.2 Localised Grey Matter Atrophy in Multiple Sclerosis and Clinically Isolated Syndrome—A Coordinate-Based Meta-

Analysis, Meta-Analysis of Networks, and Meta Regression of Voxel-Based Morphometry Studies

GM atrophy regions involving the dorsal striatum, primary motor cortex, primary somatosensory cortex, insular cortex, auditory cortex and the relay station of the brain were identified cortically and subcortically in MS or CIS. The regions demonstrating significant effect sizes involved cortical and DGM regions, namely- bilateral Thalamus, Superior temporal gyrus (L), bilateral Putamen, Postcentral gyrus (L), Precentral gyrus (R) and Insula (R).

Further, a network Meta-analysis has been conducted[143], that works on the assumption that in case of the activation pattern reported by independent studies being consistent, the relative magnitude of these Z scores might also show consistency.

The estimated statistical effect sizes may be important for powering prospective studies of GM atrophy in MS to test specific hypotheses and can be used as outcome measures of immunomodulatory or neuroprotective clinical trials.

The strengths of this meta-analysis involve the utilization of ClusterZ algorithm, with the novelty of meta-regression. The use of standardized effect sizes makes meta-regression possible by looking for significant correlation between a specified covariate and the standardized effect size in each cluster.

7.2.1 Limitations

A well-done meta-analysis of badly designed studies is bound to yield invalid results. Primary studies dealing with bias and confounding might cause major problems for meta-analysis. In order to avoid the problem of including low quality studies, differences in study quality could have been explored by the meta-analysts. This could be done by applying sensitivity

analysis, by assessment of the effect of excluding studies with certain methodological weaknesses on the summary effect in the meta-analysis.

7.3 Voxel-based morphometry

Previous imaging studies conducted to assess the relationship between WM damage and GM atrophy have raised the concern of MS WM lesions having an effect on measures of GM volume by inducing voxel misclassification during intensity-based tissue segmentation.[260]

Considering the bias that hypointense WM lesions can have on tissue segmentation, lesion masks can be created followed by lesion filling. Optimised VBM protocol[247] can be adopted for the assessment of GM density alterations in MS.

There are cases when normalization might result in the misinterpretation of structural differences, not directly related to GM or WM volumes, as volumetric differences. An example would be when the size of the ventricles differs significantly between two or more experimental groups. If the ventricles of one experimental group are enlarged during normalisation, the surrounding GM and WM also may be enlarged. This is because the parameters of the normalisation only encode highly smooth, low frequency deformations which may not distinguish between the ventricles and the surrounding tissue. As a result, structural differences pertaining to ventricular volume may show up in a VBM study of GM volumes. A way of minimizing this potential source of error is to perform the normalisation using the segmented GM and WM volumes rather than on the whole brain images. If all the data entering into the statistical analysis are only derived from GM, then any significant differences must be due to GM. The limitation of this approach, however, would be that the segmentation will be required to be performed on images in native space.

However the Bayesian priors, which encode a priori knowledge about the spatial distribution of different tissues in normal subjects, are in stereotactic space. A way of sidestepping this problem is to use an iterative version of segmentation and normalisation operators. First, the original structural MRI images in native space are segmented. The resulting GM an WM images are then spatially normalized to GM and WM templates respectively to derive the optimized normalisation parameters. These parameters are further applied to the original, whole-brain structural images in native space prior to a new segmentation. This procedure, also known as “optimized VBM”, will have the effect of reduction in the misinterpretation of significant differences relative to “standard VBM”.[247]

FSL-SIENA[261] can be employed, in combination with BEaST: Brain Extraction Based on Nonlocal Segmentation Technique[262], to examine the longitudinal brain volume change over the course of intervention.

The GLM also allows the identification of regions of GM concentration that are related to specified covariates. As a further research project, the relation of GM concentration to disease duration and age, that are statistically significant covariates as revealed by the CBMAN conducted, can be applied.

The overarching hypothesis behind the thesis is that regional GM atrophy exists in MS or CIS, along with alterations in WM lesions. Although, the results of the Coordinate-Based Meta-Analysis, Meta-Analysis of Networks, and Meta Regression of Voxel-Based Morphometry Studies can be utlised for the development of a potential biomarker for neurodegeneration based on patterns of regional brain atrophy, the results from the VBM study could not be helpful due to the duration of the WIRMS clinical trial. However, future interventional trials (including possibly hookworm trials) may be designed prospectively to assess the effects of the intervention on the GM regions that we identified through our analysis to determine a potential neuroprotective effect.

Here, the recommendation refers to a further Phase 2 study to provide additional rationale for Phase 3.

1. Weinshenker, B. G. *et al.* The natural history of multiple sclerosis: a geographically based study. I. Clinical course and disability. *Brain J. Neurol.* **112 (Pt 1)**, 133–146 (1989).
2. Confavreux, C. & Vukusic, S. Natural history of multiple sclerosis: a unifying concept. *Brain J. Neurol.* **129**, 606–616 (2006).
3. Confavreux, C., Vukusic, S. & Adeleine, P. Early clinical predictors and progression of irreversible disability in multiple sclerosis: an amnesic process. *Brain J. Neurol.* **126**, 770–782 (2003).
4. Tremlett, H., Yinshan Zhao, null & Devonshire, V. Natural history of secondary-progressive multiple sclerosis. *Mult. Scler. Houndmills Basingstoke Engl.* **14**, 314–324 (2008).
5. Vukusic, S. *et al.* Pregnancy and multiple sclerosis (the PRIMS study): clinical predictors of post-partum relapse. *Brain J. Neurol.* **127**, 1353–1360 (2004).
6. Ysrraelit, M. C. & Correale, J. Impact of sex hormones on immune function and multiple sclerosis development. *Immunology* **156**, 9–22 (2019).
7. Edwards, S., Zvartau, M., Clarke, H., Irving, W. & Blumhardt, L. D. Clinical relapses and disease activity on magnetic resonance imaging associated with viral upper respiratory tract infections in multiple sclerosis. *J. Neurol. Neurosurg. Psychiatry* **64**, 736–741 (1998).
8. Panitch, H. S. Influence of infection on exacerbations of multiple sclerosis. *Ann. Neurol.* **36 Suppl**, S25-28 (1994).
9. Merelli, E. & Casoni, F. Prognostic factors in multiple sclerosis: role of intercurrent infections and vaccinations against influenza and hepatitis B.

Neurol. Sci. Off. J. Ital. Neurol. Soc. Ital. Soc. Clin. Neurophysiol. **21**, S853-856 (2000).

10. Jörg, S. *et al.* Environmental factors in autoimmune diseases and their role in multiple sclerosis. *Cell. Mol. Life Sci. CMLS* **73**, 4611–4622 (2016).

11. Marcus, J. F. & Waubant, E. L. Updates on clinically isolated syndrome and diagnostic criteria for multiple sclerosis. *The Neurohospitalist* **3**, 65–80 (2013).

12. Peterson, J. W., Bö, L., Mörk, S., Chang, A. & Trapp, B. D. Transected neurites, apoptotic neurons, and reduced inflammation in cortical multiple sclerosis lesions. *Ann. Neurol.* **50**, 389–400 (2001).

13. Goverman, J. Autoimmune T cell responses in the central nervous system. *Nat. Rev. Immunol.* **9**, 393–407 (2009).

14. Legroux, L. & Arbour, N. Multiple Sclerosis and T Lymphocytes: An Entangled Story. *J. Neuroimmune Pharmacol. Off. J. Soc. NeuroImmune Pharmacol.* **10**, 528–546 (2015).

15. Francis, D. A., Bain, P., Swan, A. V. & Hughes, R. A. An assessment of disability rating scales used in multiple sclerosis. *Arch. Neurol.* **48**, 299–301 (1991).

16. Meyer-Moock, S., Feng, Y.-S., Maeurer, M., Dippel, F.-W. & Kohlmann, T. Systematic literature review and validity evaluation of the Expanded Disability Status Scale (EDSS) and the Multiple Sclerosis Functional Composite (MSFC) in patients with multiple sclerosis. *BMC Neurol.* **14**, 58 (2014).

17. Çinar, B. P. & Yorgun, Y. G. What We Learned from The History of Multiple Sclerosis Measurement: Expanded Disability Status Scale. *Arch. Neuropsychiatry* **55**, S69–S75 (2018).

18. Dutta, R. & Trapp, B. D. Relapsing and progressive forms of multiple sclerosis – insights from pathology. *Curr. Opin. Neurol.* **27**, 271–278 (2014).

19. Katz Sand, I., Krieger, S., Farrell, C. & Miller, A. E. Diagnostic uncertainty during the transition to secondary progressive multiple sclerosis. *Mult. Scler. Houndmills Basingstoke Engl.* **20**, 1654–1657 (2014).

20. Browne, P. *et al.* Atlas of Multiple Sclerosis 2013: A growing global problem with widespread inequity. *Neurology* **83**, 1022–1024 (2014).

21. Kingwell, E. *et al.* Incidence and prevalence of multiple sclerosis in Europe: a systematic review. *BMC Neurol.* **13**, 128 (2013).

22. Ahmed, S. I., Aziz, K., Gul, A., Samar, S. S. & Bareeqa, S. B. Risk of Multiple Sclerosis in Epstein-Barr Virus Infection. *Cureus* **11**, e5699 (2019).

23. Simpson, S., Blizzard, L., Otahal, P., Van der Mei, I. & Taylor, B. Latitude is significantly associated with the prevalence of multiple sclerosis: a meta-analysis. *J. Neurol. Neurosurg. Psychiatry* **82**, 1132–1141 (2011).

24. Handel, A. E. *et al.* Smoking and multiple sclerosis: an updated meta-analysis. *PloS One* **6**, e16149 (2011).

25. Ramagopalan, S. V., Dobson, R., Meier, U. C. & Giovannoni, G. Multiple sclerosis: risk factors, prodromes, and potential causal pathways. *Lancet Neurol.* **9**, 727–739 (2010).

26. Belbasis, L., Bellou, V., Evangelou, E., Ioannidis, J. P. A. & Tzoulaki, I. Environmental risk factors and multiple sclerosis: an umbrella review of systematic reviews and meta-analyses. *Lancet Neurol.* **14**, 263–273 (2015).

27. Higgins, J. P. T. Commentary: Heterogeneity in meta-analysis should be expected and appropriately quantified. *Int. J. Epidemiol.* **37**, 1158–1160 (2008).

28. Higgins, J. P. T., Thompson, S. G. & Spiegelhalter, D. J. A re-evaluation of random-effects meta-analysis. *J. R. Stat. Soc. Ser. A Stat. Soc.* **172**, 137–159 (2009).

29. Chinn, S. A simple method for converting an odds ratio to effect size for use in meta-analysis. *Stat. Med.* **19**, 3127–3131 (2000).

30. Artemiadis, A. K., Anagnostouli, M. C. & Alexopoulos, E. C. Stress as a risk factor for multiple sclerosis onset or relapse: a systematic review. *Neuroepidemiology* **36**, 109–120 (2011).

31. Zhornitsky, S., Yong, V. W., Weiss, S. & Metz, L. M. Prolactin in multiple sclerosis. *Mult. Scler. Houndmills Basingstoke Engl.* **19**, 15–23 (2013).

32. Goulden, R., Ibrahim, T. & Wolfson, C. Is high socioeconomic status a risk factor for multiple sclerosis? A systematic review. *Eur. J. Neurol.* **22**, 899–911 (2015).

33. Ascherio, A., Munger, K. L. & Lünemann, J. D. The initiation and prevention of multiple sclerosis. *Nat. Rev. Neurol.* **8**, 602–612 (2012).

34. International Multiple Sclerosis Genetics Consortium *et al.* Genetic risk and a primary role for cell-mediated immune mechanisms in multiple sclerosis. *Nature* **476**, 214–219 (2011).

35. Bv, T. The major cause of multiple sclerosis is environmental: genetics has a minor role--yes. *Mult. Scler. Houndmills Basingstoke Engl.* **17**, 1171–1173 (2011).

36. Ascherio, A. & Munger, K. L. Environmental risk factors for multiple sclerosis. Part I: the role of infection. *Ann. Neurol.* **61**, 288–299 (2007).

37. Manouchehrinia, A. *et al.* Tobacco smoking and disability progression in multiple sclerosis: United Kingdom cohort study. *Brain J. Neurol.* **136**, 2298–2304 (2013).

38. Ponsonby, A.-L. *et al.* Exposure to infant siblings during early life and risk of multiple sclerosis. *JAMA* **293**, 463–469 (2005).

39. Poser, C. M. *et al.* New diagnostic criteria for multiple sclerosis: guidelines for research protocols. *Ann. Neurol.* **13**, 227–231 (1983).

40. van der Mei, I. a. F. *et al.* Past exposure to sun, skin phenotype, and risk of multiple sclerosis: case-control study. *BMJ* **327**, 316 (2003).

41. Levin, L. I. *et al.* Multiple sclerosis and Epstein-Barr virus. *JAMA* **289**, 1533–1536 (2003).

42. Pittas, F. *et al.* Smoking is associated with progressive disease course and increased progression in clinical disability in a prospective cohort of people with multiple sclerosis. *J. Neurol.* **256**, 577–585 (2009).

43. Sintzel, M. B., Rametta, M. & Reder, A. T. Vitamin D and Multiple Sclerosis: A Comprehensive Review. *Neurol. Ther.* **7**, 59–85 (2017).

44. Fleming, J. O. Helminth therapy and multiple sclerosis. *Int. J. Parasitol.* **43**, 259–274 (2013).

45. Correale, J. & Gaitán, M. I. Multiple sclerosis and environmental factors: the role of vitamin D, parasites, and Epstein-Barr virus infection. *Acta Neurol. Scand.* **132**, 46–55 (2015).

46. Zaccone, P., Fehervari, Z., Phillips, J. M., Dunne, D. W. & Cooke, A. Parasitic worms and inflammatory diseases. *Parasite Immunol.* **28**, 515–523 (2006).

47. Cabre, P. *et al.* Role of return migration in the emergence of multiple sclerosis in the French West Indies. *Brain J. Neurol.* **128**, 2899–2910 (2005).

48. Fleming, J. O. & Cook, T. D. Multiple sclerosis and the hygiene hypothesis. *Neurology* **67**, 2085–2086 (2006).

49. Correale, J. & Farez, M. F. The impact of parasite infections on the course of multiple sclerosis. *J. Neuroimmunol.* **233**, 6–11 (2011).

50. Runge, V. M. *et al.* Initial clinical evaluation of gadolinium DTPA for contrast-enhanced magnetic resonance imaging. *Magn. Reson. Imaging* **3**, 27–35 (1985).

51. McQuaid, S., Cunnea, P., McMahon, J. & Fitzgerald, U. The effects of blood-brain barrier disruption on glial cell function in multiple sclerosis. *Biochem. Soc. Trans.* **37**, 329–331 (2009).

52. Filippi, M., Rocca, M. A., Martino, G., Horsfield, M. A. & Comi, G. Magnetization transfer changes in the normal appearing white matter precede the appearance of enhancing lesions in patients with multiple sclerosis. *Ann. Neurol.* **43**, 809–814 (1998).

53. Werring, D. J. *et al.* The pathogenesis of lesions and normal-appearing white matter changes in multiple sclerosis: a serial diffusion MRI study. *Brain J. Neurol.* **123 (Pt 8)**, 1667–1676 (2000).

54. Goodkin, D. E. *et al.* A serial study of new MS lesions and the white matter from which they arise. *Neurology* **51**, 1689–1697 (1998).

55. Fahrbach, K. *et al.* Relating relapse and T2 lesion changes to disability progression in multiple sclerosis: a systematic literature review and regression analysis. *BMC Neurol.* **13**, 180 (2013).

56. Scalfari, A., Neuhaus, A., Daumer, M., Muraro, P. A. & Ebers, G. C. Onset of secondary progressive phase and long-term evolution of multiple sclerosis. *J. Neurol. Neurosurg. Psychiatry* **85**, 67–75 (2014).

57. Friese, M. A., Schattling, B. & Fugger, L. Mechanisms of neurodegeneration and axonal dysfunction in multiple sclerosis. *Nat. Rev. Neurol.* **10**, 225–238 (2014).

58. Nikić, I. *et al.* A reversible form of axon damage in experimental autoimmune encephalomyelitis and multiple sclerosis. *Nat. Med.* **17**, 495–499 (2011).

59. Sorbara, C. D. *et al.* Pervasive axonal transport deficits in multiple sclerosis models. *Neuron* **84**, 1183–1190 (2014).

60. Leray, E. *et al.* Evidence for a two-stage disability progression in multiple sclerosis. *Brain* **133**, 1900 (2010).

61. Zéphir, H. Progress in understanding the pathophysiology of multiple sclerosis. *Rev. Neurol. (Paris)* **174**, 358–363 (2018).

62. Kuhlmann, T., Lingfeld, G., Bitsch, A., Schuchardt, J. & Brück, W. Acute axonal damage in multiple sclerosis is most extensive in early disease stages and decreases over time. *Brain J. Neurol.* **125**, 2202–2212 (2002).

63. Anderton, S. M. & Liblau, R. S. Regulatory T cells in the control of inflammatory demyelinating diseases of the central nervous system. *Curr. Opin. Neurol.* **21**, 248–254 (2008).

64. Murphy, E. L. Multiple sclerosis. By McAlpine, Compston, and Lumsden. *Ir. J. Med. Sci. 1926-1967* **30**, 370–370 (1955).

65. Lublin, F. D. & Reingold, S. C. Defining the clinical course of multiple sclerosis: results of an international survey. National Multiple Sclerosis Society (USA) Advisory Committee on Clinical Trials of New Agents in Multiple Sclerosis. *Neurology* **46**, 907–911 (1996).

66. Paz Soldán, M. M. *et al.* Relapses and disability accumulation in progressive multiple sclerosis. *Neurology* **84**, 81–88 (2015).

67. Montalban, X. *et al.* Ocrelizumab versus Placebo in Primary Progressive Multiple Sclerosis. *N. Engl. J. Med.* **376**, 209–220 (2017).

68. Hawker, K. *et al.* Rituximab in patients with primary progressive multiple sclerosis: results of a randomized double-blind placebo-controlled multicenter trial. *Ann. Neurol.* **66**, 460–471 (2009).

69. Lublin, F. D. & Reingold, S. C. Defining the clinical course of multiple sclerosis: results of an international survey. National Multiple Sclerosis Society (USA) Advisory Committee on Clinical Trials of New Agents in Multiple Sclerosis. *Neurology* **46**, 907–911 (1996).

70. Polman, C. H. *et al.* Diagnostic criteria for multiple sclerosis: 2010 Revisions to the McDonald criteria. *Ann. Neurol.* **69**, 292–302 (2011).

71. McDonald, W. I. *et al.* Recommended diagnostic criteria for multiple sclerosis: guidelines from the International Panel on the diagnosis of multiple sclerosis. *Ann. Neurol.* **50**, 121–127 (2001).

72. Miller, D. H., Chard, D. T. & Ciccarelli, O. Clinically isolated syndromes. *Lancet Neurol.* **11**, 157–169 (2012).

73. Mathey, G., Michaud, M., Pittion-Vouyovitch, S. & Debouverie, M. Classification and diagnostic criteria for demyelinating diseases of the central nervous system: Where do we stand today? *Rev. Neurol. (Paris)* **174**, 378–390 (2018).

74. Kurtzke, J. F. *et al.* STUDIES ON THE NATURAL HISTORY OF MULTIPLE SCLEROSIS: 7. Correlates of Clinical Change in an Early Bout. *Acta Neurol. Scand.* **49**, 379–395 (1973).

75. Polman, C. H. *et al.* Diagnostic criteria for multiple sclerosis: 2005 revisions to the 'McDonald Criteria'. *Ann. Neurol.* **58**, 840–846 (2005).

76. Eriksson, M., Andersen, O. & Runmarker, B. Long-term follow up of patients with clinically isolated syndromes, relapsing-remitting and secondary

progressive multiple sclerosis. *Mult. Scler. Houndmills Basingstoke Engl.* **9**, 260–274 (2003).

77. Confavreux, C., Vukusic, S., Moreau, T. & Adeleine, P. Relapses and progression of disability in multiple sclerosis. *N. Engl. J. Med.* **343**, 1430–1438 (2000).

78. Martinelli, V. *et al.* Multiple biomarkers improve the prediction of multiple sclerosis in clinically isolated syndromes. *Acta Neurol. Scand.* **136**, 454–461 (2017).

79. Thompson, A. J. *et al.* Diagnosis of multiple sclerosis: 2017 revisions of the McDonald criteria. *Lancet Neurol.* **17**, 162–173 (2018).

80. Confavreux, C., Aimard, G. & Devic, M. Course and prognosis of multiple sclerosis assessed by the computerized data processing of 349 patients. *Brain J. Neurol.* **103**, 281–300 (1980).

81. Filippi, M. *et al.* Quantitative brain MRI lesion load predicts the course of clinically isolated syndromes suggestive of multiple sclerosis. *Neurology* **44**, 635–641 (1994).

82. Barkhof, F. *et al.* Comparison of MRI criteria at first presentation to predict conversion to clinically definite multiple sclerosis. *Brain J. Neurol.* **120 (Pt 11)**, 2059–2069 (1997).

83. CHAMPS Study Group. MRI predictors of early conversion to clinically definite MS in the CHAMPS placebo group. *Neurology* **59**, 998–1005 (2002).

84. Brex, P. A. *et al.* Assessing the risk of early multiple sclerosis in patients with clinically isolated syndromes: the role of a follow up MRI. *J. Neurol. Neurosurg. Psychiatry* **70**, 390–393 (2001).

85. Waldman, A. *et al.* Pediatric multiple sclerosis: Clinical features and outcome. *Neurology* **87**, S74-81 (2016).

86. Institute of Medicine (US) Committee on Multiple Sclerosis: Current Status and Strategies for the Future. *Multiple Sclerosis: Current Status and Strategies for the Future*. (National Academies Press (US), 2001).

87. Amato, M. P., Ponziani, G., Bartolozzi, M. L. & Siracusa, G. A prospective study on the natural history of multiple sclerosis: clues to the conduct and interpretation of clinical trials. *J. Neurol. Sci.* **168**, 96–106 (1999).

88. Bakshi, R., Minagar, A., Jaisani, Z. & Wolinsky, J. S. Imaging of Multiple Sclerosis: Role in Neurotherapeutics. *NeuroRx* **2**, 277–303 (2005).

89. Miller, D. H. *et al.* Role of magnetic resonance imaging within diagnostic criteria for multiple sclerosis. *Ann. Neurol.* **56**, 273–278 (2004).

90. Filippi, M. *et al.* Assessment of lesions on magnetic resonance imaging in multiple sclerosis: practical guidelines. *Brain J. Neurol.* **142**, 1858–1875 (2019).

91. Cotton, F., Weiner, H. L., Jolesz, F. A. & Guttmann, C. R. G. MRI contrast uptake in new lesions in relapsing-remitting MS followed at weekly intervals. *Neurology* **60**, 640–646 (2003).

92. Miller, D. H. *et al.* Serial gadolinium enhanced magnetic resonance imaging in multiple sclerosis. *Brain J. Neurol.* **111 (Pt 4)**, 927–939 (1988).

93. Simon, J. H. *et al.* Standardized MR imaging protocol for multiple sclerosis: Consortium of MS Centers consensus guidelines. *AJNR Am. J. Neuroradiol.* **27**, 455–461 (2006).

94. Filippi, M. *et al.* Magnetic resonance techniques in multiple sclerosis: the present and the future. *Arch. Neurol.* **68**, 1514–1520 (2011).

95. Stankiewicz, J. M. *et al.* Brain MRI lesion load at 1.5T and 3T vs. clinical status in multiple sclerosis. *J. Neuroimaging Off. J. Am. Soc. Neuroimaging* **21**, e50–e56 (2011).

96. Wattjes, M. P. *et al.* Does high field MRI allow an earlier diagnosis of multiple sclerosis? *J. Neurol.* **255**, 1159–1163 (2008).

97. Filippi, M. *et al.* MRI criteria for the diagnosis of multiple sclerosis: MAGNIMS consensus guidelines. *Lancet Neurol.* **15**, 292–303 (2016).

98. Rovira, À. *et al.* Evidence-based guidelines: MAGNIMS consensus guidelines on the use of MRI in multiple sclerosis-clinical implementation in the diagnostic process. *Nat. Rev. Neurol.* **11**, 471–482 (2015).

99. Solomon, A. J., Naismith, R. T. & Cross, A. H. Misdiagnosis of multiple sclerosis: Impact of the 2017 McDonald criteria on clinical practice. *Neurology* **92**, 26–33 (2019).

100. Absinta, M. *et al.* Seven-tesla phase imaging of acute multiple sclerosis lesions: a new window into the inflammatory process. *Ann. Neurol.* **74**, 669–678 (2013).

101. Louapre, C. *et al.* Beyond focal cortical lesions in MS. *Neurology* **85**, 1702–1709 (2015).

102. George, I. C. *et al.* Clinical 3-tesla FLAIR* MRI improves diagnostic accuracy in multiple sclerosis. *Mult. Scler. Houndmills Basingstoke Engl.* **22**, 1578–1586 (2016).

103. Kaunzner, U. W. & Gauthier, S. A. MRI in the assessment and monitoring of multiple sclerosis: an update on best practice. *Ther. Adv. Neurol. Disord.* **10**, 247–261 (2017).

104. Lai, M. *et al.* A preliminary study into the sensitivity of disease activity detection by serial weekly magnetic resonance imaging in multiple sclerosis. *J. Neurol. Neurosurg. Psychiatry* **60**, 339–341 (1996).

105. Bakshi, R., Hutton, G. J., Miller, J. R. & Radue, E.-W. The use of magnetic resonance imaging in the diagnosis and long-term management of multiple sclerosis. *Neurology* **63**, S3-11 (2004).

106. Bagnato, F. *et al.* Evolution of T1 black holes in patients with multiple sclerosis imaged monthly for 4 years. *Brain J. Neurol.* **126**, 1782–1789 (2003).

107. Barkhof, F. *et al.* Remyelinated lesions in multiple sclerosis: magnetic resonance image appearance. *Arch. Neurol.* **60**, 1073–1081 (2003).

108. Masdeu, J. C. *et al.* Open-ring imaging sign: highly specific for atypical brain demyelination. *Neurology* **54**, 1427–1433 (2000).

109. Filippi, M., Wolinsky, J. S., Sormani, M. P. & Comi, G. Enhancement frequency decreases with increasing age in relapsing-remitting multiple sclerosis. *Neurology* **56**, 422–423 (2001).

110. Laule, C. *et al.* Evolution of focal and diffuse magnetisation transfer abnormalities in multiple sclerosis. *J. Neurol.* **250**, 924–931 (2003).

111. Sormani, M. P. & Bruzzi, P. MRI lesions as a surrogate for relapses in multiple sclerosis: a meta-analysis of randomised trials. *Lancet Neurol.* **12**, 669–676 (2013).

112. Bermel, R. A. *et al.* Predictors of long-term outcome in multiple sclerosis patients treated with interferon β. *Ann. Neurol.* **73**, 95–103 (2013).

113. Giovannoni, G. *et al.* Is it time to target no evident disease activity (NEDA) in multiple sclerosis? *Mult. Scler. Relat. Disord.* **4**, 329–333 (2015).

114. Kappos, L. *et al.* Inclusion of brain volume loss in a revised measure of 'no evidence of disease activity' (NEDA-4) in relapsing-remitting multiple sclerosis. *Mult. Scler. Houndmills Basingstoke Engl.* **22**, 1297–1305 (2016).

115. Rotstein, D. L., Healy, B. C., Malik, M. T., Chitnis, T. & Weiner, H. L. Evaluation of no evidence of disease activity in a 7-year longitudinal multiple sclerosis cohort. *JAMA Neurol.* **72**, 152–158 (2015).

116. Calabrese, M. *et al.* Detection of cortical inflammatory lesions by double inversion recovery magnetic resonance imaging in patients with multiple sclerosis. *Arch. Neurol.* **64**, 1416–1422 (2007).

117. Calabrese, M. & Gallo, P. Magnetic resonance evidence of cortical onset of multiple sclerosis. *Mult. Scler. Houndmills Basingstoke Engl.* **15**, 933–941 (2009).

118. Giorgio, A. *et al.* Cortical lesions in radiologically isolated syndrome. *Neurology* **77**, 1896–1899 (2011).

119. Audoin, B. *et al.* Atrophy mainly affects the limbic system and the deep grey matter at the first stage of multiple sclerosis. *J. Neurol. Neurosurg. Psychiatry* **81**, 690–695 (2010).

120. Calabrese, M. *et al.* The predictive value of gray matter atrophy in clinically isolated syndromes. *Neurology* **77**, 257–263 (2011).

121. Rocca, M. A. *et al.* Brain MRI atrophy quantification in MS. *Neurology* **88**, 403–413 (2017).

122. Calabrese, M. *et al.* Cortical atrophy is relevant in multiple sclerosis at clinical onset. *J. Neurol.* **254**, 1212 (2007).

123. Fisher, E., Lee, J. C., Nakamura, K. & Rudick, R. A. Gray matter atrophy in multiple sclerosis: a longitudinal study. *Ann. Neurol.* **64**, 255–65 (2008).

124. Bishop, C. A. *et al.* Analysis of ageing-associated grey matter volume in patients with multiple sclerosis shows excess atrophy in subcortical regions. *NeuroImage Clin.* **13**, 9–15 (2016).

125. Bergsland, N. *et al.* Subcortical and cortical gray matter atrophy in a large sample of patients with clinically isolated syndrome and early relapsing-remitting multiple sclerosis. *AJNR Am J Neuroradiol* **33**, 1573–8 (2012).

126. Sicotte, N. L. *et al.* Regional hippocampal atrophy in multiple sclerosis. *Brain J. Neurol.* **131**, 1134–1141 (2008).

127. Nygaard, G. O. *et al.* A Longitudinal Study of Disability, Cognition and Gray Matter Atrophy in Early Multiple Sclerosis Patients According to Evidence of Disease Activity. *PloS One* **10**, e0135974 (2015).

128. Eshaghi, A. *et al.* Temporal and spatial evolution of grey matter atrophy in primary progressive multiple sclerosis. *Neuroimage* **86**, 257–264 (2014).

129. Hofstetter, L. *et al.* Progression in disability and regional grey matter atrophy in relapsing-remitting multiple sclerosis. *Mult. Scler. Houndmills Basingstoke Engl.* **20**, 202–213 (2014).

130. Houtchens, M. K. *et al.* Thalamic atrophy and cognition in multiple sclerosis. *Neurology* **69**, 1213–1223 (2007).

131. Solomon, A. J., Watts, R., Dewey, B. E. & Reich, D. S. MRI evaluation of thalamic volume differentiates MS from common mimics. *Neurol. Neuroimmunol. Neuroinflammation* **4**, (2017).

132. Schoonheim, M. M. *et al.* Thalamus structure and function determine severity of cognitive impairment in multiple sclerosis. *Neurology* **84**, 776–783 (2015).

133. Geurts, J. J. G., Calabrese, M., Fisher, E. & Rudick, R. A. Measurement and clinical effect of grey matter pathology in multiple sclerosis. *Lancet Neurol.* **11**, 1082–1092 (2012).

134. Okuda, D. T. *et al.* Radiologically isolated syndrome: 5-year risk for an initial clinical event. *PloS One* **9**, e90509 (2014).

135. De Stefano, N. *et al.* Improving the characterization of radiologically isolated syndrome suggestive of multiple sclerosis. *PloS One* **6**, e19452 (2011).

136. Tedeschi, G. *et al.* Brain atrophy and lesion load in a large population of patients with multiple sclerosis. *Neurology* **65**, 280–5 (2005).

137. Filippi, M. *et al.* Interferon beta-1a for brain tissue loss in patients at presentation with syndromes suggestive of multiple sclerosis: a randomised, double-blind, placebo-controlled trial. *Lancet Lond. Engl.* **364**, 1489–1496 (2004).

138. Pérez-Miralles, F. *et al.* Clinical impact of early brain atrophy in clinically isolated syndromes. *Mult. Scler. Houndmills Basingstoke Engl.* **19**, 1878–1886 (2013).

139. Di Filippo, M. *et al.* Brain atrophy and lesion load measures over 1 year relate to clinical status after 6 years in patients with clinically isolated syndromes. *J. Neurol. Neurosurg. Psychiatry* **81**, 204–208 (2010).

140. Steenwijk, M. D. *et al.* Cortical atrophy patterns in multiple sclerosis are non-random and clinically relevant. *Brain* **139**, 115–26 (2016).

141. Calabrese, M. *et al.* Exploring the origins of grey matter damage in multiple sclerosis. *Nat. Rev. Neurosci.* **16**, 147–158 (2015).

142. Tanasescu, R. *et al.* Hookworm Treatment for Relapsing Multiple Sclerosis: A Randomized Double-Blinded Placebo-Controlled Trial. *JAMA Neurol.* (2020) doi:10.1001/jamaneurol.2020.1118.

143. Singh, S., Tench, C. R., Tanasescu, R. & Constantinescu, C. S. Localised Grey Matter Atrophy in Multiple Sclerosis and Clinically Isolated Syndrome—A Coordinate-Based Meta-Analysis, Meta-Analysis of Networks, and Meta-Regression of Voxel-Based Morphometry Studies. *Brain Sci.* **10**, 798 (2020).

144. Pernet, C. R. The General Linear Model: Theory and Practicalities in Brain Morphometric Analyses. in *Brain Morphometry* (eds. Spalletta, G., Piras, F. & Gili, T.) 75–85 (Springer, 2018). doi:10.1007/978-1-4939-7647-8_5.

145. Short Introduction to the General Linear Model for Neuroimaging (Oxford Neuroimaging Primer Appendices Book 2). https://www.goodreads.com/book/show/53676436-short-introduction-to-the-general-linear-model-for-neuroimaging.

146. Bland, J. M. & Altman, D. G. Statistical methods for assessing agreement between two methods of clinical measurement. *Lancet Lond. Engl.* **1**, 307–310 (1986).

147. Tench, C. R., Tanasescu, R., Constantinescu, C. S., Auer, D. P. & Cottam, W. J. Coordinate based random effect size meta-analysis of neuroimaging studies. *Neuroimage* **153**, 293–306 (2017).

148. Tench, C. R., Tanasescu, R., Constantinescu, C. S., Cottam, W. J. & Auer, D. P. Coordinate based meta-analysis of networks in neuroimaging studies. *NeuroImage* **205**, 116259 (2020).

149. Tench, C. R. Coordinate based meta-analysis: new clustering algorithm, and inclusion of region of interest studies. *bioRxiv* 2020.04.05.026575 (2020) doi:10.1101/2020.04.05.026575.

150. Benjamini, Y. & Hochberg, Y. Controlling the False Discovery Rate: A Practical and Powerful Approach to Multiple Testing. *J. R. Stat. Soc. Ser. B Methodol.* **57**, 289–300 (1995).

151. Ashburner, J. & Friston, K. J. Voxel-based morphometry--the methods. *NeuroImage* **11**, 805–821 (2000).

152. Smith, S. M. *et al.* Advances in functional and structural MR image analysis and implementation as FSL. *NeuroImage* **23 Suppl 1**, S208-219 (2004).

153. Smith, S. M. Fast robust automated brain extraction. *Hum. Brain Mapp.* **17**, 143–155 (2002).

154. Zhang, Y., Brady, M. & Smith, S. Segmentation of brain MR images through a hidden Markov random field model and the expectation-maximization algorithm. *IEEE Trans. Med. Imaging* **20**, 45–57 (2001).

155. Jenkinson, M. & Smith, S. A global optimisation method for robust affine registration of brain images. *Med. Image Anal.* **5**, 143–156 (2001).

156. Jenkinson, M., Bannister, P., Brady, M. & Smith, S. Improved optimization for the robust and accurate linear registration and motion correction of brain images. *NeuroImage* **17**, 825–841 (2002).

157. [PDF] Non-linear optimisation FMRIB Technial Report TR 07 JA 1 | Semantic Scholar. https://www.semanticscholar.org/paper/Non-linear-optimisation-FMRIB-Technial-Report-TR-07-Andersson-Jenkinson/7018dff7b9e2d05f2b43a0fe8b0a3598e2f213f2.

158. Panitch, H. S., Hirsch, R. L., Schindler, J. & Johnson, K. P. Treatment of multiple sclerosis with gamma interferon: exacerbations associated with activation of the immune system. *Neurology* **37**, 1097–1102 (1987).

159. Röcken, M., Racke, M. & Shevach, E. M. IL-4-induced immune deviation as antigen-specific therapy for inflammatory autoimmune disease. *Immunol. Today* **17**, 225–231 (1996).

160. Harnett, W. & Harnett, M. M. Helminth-derived immunomodulators: can understanding the worm produce the pill? *Nat. Rev. Immunol.* **10**, 278–284 (2010).

161. Fleming, J. O. & Weinstock, J. V. Clinical trials of helminth therapy in autoimmune diseases: rationale and findings. *Parasite Immunol.* **37**, 277–292 (2015).

162. Hotez, P. J. *et al.* Hookworm infection. *N. Engl. J. Med.* **351**, 799–807 (2004).

163. Blount, D. *et al.* Immunologic profiles of persons recruited for a randomized, placebo-controlled clinical trial of hookworm infection. *Am. J. Trop. Med. Hyg.* **81**, 911–916 (2009).

164. Pritchard, D. I. & Brown, A. Is Necator americanus approaching a mutualistic symbiotic relationship with humans? *Trends Parasitol.* **17**, 169–172 (2001).

165. Mortimer, K. *et al.* Dose-ranging study for trials of therapeutic infection with Necator americanus in humans. *Am. J. Trop. Med. Hyg.* **75**, 914–920 (2006).

166. Falcone, F. & Pritchard, D. Parasite role reversal: Worms on trial. *Trends Parasitol.* **21**, 157–60 (2005).

167. Navarro, S., Ferreira, I. & Loukas, A. The hookworm pharmacopoeia for inflammatory diseases. *Int. J. Parasitol.* **43**, 225–231 (2013).

168. Pritchard, D. I., Blount, D. G., Schmid-Grendelmeier, P. & Till, S. J. Parasitic worm therapy for allergy: is this incongruous or avant-garde medicine? *Clin. Exp. Allergy J. Br. Soc. Allergy Clin. Immunol.* **42**, 505–512 (2012).

169. Feary, J. *et al.* Safety of hookworm infection in individuals with measurable airway responsiveness: a randomized placebo-controlled feasibility study. *Clin. Exp. Allergy* **39**, 1060–1068 (2009).

170. Daveson, A. J. *et al.* Effect of Hookworm Infection on Wheat Challenge in Celiac Disease – A Randomised Double-Blinded Placebo Controlled Trial. *PLoS ONE* **6**, (2011).

171. Tanasescu, R. & Constantinescu, C. S. Helminth Therapy for MS. *Curr. Top. Behav. Neurosci.* **26**, 195–220 (2015).

172. Fleming, J. O. *et al.* Probiotic helminth administration in relapsing-remitting multiple sclerosis: a phase 1 study. *Mult. Scler. Houndmills Basingstoke Engl.* **17**, 743–754 (2011).

173. Fleming, J. *et al.* Safety and efficacy of helminth treatment in relapsing-remitting multiple sclerosis: Results of the HINT 2 clinical trial. *Mult. Scler. Houndmills Basingstoke Engl.* **25**, 81–91 (2019).

174. Benzel, F. *et al.* Immune monitoring of Trichuris suis egg therapy in multiple sclerosis patients. *J. Helminthol.* **86**, 339–347 (2012).

175. Rosche, B. *et al.* Serum levels of brain-derived neurotrophic factor (BNDF) in multiple sclerosis patients with Trichuris suis ova therapy. *Parasite* **20**, (2013).

176. Voldsgaard, A. *et al.* Trichuris suis ova therapy in relapsing multiple sclerosis is safe but without signals of beneficial effect. *Mult. Scler. Houndmills Basingstoke Engl.* **21**, 1723–1729 (2015).

177. Worms for Immune Regulation of Multiple Sclerosis - Full Text View - ClinicalTrials.gov. https://clinicaltrials.gov/ct2/show/NCT01470521.

178. Tubridy, N., Ader, H., Barkhof, F., Thompson, A. & Miller, D. Exploratory treatment trials in multiple sclerosis using MRI: sample size calculations for relapsing-remitting and secondary progressive subgroups using placebo controlled parallel groups. *J. Neurol. Neurosurg. Psychiatry* **64**, 50–55 (1998).

179. Brex, P. A. *et al.* A longitudinal study of abnormalities on MRI and disability from multiple sclerosis. *N. Engl. J. Med.* **346**, 158–164 (2002).

180. Filippi, M. *et al.* Quantitative assessment of MRI lesion load in monitoring the evolution of multiple sclerosis. *Brain J. Neurol.* **118 (Pt 6)**, 1601–1612 (1995).

181. Filippi, M. *et al.* Intraobserver and interobserver variability in schemes for estimating volume of brain lesions on MR images in multiple sclerosis. *AJNR Am. J. Neuroradiol.* **19**, 239–244 (1998).

182. Tubridy, N., Ader, H., Barkhof, F., Thompson, A. & Miller, D. Exploratory treatment trials in multiple sclerosis using MRI: sample size

calculations for relapsing-remitting and secondary progressive subgroups using placebo controlled parallel groups. *J. Neurol. Neurosurg. Psychiatry* **64**, 50–55 (1998).

183. Campbell, Z. *et al.* Characterizing contrast-enhancing and re-enhancing lesions in multiple sclerosis. *Neurology* **78**, 1493–1499 (2012).

184. Lewańska, M., Siger-Zajdel, M. & Selmaj, K. No difference in efficacy of two different doses of intravenous immunoglobulins in MS: clinical and MRI assessment. *Eur. J. Neurol.* **9**, 565–572 (2002).

185. Fay, B. R. The Effect On Type I Error And Power Of Various Methods Of Resolving Ties For Six Distribution-Free Tests Of Location. *J. Mod. Appl. Stat. Methods* **5**, 4 (2006).

186. Confavreux, C., Vukusic, S., Moreau, T. & Adeleine, P. Relapses and progression of disability in multiple sclerosis. *N. Engl. J. Med.* **343**, 1430–1438 (2000).

187. Miller, D. H., Barkhof, F., Frank, J. A., Parker, G. J. M. & Thompson, A. J. Measurement of atrophy in multiple sclerosis: pathological basis, methodological aspects and clinical relevance. *Brain J. Neurol.* **125**, 1676–1695 (2002).

188. Losseff, N. A. *et al.* Progressive cerebral atrophy in multiple sclerosis. A serial MRI study. *Brain J. Neurol.* **119 (Pt 6)**, 2009–2019 (1996).

189. Dalton, C. M. *et al.* Early development of multiple sclerosis is associated with progressive grey matter atrophy in patients presenting with clinically isolated syndromes. *Brain J. Neurol.* **127**, 1101–1107 (2004).

190. Messina, S. & Patti, F. Gray matters in multiple sclerosis: cognitive impairment and structural MRI. *Mult Scler Int* **2014**, 609694 (2014).

191. Geurts, J. J. G. & Barkhof, F. Grey matter pathology in multiple sclerosis. *Lancet Neurol.* **7**, 841–851 (2008).

192. De Stefano, N. *et al.* Evidence of early cortical atrophy in MS: relevance to white matter changes and disability. *Neurology* **60**, (2003).

193. Fisniku, L. K. *et al.* Gray matter atrophy is related to long-term disability in multiple sclerosis. *Ann. Neurol.* **64**, 247–254 (2008).

194. Sailer, M. *et al.* Focal thinning of the cerebral cortex in multiple sclerosis. *Brain* **126**, 1734–44 (2003).

195. Scarpazza, C., Tognin, S., Frisciata, S., Sartori, G. & Mechelli, A. False positive rates in Voxel-based Morphometry studies of the human brain: should we be worried? *Neurosci. Biobehav. Rev.* **52**, 49–55 (2015).

196. Button, K. S. *et al.* Power failure: why small sample size undermines the reliability of neuroscience. *Nat Rev Neurosci* **14**, 365–76 (2013).

197. Bennett, C. M., Wolford, G. L. & Miller, M. B. The principled control of false positives in neuroimaging. *Soc Cogn Affect Neurosci* **4**, 417–22 (2009).

198. Popescu, V. *et al.* Grey Matter Atrophy in Multiple Sclerosis: Clinical Interpretation Depends on Choice of Analysis Method. *PLoS One* **11**, e0143942 (2016).

199. Smith, S. M. *et al.* Accurate, robust, and automated longitudinal and cross-sectional brain change analysis. *Neuroimage* **17**, 479–89 (2002).

200. Dale, A. M., Fischl, B. & Sereno, M. I. Cortical surface-based analysis. I. Segmentation and surface reconstruction. *Neuroimage* **9**, 179–94 (1999).

201. Fischl, B., Sereno, M. I. & Dale, A. M. Cortical surface-based analysis. II: Inflation, flattening, and a surface-based coordinate system. *Neuroimage* **9**, 195–207 (1999).

202. Tench, C. & Singh, S. MS meta analysis files. (2020) doi:http://doi.org/10.17639/nott.7049.

203. Talairach, J. & Tournoux, P. *Co-planar stereotaxic atlas of the human brain*. (Thieme, 1988).

204. Tench, C. R. Coordinate based meta-analysis: new clustering algorithm, and inclusion of region of interest studies. *bioRxiv* 2020.04.05.026575 (2020) doi:10.1101/2020.04.05.026575.

205. Turkeltaub, P. E. *et al.* Minimizing within-experiment and within-group effects in Activation Likelihood Estimation meta-analyses. *Hum Brain Mapp* **33**, 1–13 (2012).

206. Moher, D., Liberati, A., Tetzlaff, J., Altman, D. G., & PRISMA Group. Preferred reporting items for systematic reviews and meta-analyses: the PRISMA statement. *PLoS Med.* **6**, e1000097 (2009).

207. Martijn D. Steenwijk *et al.* What Explains Gray Matter Atrophy in Long-standing Multiple Sclerosis? *Radiology* **272**, 832–842 (2014).

208. Koskimäki, F. *et al.* Gray matter atrophy in multiple sclerosis despite clinical and lesion stability during natalizumab treatment. *Plos One* **13**, e0209326 (2018).

209. Trapp, B. D. *et al.* Axonal transection in the lesions of multiple sclerosis. *N. Engl. J. Med.* **338**, 278–285 (1998).

210. Štecková, T. *et al.* Thalamic atrophy and cognitive impairment in clinically isolated syndrome and multiple sclerosis. *J Neurol Sci* **342**, 62–68 (2014).

211. Haider, L. *et al.* Multiple sclerosis deep grey matter: the relation between demyelination, neurodegeneration, inflammation and iron. *J Neurol Neurosurg Psychiatry* **85**, 1386–95 (2014).

212. Cifelli, A. *et al.* Thalamic neurodegeneration in multiple sclerosis. *Ann. Neurol.* **52**, 650–3 (2002).

213. Azevedo, C. J. *et al.* Early CNS neurodegeneration in radiologically isolated syndrome. *Neurol. Neuroimmunol. Neuroinflammation* **2**, e102–e102 (2015).

214. Lassmann, H. Multiple sclerosis: lessons from molecular neuropathology. *Exp Neurol* **262 Pt A**, 2–7 (2014).

215. Henry, R. G. *et al.* Regional grey matter atrophy in clinically isolated syndromes at presentation. *J Neurol Neurosurg Psychiatry* **79**, 1236–44 (2008).

216. Batista, S. *et al.* Basal ganglia, thalamus and neocortical atrophy predicting slowed cognitive processing in multiple sclerosis. *J. Neurol.* **259**, 139–46 (2012).

217. Modica, C. M. *et al.* Iron and Volume in the Deep Gray Matter: Association with Cognitive Impairment in Multiple Sclerosis. *Am. J. Neuroradiol.* **36**, 57 (2015).

218. Starr, C. J. *et al.* The contribution of the putamen to sensory aspects of pain: insights from structural connectivity and brain lesions. *Brain J. Neurol.* **134**, 1987–2004 (2011).

219. Koikkalainen, J. *et al.* Shape variability of the human striatum--Effects of age and gender. *NeuroImage* **34**, 85–93 (2007).

220. Uono, S. *et al.* Putamen Volume is Negatively Correlated with the Ability to Recognize Fearful Facial Expressions. *Brain Topogr.* **30**, 774–784 (2017).

221. Kramer, J. *et al.* Early and Degressive Putamen Atrophy in Multiple Sclerosis. *Int. J. Mol. Sci.* **16**, 23195–209 (2015).

222. Li, Y. *et al.* Diffusion tensor imaging based network analysis detects alterations of neuroconnectivity in patients with clinically early relapsing-remitting multiple sclerosis. *Hum. Brain Mapp.* **34**, 3376–91 (2013).

223. Leff, A. P. *et al.* The left superior temporal gyrus is a shared substrate for auditory short-term memory and speech comprehension: evidence from 210 patients with stroke. *Brain* **132**, 3401–3410 (2009).

224. Friederici, A. D. The cortical language circuit: from auditory perception to sentence comprehension. *Trends Cogn. Sci.* **16**, 262–268 (2012).

225. Bigler, E. D. *et al.* Superior temporal gyrus, language function, and autism. *Dev. Neuropsychol.* **31**, 217–238 (2007).

226. Radua, J. *et al.* Neural response to specific components of fearful faces in healthy and schizophrenic adults. *NeuroImage* **49**, 939–946 (2010).

227. Michl, P. *et al.* Neurobiological underpinnings of shame and guilt: a pilot fMRI study. *Soc. Cogn. Affect. Neurosci.* **9**, 150–157 (2014).

228. Achiron, A. *et al.* Superior temporal gyrus thickness correlates with cognitive performance in multiple sclerosis. *Brain Struct Funct* **218**, 943–50 (2013).

229. Uddin, L. Q., Nomi, J. S., Hébert-Seropian, B., Ghaziri, J. & Boucher, O. Structure and Function of the Human Insula. *J. Clin. Neurophysiol. Off. Publ. Am. Electroencephalogr. Soc.* **34**, 300–306 (2017).

230. Finke, C. *et al. Altered basal ganglia functional connectivity in multiple sclerosis patients with fatigue*. vol. 21 (2014).

231. Jaeger, S. *et al.* Multiple sclerosis-related fatigue: Altered resting-state functional connectivity of the ventral striatum and dorsolateral prefrontal cortex. *Mult Scler* 1352458518758911 (2018) doi:10.1177/1352458518758911.

232. Lin, F. *et al.* Altered nuclei-specific thalamic functional connectivity patterns in multiple sclerosis and their associations with fatigue and cognition. *Mult Scler* 1352458518788218 (2018) doi:10.1177/1352458518788218.

233. Chiang, F. L. *et al.* Localised grey matter atrophy in multiple sclerosis is network-based: a coordinate-based meta-analysis. *Clin Radiol* **74**, 816.e19-816.e28 (2019).

234. Robinson, J. L., Laird, A. R., Glahn, D. C., Lovallo, W. R. & Fox, P. T. Metaanalytic connectivity modeling: delineating the functional connectivity of the human amygdala. *Hum Brain Mapp* **31**, 173–84 (2010).

235. Kidd, D. *et al.* Cortical lesions in multiple sclerosis. *Brain J. Neurol.* **122 (Pt 1)**, 17–26 (1999).

236. Cercignani, M., Bozzali, M., Iannucci, G., Comi, G. & Filippi, M. Magnetisation transfer ratio and mean diffusivity of normal appearing white and grey matter from patients with multiple sclerosis. *J. Neurol. Neurosurg. Psychiatry* **70**, 311–317 (2001).

237. Chard, D. T. *et al.* Brain metabolite changes in cortical grey and normal-appearing white matter in clinically early relapsing-remitting multiple sclerosis. *Brain J. Neurol.* **125**, 2342–2352 (2002).

238. Rovaris, M. *et al.* Assessment of normal-appearing white and gray matter in patients with primary progressive multiple sclerosis: a diffusion-tensor magnetic resonance imaging study. *Arch. Neurol.* **59**, 1406–1412 (2002).

239. Bakshi, R. *et al.* T2 hypointensity in the deep gray matter of patients with multiple sclerosis: a quantitative magnetic resonance imaging study. *Arch. Neurol.* **59**, 62–68 (2002).

240. Davies, G. R. *et al.* Evidence for grey matter MTR abnormality in minimally disabled patients with early relapsing-remitting multiple sclerosis. *J. Neurol. Neurosurg. Psychiatry* **75**, 998–1002 (2004).

241. Losseff, N. A. *et al.* Progressive cerebral atrophy in multiple sclerosis. A serial MRI study. *Brain J. Neurol.* **119 (Pt 6)**, 2009–2019 (1996).

242. Chard, D. T. *et al.* Brain atrophy in clinically early relapsing-remitting multiple sclerosis. *Brain J. Neurol.* **125**, 327–337 (2002).

243. Barkhof, F. The clinico-radiological paradox in multiple sclerosis revisited. *Curr. Opin. Neurol.* **15**, 239–245 (2002).

244. Ruiz, F., Vigne, S. & Pot, C. Resolution of inflammation during multiple sclerosis. *Semin. Immunopathol.* **41**, 711–726 (2019).

245. Andravizou, A. *et al.* Brain atrophy in multiple sclerosis: mechanisms, clinical relevance and treatment options. *Autoimmun. Highlights* **10**, 7 (2019).

246. Bermel, R. A. & Bakshi, R. The measurement and clinical relevance of brain atrophy in multiple sclerosis. *Lancet Neurol.* **5**, 158–170 (2006).

247. Good, C. D. *et al.* A voxel-based morphometric study of ageing in 465 normal adult human brains. *NeuroImage* **14**, 21–36 (2001).

248. Ceccarelli, A. *et al.* A voxel-based morphometry study of grey matter loss in MS patients with different clinical phenotypes. *NeuroImage* **42**, 315–322 (2008).

249. Audoin, B. *et al.* Localization of grey matter atrophy in early RRMS : A longitudinal study. *J. Neurol.* **253**, 1495–1501 (2006).

250. Khaleeli, Z. *et al.* Localized grey matter damage in early primary progressive multiple sclerosis contributes to disability. *NeuroImage* **37**, 253–261 (2007).

251. Morgen, K. *et al.* Evidence for a direct association between cortical atrophy and cognitive impairment in relapsing-remitting MS. *NeuroImage* **30**, 891–898 (2006).

252. Pagani, E. *et al.* Regional brain atrophy evolves differently in patients with multiple sclerosis according to clinical phenotype. *AJNR Am. J. Neuroradiol.* **26**, 341–346 (2005).

253. Prinster, A. *et al.* Grey matter loss in relapsing-remitting multiple sclerosis: a voxel-based morphometry study. *NeuroImage* **29**, 859–867 (2006).

254. Sepulcre, J. *et al.* Regional gray matter atrophy in early primary progressive multiple sclerosis: a voxel-based morphometry study. *Arch. Neurol.* **63**, 1175–1180 (2006).

255. Favaretto, A., Lazzarotto, A., Margoni, M., Poggiali, D. & Gallo, P. Effects of disease modifying therapies on brain and grey matter atrophy in relapsing remitting multiple sclerosis. *Mult. Scler. Demyelinating Disord.* **3**, 1 (2018).

256. Hohlfeld, R. & Wekerle, H. Autoimmune concepts of multiple sclerosis as a basis for selective immunotherapy: From pipe dreams to (therapeutic) pipelines. *Proc. Natl. Acad. Sci. U. S. A.* **101**, 14599–14606 (2004).

257. Kleinewietfeld, M. & Hafler, D. A. Regulatory T cells in autoimmune neuroinflammation. *Immunol. Rev.* **259**, 231–244 (2014).

258. Constantinescu, C. S. & Gran, B. The essential role of T cells in multiple sclerosis: a reappraisal. *Biomed. J.* **37**, 34–40 (2014).

259. Gilmore, C. P. *et al.* Regional variations in the extent and pattern of grey matter demyelination in multiple sclerosis: a comparison between the cerebral cortex, cerebellar cortex, deep grey matter nuclei and the spinal cord. *J. Neurol. Neurosurg. Psychiatry* **80**, 182–187 (2009).

260. Gelineau-Morel, R. *et al.* The effect of hypointense white matter lesions on automated gray matter segmentation in multiple sclerosis. *Hum. Brain Mapp.* **33**, 2802–2814 (2011).

261. Smith, S. M. *et al.* Accurate, robust, and automated longitudinal and cross-sectional brain change analysis. *NeuroImage* **17**, 479–489 (2002).

262. Nakamura, K. *et al.* Improving the SIENA performance using BEaST brain extraction. *PloS One* **13**, e0196945 (2018).